Toward Large-Scale DER Aggregation: Competitive Aggregation, Operation Support, and ISO-Aggregator-Utility Coordination

Final Project Report

M-46

Power Systems Engineering Research Center
Empowering Minds to Engineer
the Future Electric Energy System

Toward Large-Scale DER Aggregation:
Competitive Aggregation, Operation Support, and ISO-Aggregator-Utility Coordination

Final Project Report

Project Team
Lang Tong, Project Leader
Timothy D. Mount
Cornell University

Subhonmesh Bose
University of Illinois, Urbana-Champaign

Meng Wu
Arizona State University

Graduate Students
Cong Chen
Siying Li
Ahmed Alahmed
Cornell University

Mohammad Mousavi
Arizona State University

PSERC Publication 25-02

December 2025

For information about this project, contact:

Professor Lang Tong
School of Electrical and Computer Engineering
Cornell University, Ithaca, New York 14853

Power Systems Engineering Research Center

The Power Systems Engineering Research Center (PSERC) is a multi-university Center conducting research on challenges facing the electric power industry and educating the next generation of power engineers. More information about PSERC can be found at the Center's website: http://www.pserc.org.

For additional information, contact:

Power Systems Engineering Research Center
Arizona State University
527 Engineering Research Center
Tempe, Arizona 85287-5706
Phone: 480-965-1643
Fax: 480-727-2052

Notice Concerning Copyright Material

Acknowledgements

We wish to thank the following PSERC industry advisors and researchers who have interacted with us during the duration of this project. Their comments, suggestions, and advice helped us navigate the nascent field DER aggregation under FERC Order 2222:

CAISO: Clyde Loutan
EPRI : Nikita Singhai
ISONE: Mingguo Hong, Tongxin Zheng
PJM: Hong Chen, Jianzhong Tong
MISO: Anupam Thatte
NYISO: Mike Swider
RTE: Patrick Panciatici
SPP: Harvey Scribner
SRP: Bo Gong

Executive Summary

This report summarizes research outcomes from project M46 in the PSERC market stem. Led by Professor Lang Tong (Lead PI, Cornell University), Professor Subhonmesh Bose (University of Illinois Urbana-Champaign), and Professor Meng Wu (Arizona State University), this project focused on the theoretical and practical challenges of aggregating distributed energy resources in distribution systems for wholesale market participation under the general framework of FERC Order 2222.

Aggregating distributed energy resources in distribution systems for wholesale market participation involves complex system and market interactions. This project pursued a bottom-up approach to address key technological barriers at each market interface: (i) the interfaces between a distributed energy resource (DER) aggregator (DERA) and its customers where generation, storage, and flexible demand resources are aggregated, (ii) the interface between DERAs and a wholesale market operator (ISO/RTO) where DERAs participate in wholesale energy, reserve and regulation markets, (iii) the interface between DERAs and a distribution utility where the utility provides planning and operation support for delivering the aggreged DER from end customers to the wholesale markets, and (iv) the interface between a distribution utility and an ISO where the ISO maximizes net benefits of market participants and mitigates risk subject to system constraints.

This project developed aggregation models, optimal aggregation strategies for DERAs, and coordination mechanisms for aggregators, distribution utilities, and wholesale market operators at multiple market interfaces, as well as aggregators' wholesale market participation approaches. Among the most significant outcomes of the project are an auction mechanism that defines DERAs' passways to the transmission system without interfering with the normal operations of the distribution utility, a competitive aggregation strategy that ensures customers of DERA with higher consumer surplus than that under the default regulated retail tariff, and a virtual storage participation model in the wholesale market achieving the same market efficiency as if distributed energy resources participating directly in the wholesale market.
In particular, this project investigates large-scale, competitive, and profit-maximizing aggregation technologies that benefit DERA customers more than the prevailing net energy metering-based retail tariffs. The project examines the impacts of DER aggregation uncertainties at all interfaces and develops risk mitigation strategies. The project investigates distribution system planning and operation solutions supporting DER aggregation, DERA bidding strategies in the wholesale markets, and ISO market clearing and settlement solutions. The project delivers technical assessments and comparative studies on the feasibility and cost/benefit analysis.

This project contributed to the graduate education of 6 students, giving them opportunities to interact with industry and pursue fundamental yet practically impactful research. Student research resulted in several significant awards, including the 2025 PES Outstanding Doctoral Dissertation Award, the 2023 PESGM Prize Conference Award, and several PESGM Best Paper Session selections.

Part I: Wholesale Market Participation of DERAs: DSO-DERA-ISO Coordination

The landmark ruling of the Federal Energy Regulatory Commission (FERC) Order 2222 aims to remove barriers to the direct participation of distributed energy resource aggregators (DERAs) in the wholesale market operated by ISOs/RTOs. Since distributed energy resources (DERs) originate in a distribution network, aggregated DERs must pass through the distribution grid managed by a distribution system operator (DSO) that can be the distribution utility or an independent entity. A coordination mechanism among the DSO, ISO, and DERAs is necessary to ensure system reliability and open access to all DERAs. FERC Order 2222 recognizes the significance of DSO-DERA-ISO coordination while leaving the specifics of the coordination design to the regulators, market operators, and stakeholders.

This work develops a novel DSO-DERA-ISO coordination mechanism aimed at achieving efficient and reliable multi-DERA aggregations with minimal deviations from existing DSO and ISO/RTO interaction models. Specifically, we propose a forward auction run by the DSO that allows DERAs to acquire network access limits–the right to inject or withdraw any amount of power within those limits over which the auction outcomes stand. These limits are auctioned off in a way that all power transactions from DERAs within these limits will satisfy distribution system operation constraints. Thus, DERA's wholesale market interaction with the ISO in real-time can be agnostic to these operational constraints, and ISOs can dispatch DERs without direct visibility into the distribution network. The DERA-ISO interaction can include models such as demand response, virtual storage, etc., and any way they choose to operate the DERs will not violate distribution network security as long as they remain within the network access limits they acquire from the DSO-operated auction. Consequently, our design removes the need for DSO's interventions in ISO's real-time dispatch and DERAs' aggregation actions under normal system operating conditions.

We consider two network access allocation mechanisms. First, a robust optimization-based market clearing formulation for network access is proposed, which guarantees satisfaction of network constraints when DERAs aggregate within their acquired access limits, thus removing the need for DSO to participate in real-time DERA-ISO interactions. DERAs do not even need knowledge of the underlying physical network when its aggregation strategy respects said limits. The robust access allocation can be conservative in that it assumes the worst-case aggregation and network operating conditions. Second, we develop a risk-based stochastic allocation mechanism that allows DSO to share the common network resources subject to an acceptable risk constraint on network security violations. For both the robust and stochastic access limit auctions, we provide theoretical analyses and empirical studies to characterize and quantify access allocation properties, including the nonnegative surpluses for DSO, the benefits of participating in the access limit auction for DERAs, the behavior of access allocation prices, and extensive numerical comparisons.

Part II: Wholesale Market Participation of DERAs: Competitive DER Aggregation

We address open problems in the direct participation of distributed energy resource aggregators (DERAs) in the wholesale electricity market operated by regional transmission organizations and independent system operators (RTOs/ISOs), under the general framework of FERC order 2222. We focus on the aggregation strategy of a profit-seeking DERA, whose industrial, commercial, and residential customers have competing service providers, such as their incumbent regulated utilities.

The central theme of this work is to develop profitable and competitive aggregation strategies to attract and retain customers. By competitive aggregation, we mean that the benefits of the DERA customers must be no less than those offered by electricity provider benchmarks. An example of such a benchmark is the incumbent utility or a community choice aggregator (CCA) adopting net energy metering (NEM) policies, offering strong incentives to prosumers with behind-the-meter (BTM) DERs. A major barrier to DERA's entry into direct wholesale market participation is the lack of an effective aggregation strategy and participation model, which would make DER aggregation a profitable venture.

The technical challenge of designing a profitable and competitive DER aggregation is twofold. First, the DERA plays a dual role in the aggregation process: an energy supplier to its customers in the retail market and a producer/demand in the wholesale market. Its aggregation must consider retail competition, distribution network access limits, and its overall revenue adequacy. To this end, a DERA needs to derive profit-maximizing bids/offers from its competitive aggregation. Second, competitive aggregation requires the DERA to offer more attractive pricing to its customers than the regulated tariff and shield them from the volatility of wholesale market prices.

In this project, we develop a DERA aggregation model that aggregates customers across multiple locations in distribution networks and incorporates security constraints on network injection and withdrawal limits. We further investigate the competitive aggregation impact on market efficiency, price stability, and long-run equilibrium. First, we propose a DER aggregation approach based on a constrained convex optimization that maximizes DERA surplus while providing higher customer surpluses than those offered by a competing aggregation model. We show that such a competitive DER aggregation, despite the aggregation involving real-time wholesale locational marginal price (LMP), has an energy cost no greater than the regulated NEM tariff. This implies that the proposed DER aggregation mechanism ensures price stability regardless of the volatility of the wholesale market LMP.

Second, we propose a virtual storage model for DERA's wholesale market participation compatible with the practical continuous storage facility participation considered by ISOs under FERC order 841. The DERA bidding curve is derived from the closed-form solution of the proposed DERA model. While the aggregation optimization explicitly involves wholesale market LMP, the virtual storage bidding curves do not require forecasting of LMP. We show that the proposed DERA wholesale market participation results in market efficiency equal to what is achievable when DERA's customers participate directly in the wholesale market.

Finally, we derive the benefit function of DERA over distribution network injection and withdrawal access limits. DERAs compete in the distribution network access auction proposed in Part I to acquire network access, and we empirically evaluate the number of surviving DERAs in

the long-run competitive equilibrium. We also present a set of numerical results, comparing the surplus distribution of the proposed competitive aggregation solution with those of various alternatives, including the regulated utility. Among significant insights gained are the higher social surplus, customer surplus, and DERA surplus achievable in the proposed competitive DERA model, when compared to other alternatives.

Part III: Coordinating Transmission and Distribution System Operations for Intensive DER Integration: A Parametric Programming Approach

Part III of this report establishes full-scale online transmission and distribution (T&D) coordination in future DER-rich markets by developing theoretical coordination frameworks, low-time-complexity algorithms, and distribution system pricing designs. To ensure real-world applicability, we strictly follow several design requirements for DER-rich T&D-coordinated markets. 1) Under extremely limited communications between T&D systems, T&D operation should be coordinated with minimal T&D communications. 2) To respect data ownership and model confidentiality, exchanging T&D system models should be avoided. 3) To enable a smooth transition from today's established ISO markets, T&D coordination should minimize the changes to ISO's existing market operations. 4) T&D-coordinated markets should guarantee optimal operation while satisfying all the operating constraints for the entire T&D systems. 5) To enable online operations, computations of large-scale T&D-coordinated markets should be fast.
The above requirements call for fast online coordination of a large-scale decentralized network optimization problem under extremely limited communications and zero model exchange, which is theoretically and computationally challenging.

To address the above technical challenges, three chapters are presented in Part III of this report.

Chapter 1 presents theoretical frameworks for T&D-coordinated market operation with guaranteed real-world applicability, leveraging parametric-programming-based multilevel system decomposition. This chapter presents a framework to coordinate ISO and DSO operations, compatible with the current wholesale market structure, without introducing additional changes to the existing wholesale market clearing procedure. In this coordination framework, DER aggregators participate in the wholesale market through coordination with the DSO, which ensures the secure operation of the distribution grid. A parametric programming approach is proposed to construct the bid-in cost function for the DSO (to be submitted to the ISO) and to run the DSO-level market-clearing procedure, which is based on offers collected from DER aggregators. The parametric-programming-based ISO-DSO coordination enables complete decoupling between the solution process of the ISO and DSO optimization sub-problems. This avoids iterative ISO-DSO communications within each wholesale market clearing interval and allows the ISO and DSO to exchange the minimal amount of public data only after each entity reaches its optimal solution. The proposed approach requires no exchange of private/confidential ISO or DSO grid model data.

Chapter 2 presents distribution system pricing designs that can efficiently and economically support T&D-coordinated economic dispatch via parametric programming. This chapter extends the T&D coordination framework in Chapter 1 by developing theoretical justifications and

thorough discussions for the T&D-coordinated pricing problem. Specifically, we prove and discuss 1) the relationship between the T&D-coordinated dispatch model and the T&D-coordinated pricing model, which together guarantee the T&D operation optimality for both the dispatch and pricing processes; and 2) the non-profit characteristics of the DSO under the proposed T&D-coordinated pricing model. One interesting finding is that, to ensure zero T&D model exchange and minimal T&D communication in the parametric programming-based T&D coordination framework, the optimal prices for aggregated DERs in the distribution system cannot be directly obtained from the dual of the DSO economic dispatch problem. Instead, a separate DSO pricing model is needed to generate accurate price signals for DSO-level resources and to coordinate with the ISO-level pricing and dispatch process.

Chapter 3 presents low-time-complexity algorithms for online T&D-coordinated market operation by developing minimum-cost flow algorithms and cutting-plane methods. In this chapter, we introduce two algorithms for addressing the ISO-DSO coordination problem, as initially presented in Chapter 1. The first algorithm focuses on solving the ISO-DSO coordination parametric programming problem without accounting for voltage constraints. The second algorithm builds on the first by dynamically incorporating voltage constraints to determine a solution that satisfies all of them. We provide mathematical proofs to demonstrate the optimality of both algorithms. Furthermore, we extend the algorithms to accommodate unbalanced three-phase systems.

Project Publications:

[1] A. N. Madavan, N. Dahlin, S. Bose, and L. Tong, "Risk-Sensitive Security-Constrained Economic Dispatch: Pricing and Algorithm Design," to appear in *IEEE Transactions on Power Systems*, doi: 10.1109/TPWRS.2025.3589590.

[2] C. Chen, S. Li and L. Tong, "Multi-Interval Energy-Reserve Co-Optimization With SoC-Dependent Bids From Battery Storage," in *IEEE Transactions on Power Systems*, vol. 40, no. 4, pp. 3008-3016, July 2025, doi: 10.1109/TPWRS.2024.3509913.

[3] A. S. Alahmed, G. Cavraro, A. Bernstein, and L. Tong, "A Decentralized Market Mechanism for Energy Communities Under Operating Envelopes," in *IEEE Transactions on Control of Network Systems*, vol. 12, no. 1, pp. 313-324, March 2025, doi: 10.1109/TCNS.2024.3466651.

[4] C. Chen, S. Bose, T. D. Mount and L. Tong, "Wholesale Market Participation of DERAs: DSO-DERA-ISO Coordination," in *IEEE Transactions on Power Systems*, vol. 39, no. 5, pp. 6605-6614, Sept. 2024, doi: 10.1109/TPWRS.2024.3352003.

[5] A. S. Alahmed and L. Tong, "Dynamic Net Metering for Energy Communities," in *IEEE Transactions on Energy Markets, Policy and Regulation*, vol. 2, no. 3, pp. 289-300, Sept. 2024, doi: 10.1109/TEMPR.2024.3354162.

[6] C. Chen, A. S. Alahmed, T. D. Mount, and L. Tong, "Competitive DER aggregation for participation in wholesale markets," in Proceedings of the 56th Hawaii International Conference on System Sciences.

[7] C. Chen, S. Bose, and L. Tong, "DSO-DERA Coordination for the Wholesale Market Participation of Distributed Energy Resources," *Proc. of IEEE Power & Energy Society General Meeting*, 2023. **(IEEE PESGM Prize Conference Paper Award)**

[8] A. S. Alahmed and L. Tong, "Resource Sharing in Energy Communities: A Cooperative Game Approach," *2024 IEEE Power & Energy Society General Meeting (PESGM)*, Seattle, WA,

USA, 2024, pp. 1-5, doi: 10.1109/PESGM51994.2024.10688636. **(IEEE PESGM Best Paper Session)**
[9] A. S. Alahmed, G. Cavraro, A. Bernstein, and L. Tong, "Network-Aware and Welfare-Maximizing Dynamic Pricing for Energy Sharing," *2024 IEEE 63rd Conference on Decision and Control (CDC)*, Milan, Italy, 2024, pp. 859-865, doi: 10.1109/CDC56724.2024.10885977.
[10] M. Mousavi and M. Wu, "Transmission and Distribution Coordination Framework Using Parametric Programming: Optimal Pricing in The Distribution Systems ," *Hawaii International Conference on System Sciences (HICSS),* 2023.
[11] Coordinating Transmission and Distribution Systems Operations for Intensive DER Integration - Part I: A Parametric Programming Framework, under review for "*IEEE Transactions on Energy Markets, Policy and Regulation*".
[12] Coordinating Transmission and Distribution Systems Operations for Intensive DER Integration - Part II: An Efficient Algorithm, under review for "*IEEE Transactions on Energy Markets, Policy and Regulation*".

Student Theses:

[1] Cong Chen, "Future Power Systems Mechanism Designs: Storage and Distributed Energy Resource Integration," Cornell University, May 2024, **(2025 IEEE PES Outstanding Doctoral Dissertation Award** and **2024 Cornell ECE Best Thesis Award.)**
[2] Ahmed Alahmed, "Integration of Distributed Energy Resources: Optimal Decisions, Mechanism Design, and Aggregations," Cornell University, August 2024.
[3] Mohammad Mousavi, "Distribution System Operator (DSO) Design for Distributed Energy Resources Market Participation", Arizona State University, May 2024.

Part I

Wholesale Market Participation of DERAs: DSO-DERA-ISO Coordination

Subhonmesh Bose

University of Illinois Urbana-Champaign

Lang Tong
Timothy D. Mount
Cong Chen, Graduate Student
Siying Li, Graduate Student

Cornell University

For information about this project, contact:

Subhonmesh Bose
University of Illinois Urbana-Champaign
boses@illinois.edu

Power Systems Engineering Research Center

The Power Systems Engineering Research Center (PSERC) is a multi-university Center conducting research on challenges facing the electric power industry and educating the next generation of power engineers. More information about PSERC can be found at the Center's website: http://www.pserc.org.

For additional information, contact:

Power Systems Engineering Research Center
Arizona State University
527 Engineering Research Center
Tempe, Arizona 85287-5706
Phone: 480-965-1643
Fax: 480-727-2052

Table of Contents

List of Figures

List of Tables

1. Introduction

The landmark ruling of the Federal Energy Regulatory Commission (FERC) Order 2222 in [1] aims to remove barriers to the direct participation of distributed energy resource aggregators (DERAs) in the wholesale market operated by independent system operators (ISOs) (or regional transmission operators). Since distributed energy resources (DERs) originate in a distribution network, aggregated DERs must pass through the distribution grid managed by a distribution system operator (DSO) that can be the distribution utility or an independent entity. A coordination mechanism among the DSO, ISO, and DERAs is necessary to ensure system reliability and open access to all DERAs. FERC Order 2222 recognizes the significance of DSO-DERA-ISO coordination while leaving the specifics of the coordination design to the regulators, market operators, and stakeholders.

DSO-DERA-ISO coordination poses significant theoretical and practical challenges. Net power injections from DERAs will likely depend on wholesale market conditions such as wholesale locational marginal prices (LMPs), real-time regulation service needs, and available behind-the-meter DERs in the distribution system. Notwithstanding these uncertainties, the DSO must ensure the reliable operation of the distribution grid, both in delivering services to all customers and allowing DERAs to offer services to the wholesale market. Moreover, any coordination mechanism must provide open and nondiscriminatory access to multiple competing DERAs operating over the same distribution network.

DSO-DERA-ISO coordination has been actively debated since the release of FERC Order 2222. In [2], coordination models have been classified into four categories, ranging from the least to the most DSO involvement. Type I models assume no DSO control (see, e.g., [3, 4]), because installed DER capacities are deemed to lie within the network's hosting capacity limits. One approach is to impose strict net injection limits [5, 6] on individual prosumers so that the system's reliability is ensured as long as the limits are respected. In Type II models, e.g., [7–9], the DSO strives to prevent constraint violations, considering the randomness of power injections from DERs. Type III models involve coordination among DERAs, DSO, and ISO, where DERAs can provide distribution grid services in addition to delivering wholesale market products (see, e.g., [10, 11]). Type IV models require DERA aggregation through the DSO, with the DSO performing all reliability functions and participating in the wholesale market on behalf of the DERAs as in [12–15].

In this paper, we develop a Type II DSO-DERA-ISO coordination mechanism aimed at achieving efficient and reliable multi-DERA aggregations without significant deviations from existing DSO and ISO/RTO interaction models. Fig. 1.1 illustrates the power, financial, and control interactions among DSO, DERA, and ISO. Our coordination approach decouples the complex DSO-DERA-ISO interactions into nearly independent, pairwise interactions. In particular, we propose a *forward auction* run by the DSO that allows DERAs to acquire *network access limits*–the right to inject or

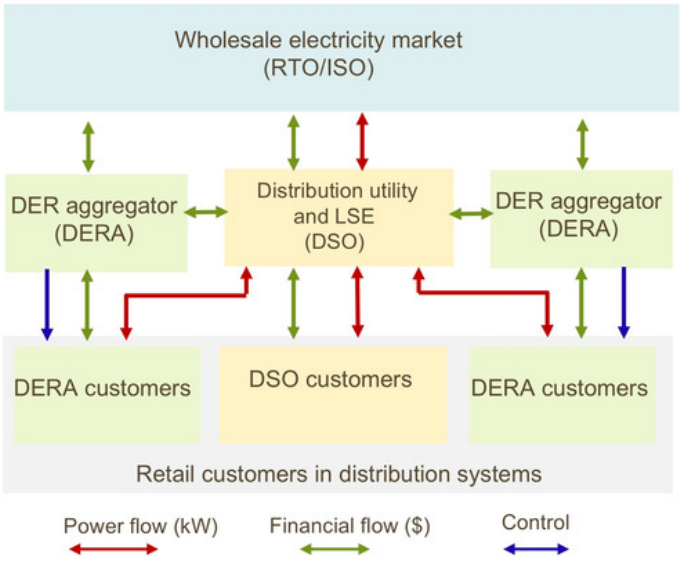

Figure 1.1: Power flow, financial flow, and control interactions in the DSO-DERA-ISO coordination model.

withdraw any amount of power within those limits over which the auction outcomes stand. These limits are auctioned off in a way that *all* power transactions from DERAs within these limits will satisfy distribution system operation constraints. Thus, DERA's wholesale market interaction with the ISO in real-time can be agnostic to these operational constraints, and ISOs can dispatch DERs without direct visibility into the distribution network. The DERA-ISO interaction can include models such as demand response, virtual storage, etc., and *any* way they choose to operate the DERs will not violate distribution network security as long as they remain within the network access limits they acquire from the DSO-operated auction. Thus, our design removes the need for DSO's interventions in ISO's real-time dispatch and DERAs' aggregation actions under normal system operating conditions.

We consider two network access allocation mechanisms. Sec. 3 presents a robust optimization-based market clearing formulation for network access, which guarantees satisfaction of network constraints when DERAs aggregate within their acquired access limits, thus removing the need for DSO to participate in real-time DERA-ISO interactions. DERAs do not even need knowledge of the underlying physical network when its aggregation strategy respects said limits.

The robust access allocation can be conservative in that it assumes the worst-case aggregation and network operating conditions. We present a risk-based stochastic allocation mechanism in Sec. 4 that allows DSO to share the common network resources subject to an acceptable risk constraint on network security violations. For both the robust and stochastic access limit auctions, we provide theoretical analyses and empirical studies to characterize and quantify access allocation properties, including the nonnegative surpluses for DSO, the benefits of participating in the access limit auction for DERAs, the behavior of access allocation prices, and a comparison of the two formulations.

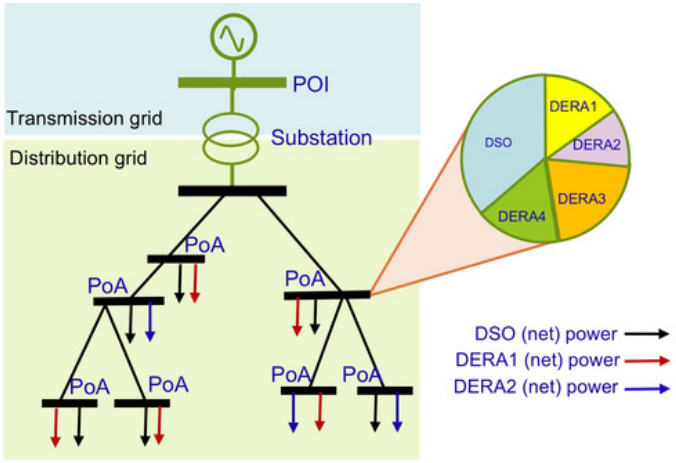

Figure 1.2: The distribution system and DER resources.

Our DSO-DERA coordination mechanism via access limits shares both parallels and important differences with two distant relatives. One is the transmission right allocation problem for participants with bilateral contracts considered in the early years of wholesale market deregulation. Allocating physical transmission rights was deemed impractical and unnecessary (see [16]) with the "loop-flow" problem in meshed transmission networks. Ultimately, wholesale markets evolved to adopt a centrally coordinated economic dispatch run by the ISO, where bilateral transactions are protected from the risks of LMP fluctuations using derivatives such as financial transmission rights. In our proposed coordination mechanisms, no central authority coordinates DERAs in real-time. Making access limit allocation *physical* allows DERAs to inject or withdraw any amount of power within their purchased access limits. The loop-flow problem does not affect our design, thanks to the radial nature of distribution networks. Also, we deliberately separate access limit allocation from real-time decisions; we envision the forward auction for access limits to run once a day or a week. We posit that tight coordination of dispatch decisions via a centralized market mechanism, matched to that operated by the ISO, may be impractical in the near-term and possibly unnecessary, owing to smaller trade volumes and less stringent system constraints in the distribution grid.

Second, our mechanism is reminiscent of the notion of operating envelopes defined by DSO-imposed net nodal DER injection and withdrawal limits. For instance, an Australian market imposes 5kW net-injection limits on residential customers with DERs [5]. Instead of using pre-determining dynamic operating envelopes as in [6, 8, 9], we auction off these envelopes among competing DERAs based on each DERA's aggregation needs and aggregation strategy.

The paper is organized as follows. We begin with the preliminaries of the network and the DSO-DERA-ISO coordination models in Sec. 2. Then, we present the robust and the stochastic network access allocation problems and their properties in Sec. 3 and Sec. 4, respectively. A simple yet illustrative example is discussed in Sec. 5. Then, we provide a numerical case study on a 141-bus distribution network in Sec. 6. Theoretical claims are proven in the appendix of [**?**].

Symbol	Meaning
$\boldsymbol{p}_0, \overline{\boldsymbol{p}}_0, \underline{\boldsymbol{p}}_0$	power injections and network accesses of DSO
$\boldsymbol{p}_k, \overline{\boldsymbol{C}}_k, \underline{\boldsymbol{C}}_k$	power injections and network accesses of DERA k
$\overline{C}_k^{\min}, \underline{C}_k^{\min}$	minimum injection/withdrawal access of DERA k
$\overline{P}^{\max}, \underline{P}^{\max}$	injection/withdrawal access limits of the network
φ_k	utility of DERA k, induced by its bid
J:	operational cost of DSO
$\boldsymbol{A}$:	network parameters for linearized power flow
$\overline{b}, \underline{b}$	limits on network voltage/power flows
K, S	total number of DERAs and scenarios

Table 1.1: Major symbols

Iteration	Step in Algorithm 1	Aggregate cost ($/h)	Run-time (in ms)
1	Step 1 to compute y^*	9897.7	113.6
1	Step 2 to compute ξ^{opt}	9910.3	99.6
2	Step 3 to compute y^*	9899.3	93.4
2	Step 4 to compute ξ^{opt}	9899.3	121.5

Table 1.2: Evolution of aggregate cost of some algorithm.

2. Network and Coordination Models

Consider K DERAs operating over a radial distribution network across N buses shown in Fig. 1.2, where bus 1 is the reference bus. Let the power injection profile from DERA k across the network be given by $\boldsymbol{p}_k \in \mathbb{R}^N$, and the total DERA net injection to the system is given by $\sum_{k=1}^{K} \boldsymbol{p}_k$. Let the power injection profile from the DSO's customers be given by $\boldsymbol{p}_0 \in \mathbb{R}^N$. Assuming a uniform power factor for all power injections, the reactive power injection profile is given by $\alpha\left(\sum_{k=1}^{K} \boldsymbol{p}_k + \boldsymbol{p}_0\right)$. This assumption simplifies our presentation but is not crucial to the design of our auctions. These real and reactive power injections then induce power flows and voltage magnitudes over the distribution network that are related via the power flow equations. In this work, we adopt a linear distribution power flow (LinDistFlow) model [17] adopted from [18]. Voltage and line capacity/thermal limits define security constraints. As explained in the appendix of [**?**], these constraints take the form,

$$\underline{\boldsymbol{b}} \leq \boldsymbol{A}\left(\sum_{k=1}^{K} \boldsymbol{p}_k + \boldsymbol{p}_0\right) \leq \overline{\boldsymbol{b}}. \tag{2.1}$$

Inequalities are interpreted element-wise.

With the linearized network model, we propose forward auctions for DSO-DERA coordination. In these auction models, the DERAs bid for injection/withdrawal *access* at various buses of the distribution network, where the DERA commands DERs from its customers; see Fig. 1.2. In Sec. 3 and Sec. 4, we describe, respectively the robust and the stochastic, optimization problems to clear the forward auctions and the settlements for the DERAs. The auctions determine the *range* of injection and withdrawal access for each DERA at each bus of the network, and the DERAs' payments to acquire those access limits. We thus design the auction of an operating envelope, where the DERA can inject/withdraw *any* amount of power from the DERs they command within this envelope that they purchase from the DSO. Thus, the real-time power of DERA stays within the limits/envelopes they purchase at the points of aggregation (PoAs) from the DSO through the proposed forward auctions. Our network model contains buses at the PoAs, but we do not model individual customers/DERs downstream from the PoAs. Transactions between a DERA and the ISO occur at the point of interconnection (PoI).

Our auctions for network access are hosted ahead of real-time operations–it can be a few hours to a week in advance of power delivery. To participate, all DERAs must submit their bids/offers to this forward auction and they are cleared simultaneously. Through this auction, DERAs get access to limits/capacities that they must obey during real-time operations. Since the auction outcome binds over multiple real-time interactions, we account for the range of possible operating conditions through robust and stochastic programming based auction-clearing formulations.

3. The Robust Auction Model

We now design an auction for network access that accounts for a variety of real-time operating conditions through a robust optimization formulation. Specifically, let $\underline{\boldsymbol{C}}_k \in \mathbb{R}^N$ and $\overline{\boldsymbol{C}}_k \in \mathbb{R}^N$ denote the vectors of (real) power withdrawal and injection capacity limits acquired by DERA k. Then, all power injections from assets controlled by DERA k must respect $\boldsymbol{p}_k \in [-\underline{C}_k, \overline{C}_k]$. Let the DSO's own customers have net power injections $\boldsymbol{p}_0$ that take values in the set $[-\underline{p}_0, \overline{p}_0]$. Given these ranges of the various power injections, the DSO solves,

$$
\begin{aligned}
\underset{\underline{C},\overline{C},\overline{P},\underline{P}}{\text{maximize}} \quad & \sum_{k=1}^{K} \varphi_k(\underline{C}_k, \overline{C}_k) - J(\overline{\boldsymbol{P}}, \underline{\boldsymbol{P}}), && \text{(3.1a)}\\
\text{subject to} \quad & \overline{C}_k^{\min} \le \overline{C}_k, \;\; \underline{C}_k^{\min} \le \underline{C}_k, && \text{(3.1b)}\\
& \overline{P} \le \overline{P}^{\max}, \;\; \underline{P} \le \underline{P}^{\max}, && \text{(3.1c)}\\
& \overline{P} = \sum_{k=1}^{K} \overline{C}_k + \overline{p}_0, && \text{(3.1d)}\\
& \underline{P} = \sum_{k=1}^{K} \underline{C}_k + \underline{p}_0, && \text{(3.1e)}\\
& \underline{b} \le \boldsymbol{A}\left(\sum_{k=1}^{K} \boldsymbol{p}_k + \boldsymbol{p}_0\right) \le \overline{b}, && \text{(3.1f)}\\
& \text{for all } \boldsymbol{p}_k \in [-\underline{C}_k, \overline{C}_k], \boldsymbol{p}_0 \in [-\underline{p}_0, \overline{p}_0], && \text{(3.1g)}\\
& \text{for } k = 1, \ldots, K.
\end{aligned}
$$

Here, DERA k provides the bid $\varphi_k : \mathbb{R}^{2N} \to \mathbb{R}$ to the DSO, where $\varphi_k(\underline{\boldsymbol{C}}_k, \overline{\boldsymbol{C}}_k)$ represents DERA k's willingness to pay for power transactions. Bid/offer construction for φ_k depends on the DERA's aggregation strategy; we refer to our work in [19] for a candidate construction. Let $\overline{\boldsymbol{P}} \in \mathbb{R}^N$ and $\underline{\boldsymbol{P}} \in \mathbb{R}^N$ represent the vectors of the total injection and withdrawal capacities, respectively. Also, define $\overline{C} := (\overline{C}_k), \underline{C} := (\underline{C}_k)$ as the matrices that collect the access limits across the K DERAs. The operational cost of the DSO is encoded in $J : \mathbb{R}^{2N} \to \mathbb{R}$ that is assumed to be convex and non-decreasing. Being a regulated monopoly running the distribution grid, we anticipate that J will include the cost of reactive power support, network maintenance, line losses, etc. required to maintain quality of service to existing retail customers. See [20] for example cost component constructions. The objective function then represents the induced social surplus from DERAs' bids and DSO's costs. Let φ_k be concave and non-decreasing for each k. Additionally, $(\overline{C}_k^{\min}, \underline{C}_k^{\min})$ are the vectors of minimum injection and withdrawal capacities that DERA k is willing to acquire across the network, and $(\overline{P}^{\max}, \underline{P}^{\max})$ are the vectors of the maximum injection and withdrawal capacities across the network. All capacity limits are assumed nonnegative. Equations (3.1b) and (3.1c) encode the DERAs' minimum access requirements and the DSO's maximum access limits,

respectively. Equations (3.1d) and (3.1e) define the total injection and withdrawal accesses in terms of DSO's access limits and those sold to individual DERAs. With the linearized network model in (2.1), the relations in (3.1f) and (3.1g) enforce the engineering constraints of the grid for *every possible* power injection profile from the DSO's customers and those of all DERAs within their acquired capacities.

The formulation in (3.1) contains robust constraint enforcement in (3.1f)-(3.1g), but it admits a reformulation as a classic convex program that we present next. The result requires additional notation. For any scalar z, define $z_+ := \max\{z, 0\}$ and $z_- := z_+ - z$. Define the same for a matrix/vector, where the operations are carried element-wise.

Lemma 1. *Problem* (3.1) *is equivalent to*

$$\begin{aligned}
&\underset{\underline{C},\overline{C},\overline{P},\underline{P}}{\textit{maximize}} && \sum_{k=1}^{K} \varphi_k(\underline{C}_k, \overline{C}_k) - J(\overline{\boldsymbol{P}}, \underline{\boldsymbol{P}}), && \text{(3.2a)}\\
&\textit{subject to} && \textit{for } k = 1, \dots, K, \\
&\overline{\boldsymbol{\eta}}, \underline{\boldsymbol{\eta}}: && \overline{C}_k^{min} \le \overline{C}_k, \;\; \underline{C}_k^{min} \le \underline{C}_k, && \text{(3.2b)}\\
&\overline{\boldsymbol{\omega}}, \underline{\boldsymbol{\omega}}: && \overline{P} \le \overline{P}^{max}, \;\; \underline{P} \le \underline{P}^{max}, && \text{(3.2c)}\\
&\overline{\boldsymbol{\lambda}}: && \overline{P} = \sum_{k=1}^{K} \overline{C}_k + \overline{p}_0, && \text{(3.2d)}\\
&\underline{\boldsymbol{\lambda}}: && \underline{P} = \sum_{k=1}^{K} \underline{C}_k + \underline{p}_0, && \text{(3.2e)}\\
&\overline{\boldsymbol{\mu}}: && \boldsymbol{A}_+ \overline{\boldsymbol{P}} + \boldsymbol{A}_- \underline{\boldsymbol{P}} \le \overline{b}, && \text{(3.2f)}\\
&\underline{\boldsymbol{\mu}}: && \underline{b} \le -\boldsymbol{A}_+ \underline{\boldsymbol{P}} - \boldsymbol{A}_- \overline{\boldsymbol{P}}. && \text{(3.2g)}
\end{aligned}$$

We remark that for the linear power flow model developed in the appendix of [**?**], $\boldsymbol{A} = \boldsymbol{A}_+$ and $\boldsymbol{A}_- = \boldsymbol{0}$. Our auction mechanism and its properties hold more generally for any linear approximation to power flow equations, and hence, we present our results with a more general $\boldsymbol{A}$. Associate Lagrange multipliers with the various constraints in (3.2) as shown. We now introduce the prices that will define the settlements with the DERAs using the *optimal* Lagrange multipliers (indicated with $\star$) for (3.2).

Definition 1 (LMAP-R)**.** *For the robust access allocation problem* (3.2)*, the locational marginal access price for access limits to the distribution network is defined by the vector of optimal dual solutions* $\overline{\boldsymbol{\lambda}}^\star \in \mathbb{R}^N, \underline{\boldsymbol{\lambda}}^\star \in \mathbb{R}^N$ *of* (3.2)*.*

Specifically, the injection and the withdrawal access price at bus i are given by $\overline{\lambda}^{(i)}$ and $\underline{\lambda}^{(i)}$, respectively. With these prices, for obtaining injection and withdrawal access of $\overline{\boldsymbol{C}}_k$ and $\underline{\boldsymbol{C}}_k$, respectively,

DERA k pays

$$\mathscr{P}_k(\overline{C}_k^\star, \underline{C}_k^\star) = \overline{\boldsymbol{\lambda}}^{\star\mathsf{T}}\overline{C}_k^\star + \underline{\boldsymbol{\lambda}}^{\star\mathsf{T}}\underline{C}_k^\star \tag{3.3}$$

to the DSO. Having derived the prices from an auction that is reminiscent of the economic dispatch problem solved by RTO/ISO in wholesale electricity markets, LMAP-R shares strong parallels with locational marginal prices (LMPs). For example, LMAP-R is nodally uniform. That is, all DERAs pay the same injection and withdrawal access price at a specific distribution bus. These prices, however, may differ across locations in the distribution network.

The second parallel between LMAP-R and LMP comes from the interpretations of these prices as sensitivities of the optimal objective function value of the market clearing problem to nodal parameters. For LMPs, the price of a bus equals the sensitivity of the optimal power procurement costs to nodal demands. For LMAP-R, it is the sensitivity of the induced social welfare $\mathscr{W}$ to DSO's own access limits $\overline{\boldsymbol{p}}_0$, $\underline{\boldsymbol{p}}_0$. More precisely, define the optimal social welfare from the optimal value of (3.2) as $\mathscr{W}^\star(\overline{\boldsymbol{p}}_0, \underline{\boldsymbol{p}}_0)$. Then, envelope theorem, per [21, Chapter 7], states that when $\mathscr{W}^\star$ is differentiable,

$$\overline{\boldsymbol{\lambda}}^\star = -\nabla_{\overline{\boldsymbol{p}}_0}\mathscr{W}^\star(\overline{\boldsymbol{p}}_0, \underline{\boldsymbol{p}}_0),\ \underline{\boldsymbol{\lambda}}^\star = -\nabla_{\underline{\boldsymbol{p}}_0}\mathscr{W}^\star(\overline{\boldsymbol{p}}_0, \underline{\boldsymbol{p}}_0), \tag{3.4}$$

which represents the marginal decrease in social welfare when supporting network access by DSO rather than selling access to DERAs. We further shed light on the contributions of network parameters to LMAP-Rs in our next result.

Proposition 1. *LMAP-R satisfies*

$$\begin{aligned}
\overline{\boldsymbol{\lambda}}^\star &= \nabla_{\overline{\boldsymbol{P}}} J(\overline{\boldsymbol{P}}^\star, \underline{\boldsymbol{P}}^\star) + \boldsymbol{A}_+^\mathsf{T}\overline{\boldsymbol{\mu}}^\star + \boldsymbol{A}_-^\mathsf{T}\underline{\boldsymbol{\mu}}^\star + \overline{\boldsymbol{\omega}}^\star, \\
\underline{\boldsymbol{\lambda}}^\star &= \nabla_{\underline{\boldsymbol{P}}} J(\overline{\boldsymbol{P}}^\star, \underline{\boldsymbol{P}}^\star) + \boldsymbol{A}_-^\mathsf{T}\overline{\boldsymbol{\mu}}^\star + \boldsymbol{A}_+^\mathsf{T}\underline{\boldsymbol{\mu}}^\star + \underline{\boldsymbol{\omega}}^\star.
\end{aligned} \tag{3.5}$$

The first term in (3.5) equals the DSO's marginal cost for disseminating access limits at the optimum of (3.2). Our result then characterizes the price markup in LMAP-R above said marginal cost. Specifically, if voltage and line constraints are non-binding, and the access allocations do not reach the injection limits, the remaining terms in $\overline{\boldsymbol{\lambda}}^\star, \underline{\boldsymbol{\lambda}}^\star$ vanish. In addition, if DSO's operational cost structure is additive and uniform across the buses of the distribution network, then LMAP-Rs become equal at all buses. The tighter the constraints on total access limits being auctioned (encoded in the entries of $\overline{P}^{\max}$, $\underline{P}^{\max}$) are, and the more stringent the network constraints (represented in the entries of $\overline{\boldsymbol{b}}$, $\underline{\boldsymbol{b}}$) are, we expect LMAP-Rs to differ from DSO's marginal costs.

Next, we investigate DSO's and the DERAs' surplus at an optimal robust access allocation. Define DSO's surplus as

$$\Pi^{\text{DSO}} := \sum_{k=1}^{K} \mathscr{P}_k(\overline{C}_k^\star, \underline{C}_k^\star) - \left(J(\overline{\boldsymbol{P}}^\star, \underline{\boldsymbol{P}}^\star) - J(\overline{p}_0, \underline{p}_0)\right). \tag{3.6}$$

The first term equals the total rent that the DSO collects from the DERAs. The second summand equals the cost that the DSO affords when allowing DERAs to operate over the distribution network. Specifically, $J(\overline{\boldsymbol{P}}^\star, \underline{\boldsymbol{P}}^\star)$ equals the cost of the net injection and withdrawal access $\overline{\boldsymbol{P}}^\star, \underline{\boldsymbol{P}}^\star$ when the DSO provides the network accesses for DERAs and itself, and $J(\overline{p}_0, \underline{p}_0)$ equals the operational cost for access required to support the DSO's customers alone. Thus, the last summand in (3.6) measures the cost of the DSO when supporting the network accesses to the DERAs. Next, define DERA k's surplus as

$$\Pi_k^{\text{DERA}} := \varphi_k(\underline{C}_k, \overline{C}_k) - \mathscr{P}_k(\overline{C}_k^\star, \underline{C}_k^\star), \tag{3.7}$$

which equals the induced utility (inferred from the bid) minus the payment to the DSO.

Proposition 2. *(i)* $\Pi^{DSO} \geq 0$*, (ii)* $\Pi_k^{DERA} \geq 0$*, if* $\varphi_k(\mathbf{0}, \mathbf{0}) \geq 0$ *and one of the following two conditions holds: (a)* $\overline{C}_k^{min} = \mathbf{0}, \underline{C}_k^{min} = \mathbf{0}$*, or (b) the constraints in* (3.2b) *are non-binding at optimality, i.e.,* $\overline{C}_k^\star > \overline{C}_k^{min}, \underline{C}_k^\star > \underline{C}_k^{min}$.

The last result suggests that DSO always gains from running the auction in that its surplus is nonnegative. For DERAs, nonnegative surplus is assured under certain sufficient conditions. Among these conditions, $\varphi_k(\mathbf{0}, \mathbf{0}) \geq 0$ is natural as one expects the inferred utility of DERA to be nonnegative for any nonnegative value of the access limits.

The condition $\overline{\boldsymbol{C}}_k = \underline{\boldsymbol{C}}_k = 0$ indicates that DERA k may obtain zero network access limits at some buses. Such a condition is violated when the DERA may require a minimum demand to be met or net injection cannot be curtailed beyond a threshold. In such an event, the DERA may need side-payments to make the auction outcome favorable for its participation. The design and discussion of side-payments are relegated to a future effort. We remark that this phenomenon is reminiscent of the challenge in wholesale markets where minimum generation constraints can negate a generator's rationale for market participation. Additionally, we expect the lower bounds $\overline{C}_k^{\min}, \underline{C}_k^{\min}$ to be non-binding for DERAs that are *marginal* to the auction, i.e., when their marginal implied costs define the prices.

Our next result sheds light on how LMAP-Rs behave along the distribution feeder. Unlike our last two results, the next one specifically utilizes the power flow model presented in the appendix of [**?**]. To present the result, we need additional notation. We say bus n is an *ancestor* of bus m in the distribution network if n lies on the unique (undirected) path from the reference bus to bus m.

Proposition 3. *When J is linear and homogeneous across buses* ($J(\overline{\boldsymbol{P}}, \underline{\boldsymbol{P}}) = \sum_{i=1}^N \overline{J} \cdot \overline{P}^{(i)} + \sum_{i=1}^N \underline{J} \cdot \underline{P}^{(i)}$) *and the constraints in* (3.2c) *are non-binding at all buses, then* $\overline{\lambda}^{(n)\star} \geq \overline{\lambda}^{(m)\star}$ *and* $\underline{\lambda}^{(n)\star} \geq \underline{\lambda}^{(m)\star}$*, if bus n is an ancestor of bus m.*

Said differently, LMAP-Rs do not decrease along the network away from the substation under certain conditions. Our numerical experiments reveal that these conditions are only sufficient for price monotonicity; the monotonic trend holds even when these conditions are not met. Such

a price monotonicity reveals that it is costlier to guarantee the voltage limits and line capacity limits for the leaf buses, compared to those closer to the substation. The non-binding nature of the constraints is only *sufficient* for the conclusion to hold; our simulations will show that they are *not* necessary.

4. The Stochastic Auction Design

The robust access allocation requires the network constraints to be satisfied for *all possible* injections from DERAs' and the DSO's customers. Naturally, the resulting allocations are dictated by the worst-case power injection/withdrawal combinations during the forward auction and fully ignore the statistics of network usage. Such an approach inherently limits the DERAs' collective network access. We present in this section a risk-based stochastic allocation mechanism that allows *controlled violation* of the network constraints in the access allocation auction in a way that accounts for the statistics of power transactions by DSO's customers. Stochastic resource allocation with controlled violation is common in many areas, especially in computer systems and communication networks, where the resources are constrained and usage patterns are random, especially over time. Such an allocation builds on the premise that random usage patterns often do not overlap, and this time-multiplexing allows higher access limits to be accommodated than the roubust counterpart Notice that we allow for possible controlled violations only in the forward auction. Said violations in the auction do not amount to actual violations in real time. In practice, DSO can implement mechanisms to curtail access to enforce reliability constraints in real-time; we side-step such considerations and purely focus on the merits of a stochastic forward auction.

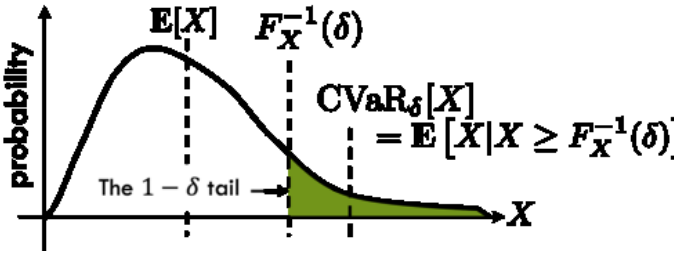

Figure 4.1: CVaR of a random variable X.

When the power transactions by DSO's customers are considered random, the power flows and the bus voltages become random quantities. In the forward auction, we limit the *risk* of constraint violations, where we measure this risk via the conditional value at risk (CVaR) measure. CVaR, analyzed and popularized by [22, 23], has recently been advocated in power system planning, e.g., in [24]. For a random variable (think loss) X with smooth cumulative distribution function F_X, CVaR at level $\delta \in [0,1)$ equals the conditional mean of X over the $(1-\delta)$-tail of the distribution (see Figure 4.1).

For power flows over a certain distribution line, CVaR_δ measures the average value among the top $1-\delta$ fraction of the largest power flow values. Thus, by constraining the $\text{CVaR}_{0.99}$ value of the line flow below a threshold $\overline{b}$, for example, implies that not only 99% of the power flows are below $\overline{b}$, but also the average power flow among the worst (largest) 1% is below $\overline{b}$. In other words, the CVaR-based constraint restricts both the probability and the extent of the line limit violation.

Following [23], CVaR is defined as

$$\mathrm{CVaR}_{\delta}[X] := \underset{t\in\mathbb{R}}{\text{minimize}} \left\{ t + \frac{1}{1-\delta}\mathbb{E}[X-t]_{+} \right\} \tag{4.1}$$

for random variables X with general distributions.

Given the distribution of $\boldsymbol{p}_0$, the risk-aware access limit auction becomes,

$$\begin{aligned}
\underset{\underline{C},\overline{C}}{\text{maximize}} \quad & \sum_{k=1}^{K} \varphi_k(\underline{C}_k, \overline{C}_k) - \mathbb{E}[J(\overline{\boldsymbol{P}}, \underline{\boldsymbol{P}})], && \text{(4.2a)}\\
\text{subject to} \quad & (3.1\text{b}) - (3.1\text{e}), \\
& \mathrm{CVaR}_{\delta}[\boldsymbol{A}(\sum_{k=1}^{K} \boldsymbol{p}_k + \boldsymbol{p}_0)] \le \overline{b}, && \text{(4.2b)}\\
& \mathrm{CVaR}_{\delta}[-\boldsymbol{A}(\sum_{k=1}^{K} \boldsymbol{p}_k + \boldsymbol{p}_0)] \le -\underline{b}, && \text{(4.2c)}\\
& \text{for all } \boldsymbol{p}_k \in [-\underline{C}_k, \overline{C}_k], \text{for } k = 1, ..., K.
\end{aligned}$$

Compared to the robust network model in (3.1), the risk-constrained mechanism differs in three aspects. First, $\overline{\boldsymbol{P}}, \underline{\boldsymbol{P}}$ in this formulation is random, and hence, (3.1c) imposes the upper bounds for all possible values of $\boldsymbol{p}_0$. Second, we consider the DSO's *expected* operational cost to serve the random $\overline{\boldsymbol{P}}, \underline{\boldsymbol{P}}$ in the objective function. In effect, we maximize the average induced social surplus. Third, and most importantly, we impose CVaR constraints on network limit violations in (4.2b) and (4.2c) for all possible values of injections/withdrawals from assets controlled by DERAs within their acquired access limits. These constraints are such that for *any* power transactions by DERAs within their access limits, they limit network constraint violation probabilities below $1-\delta$ and ensure that the average magnitude of those risky power flows/voltages remains within the specified limits. By imposing the constraint for all $\boldsymbol{p}_k \in [-\underline{C}_k, \overline{C}_k]$, this formulation inherits the benefits of decoupled DERA-DSO operations from the robust formulation. Specifically, any real-time DERA-ISO contract within the DERA's acquired limit imposes at most a pre-defined level of security risk to the distribution network. Said risk stems from the uncertainty in power transactions from DSO's customers alone for which they typically have statistics from historical data.

Next, we present a scenario-approach to approximate (4.2). Consider S independent and identically distributed samples $\boldsymbol{p}_0[1], \ldots, \boldsymbol{p}_0[S]$ for the injection of DSO's customers $\boldsymbol{p}_0$. Using (4.1) and replacing all expectations with empirical means over S samples, we arrive at the following optimization program for stochastic access allocation. The detailed derivation is relegated to the appendix of [**?**].

$$\underset{\substack{\overline{C},\underline{C},\overline{P}[s],\underline{P}[s],\\ \bar{t},\underline{t},\underline{\gamma}[s],\overline{\gamma}[s]}}{\text{maximize}} \quad \sum_{k=1}^{K} \varphi_k(\underline{C}_k,\overline{C}_k) - \frac{1}{S}\sum_{s=1}^{S} J(\overline{\boldsymbol{P}}[s],\underline{\boldsymbol{P}}[s]), \tag{4.3a}$$

$$\text{such that} \quad \text{for } k=1,\ldots,K,\ s=1,\ldots,S,$$

$$\overline{\boldsymbol{\eta}},\underline{\boldsymbol{\eta}}: \quad \overline{C}_k^{\min} \le \overline{C}_k,\ \underline{C}_k^{\min} \le \underline{C}_k, \tag{4.3b}$$

$$\overline{\boldsymbol{\omega}}[s],\underline{\boldsymbol{\omega}}[s]: \quad \overline{P}[s] \le \overline{P}^{\max},\ \underline{P}[s] \le \underline{P}^{\max}, \tag{4.3c}$$

$$\overline{\boldsymbol{\lambda}}[s]: \quad \overline{P}[s] = \sum_{k=1}^{K} \overline{C}_k + \boldsymbol{p}_0[s], \tag{4.3d}$$

$$\underline{\boldsymbol{\lambda}}[s]: \quad \underline{P}[s] = \sum_{k=1}^{K} \underline{C}_k - \boldsymbol{p}_0[s], \tag{4.3e}$$

$$\overline{\boldsymbol{\beta}}[s]: \quad \boldsymbol{A}_+\overline{P}[s] + \boldsymbol{A}_-\underline{P}[s] - \overline{b} - \bar{t} \le \overline{\gamma}[s], \tag{4.3f}$$

$$\overline{\boldsymbol{\alpha}}[s]: \quad \mathbf{0} \le \overline{\gamma}[s], \tag{4.3g}$$

$$\overline{\boldsymbol{\mu}}: \quad \bar{t} + \frac{1}{1-\delta}\frac{1}{S}\sum_{s=1}^{S} \overline{\gamma}[s] \le \mathbf{0}, \tag{4.3h}$$

$$\underline{\boldsymbol{\beta}}[s]: \quad \boldsymbol{A}_-\overline{P}[s] + \boldsymbol{A}_+\underline{P}[s] + \underline{b} - \underline{t} \le \underline{\gamma}[s], \tag{4.3i}$$

$$\underline{\boldsymbol{\alpha}}[s]: \quad \mathbf{0} \le \underline{\gamma}[s], \tag{4.3j}$$

$$\underline{\boldsymbol{\mu}}: \quad \underline{t} + \frac{1}{1-\delta}\frac{1}{S}\sum_{s=1}^{S} \underline{\gamma}[s] \le \mathbf{0}. \tag{4.3k}$$

Sample average approximations for such stochastic programs are known to become more accurate with growing number of samples, as [25] suggests. Thus, the solution of (4.3) should approach that of (3.2) as $S \to \infty$. One expects that when $\delta \uparrow 1$, the stochastic model constraints (4.3f)-(4.3k) roughly approximate network security constraints (3.2f)-(3.2g) from the robust auction model. Per our experiments, even with $\delta = 0.99$, the resulting social welfare can be significantly higher than from the robust auction ($\sim$20%), upon tolerating only 1% network security constraint violation risk at a few buses.

To define the settlement mechanism from the above auction, associate Lagrange multipliers with the constraints in (4.3) as shown and denote optimal values of variables with ($\star$).

Definition 2 (LMAP-S)**.** *For the stochastic allocation mechanism, the locational marginal access prices for injection and withdrawal access limits to the distribution network are defined by the vectors* $\overline{\boldsymbol{\Lambda}}^\star := \sum_{s=1}^{S} \overline{\boldsymbol{\lambda}}^\star[s] \in \mathbb{R}^N$ *and* $\underline{\boldsymbol{\Lambda}}^\star := \sum_{s=1}^{S} \underline{\boldsymbol{\lambda}}^\star[s] \in \mathbb{R}^N$*, respectively, obtained from the optimal Lagrange multipliers* $\overline{\boldsymbol{\lambda}}^\star[s], \underline{\boldsymbol{\lambda}}^\star[s]$ *of* (4.3)*.*

With LMAP-S, DERA k's payment to the DSO is given by

$$\tilde{\mathscr{P}}_k(\overline{C}_k^\star,\underline{C}_k^\star) = \overline{\boldsymbol{\Lambda}}^{\star\mathsf{T}}\overline{C}_k^\star + \underline{\boldsymbol{\Lambda}}^{\star\mathsf{T}}\underline{C}_k^\star. \tag{4.4}$$

$$\begin{aligned}\overline{\Lambda}^{\star} &= \sum_{s=1}^{S} \tfrac{1}{S} \nabla_{\overline{\boldsymbol{P}}[s]} J(\overline{\boldsymbol{P}}^{\star}[s], \underline{\boldsymbol{P}}^{\star}[s]) + \sum_{s=1}^{S} \left(\boldsymbol{A}_{+}^{\intercal} \overline{\boldsymbol{\beta}}^{\star}[s] + \boldsymbol{A}_{-}^{\intercal} \underline{\boldsymbol{\beta}}^{\star}[s] + \overline{\boldsymbol{\omega}}^{\star}[s] \right), \\ \underline{\Lambda}^{\star} &= \sum_{s=1}^{S} \tfrac{1}{S} \nabla_{\underline{\boldsymbol{P}}[s]} J(\overline{\boldsymbol{P}}^{\star}[s]), \underline{\boldsymbol{P}}^{\star}[s]) + \sum_{s=1}^{S} \left(\boldsymbol{A}_{+}^{\intercal} \underline{\boldsymbol{\beta}}^{\star}[s] + \boldsymbol{A}_{-}^{\intercal} \overline{\boldsymbol{\beta}}^{\star}[s] + \underline{\boldsymbol{\omega}}^{\star}[s] \right).\end{aligned} \tag{4.7}$$

These locational prices are dependent on the forecast scenarios but are uniform at each distribution bus. DERA k's induced surplus in the stochastic auction equals

$$\tilde{\Pi}_k^{\text{DERA}} = \varphi_k(\underline{C}_k^{\star}, \overline{C}_k^{\star}) - \tilde{\mathscr{P}}_k(\overline{C}_k^{\star}, \underline{C}_k^{\star}) \tag{4.5}$$

$\mathbb{E}[X]$ and the DSO's sample average surplus equals

$$\begin{aligned}\tilde{\Pi}^{\text{DSO}} := &\sum_{k=1}^{K} \mathscr{P}_k(\overline{C}_k^{\star}, \underline{C}_k^{\star}) \\ &- \frac{1}{S} \sum_{s=1}^{S} (J(\overline{\boldsymbol{P}}^{\star}[s], \underline{\boldsymbol{P}}^{\star}[s]) - J(\overline{p}_0[s], \underline{p}_0[s])).\end{aligned} \tag{4.6}$$

With this notation, we now present the properties of the stochastic allocation in the next result.

Proposition 4. *The following statements hold for the stochastic network access allocation* (4.3)*:*

(a) LMAP-S satisfies (4.7)*.*

(b) $\tilde{\Pi}^{DSO} \geq 0$*.*

(c) $\tilde{\Pi}_k^{DERA} \geq 0$*, if* $\varphi_k(\mathbf{0}, \mathbf{0}) \geq 0$ *and one of the following two conditions holds: (a)* $\overline{C}_k^{min} = \mathbf{0}, \underline{C}_k^{min} = \mathbf{0}$*, or (b) the constraints in* (4.3b) *are non-binding at optimality, i.e.,* $\overline{C}_k^{\star} > \overline{C}_k^{min}, \underline{C}_k^{\star} > \underline{C}_k^{min}$*.*

(d) When J is linear and homogeneous across buses ($J(\overline{\boldsymbol{P}}[s], \underline{\boldsymbol{P}}[s]) = \sum_{i=1}^{N} \overline{J} \cdot \overline{P}^{(i)}[s] + \sum_{i=1}^{N} \underline{J} \cdot \underline{P}^{(i)}[s]$*) and the constraints in* (4.3c) *are non-binding at all buses and scenarios, then* $\overline{\Lambda}^{(n)\star} \geq \overline{\Lambda}^{(m)\star}$ *and* $\underline{\Lambda}^{(n)\star} \geq \underline{\Lambda}^{(m)\star}$*, if bus n is an ancestor of bus m.*

Overall, this result shows that the stochastic auction outcome behaves similarly to the robust counterpart recorded in Propositions 1-3. Specifically, LMAP-S admits a sensitivity interpretation and is monotonic along the distribution feeder under similar sufficient conditions as LMAP-R. The resulting settlement covers DSO's operating cost (on average) and DERAs have nonnegative surpluses under similar sufficient conditions as the robust auction.

5. An Illustrative Example

We illustrate the properties of our access allocation mechanisms via a 4-bus network example with two different DERAs operating at two of the buses as shown in the right of Fig. 5.1. The bids of the DERAs and the DSO's cost is shown in the left of Fig. 5.1. Capacity limits for lines 2-3, 2-4, and 1-2 are taken as 1,1,2 (p.u.), respectively. The minimum access requirements of DERAs are zero, *i.e.,* $\overline{C}_k^{\min} = \mathbf{0}, \underline{C}_k^{\min} = \mathbf{0}$, for $k = 1, 2$, and the maximum access available is $\overline{P}^{\max} = 1$ p.u., $\underline{P}^{\max} = 1$ p.u. over all buses. DSO's customers have injections ranging over $[-0.15, 0.15]$ p.u. at all buses. We ignore voltage constraints for simplicity. For the stochastic model, we set $\delta = 0.9$ and draw 2000 scenarios for $\boldsymbol{p}_0$ for which each entry is i.i.d. truncated normal distributions with mean zero and standard deviation (σ) of 0.05 over $[-0.15, 0.15]$, all in per units.

$$\varphi_1 := -100[\underline{C}_1^{(3)}]^2 + 580\underline{C}_1^{(3)} + 126,$$
$$\varphi_2 := -100[\overline{C}_2^{(4)}]^2 + 420\overline{C}_2^{(4)} + 676,$$
$$J := 96\sum_{i=1}^{4}(\overline{P}^{(i)} + \underline{P}^{(i)}).$$

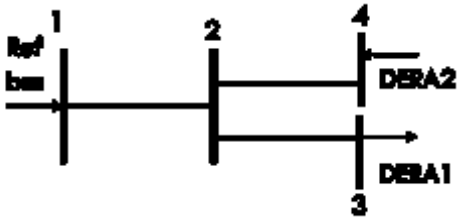

Figure 5.1: A 4-bus distribution network example.

Results from the robust and stochastic auction mechanisms are included in Tables 5.1 and 5.2. As Table 5.1 reveals, LMAP-R and LMAP-S along the bus-sequences 1-2-3 and 1-2-4 increase, aligned with the conclusions of Propositions 3 and 4. The surpluses of the DERAs and the DSO in Table 5.2 are non-negative and hence, align with the results of Propositions 2 and 4. Notice that compared to the robust allocation model, the stochastic allocation yields lower access prices,

Allocation	Parameter	Bus 1	Bus 2	Bus 3	Bus 4
Robust	$\underline{C}_1^{(i)\star}$	0	0	0.85	0
	$\underline{\lambda}^{(i)\star}$	96	96	410	96
	$\overline{C}_2^{(i)\star}$	0	0	0	0.85
	$\overline{\lambda}^{(i)\star}$	96	96	96	250
Stoch ($\delta = 0.9$)	$\underline{C}_1^{(i)\star}$	0	0	0.91	0
	$\underline{\Lambda}^{(i)\star}$	96	96	397.18	96
	$\overline{C}_2^{(i)\star}$	0	0	0	0.91
	$\overline{\Lambda}^{(i)\star}$	96	96	96	237.16

Table 5.1: Access allocation result for the 4-bus example

Allocation	DERA_1	DSO	DERA_2	Social Surplus
Robust	198.25	282.6	748.25	1229.1
Stoch ($\delta = 0.90$)	209.51	404.36	759.61	1373.48

Table 5.2: Surplus distribution for the 4-bus example

higher allocations to DERAs, and higher surpluses for the DERAs and the DSO. In effect, tolerating a small security risk yields less conservative allocations supported by lower prices and higher social surplus. In practice, one should set the risk tolerances based on exhaustive simulations for which observed real-time violations of security constraints are deemed acceptable.

6. Case Study on a 141-Bus Network

We consider a 141-bus radial distribution network from [26] with 4 DERAs that aggregate households at different buses with different levels of behind-the-meter distributed generation (BTM DG). Simulations were performed on a personal computer with Intel(R) Xeon(R) Gold 6230R CPU @ 2.10GHz and 256 GB RAM. We used YALMIP [27] with Gurobi 10.0.0 [28] on MATLAB R2021a to solve the optimization problems. The robust auction took <1s; the stochastic model with 500 scenarios took <5min and with 1500 scenarios took <1hr.

Network parameters for this system, including the resistance, reactance, topology, and base values, were adopted from [26, 29]. The base value for voltage was 12.47kV and for power was 10MW. We assumed a fixed power factor of 0.98 lagging across all buses and set the line flow limits to be 20MW for all branches. The BTM DG for households under DERAs 1, 2, 3, and 4 were set to 0.2kW, 1.2kW, 3.2kW, and 4.2kW, respectively. DERAs 1-3 aggregated resources from all buses and DERA 4 only aggregated over buses 118-134. The bid-in utility function φ_k of DERA_k is assumed to equal the sum of $\varphi_k^{(i)}$ for each bus i, where DERA_k operates; $\varphi_k^{(i)}$'s are reported in Table 6.1. The derivation of $\varphi_k^{(i)}$ is relegated to part II of this paper series; a short explanation is included in the appendix of [**?**]. Minimal access limits for the DERAs are assumed uniform across all buses, values for which are in Table 6.1. DSO's operational cost is assumed to be the sum of quadratics, $\frac{1}{2}bx^2 + ax$ with $a = \$0.009/\text{kWh}, b = \$0.0005/(\text{kWh})^2$ for both the injection and withdrawal access at all buses.

Power injection $p_0^{(i)}$ from the DSO's customer at each bus i was sampled from independent truncated normal distributions with mean $\mu = 5\text{kW}$, standard deviation σ, truncated to $[\underline{p}_0^{(i)}, \overline{p}_0^{(i)}] = [\mu - 3\sigma, \mu + 3\sigma]$. We used these intervals for the robust allocation model, but utilized 1500 random samples within said intervals for the stochastic allocation results.

DERA k	$\varphi_k^{(i)}$	$\underline{C}_k^{\min}$ (kW)	$\overline{C}_k^{\min}$ (kW)
1	$-0.1[\underline{C}^{(i)}]^2 + 2.8\underline{C}^{(i)} - 1.655$	4.1	0
2	$-0.1[\underline{C}^{(i)}]^2 + 1.8\underline{C}^{(i)} + 1.513$	0	0
3	$-0.1[\overline{C}^{(i)}]^2 + 0.2\overline{C}^{(i)} + 7.393$	0	0
4	$-0.1[\overline{C}^{(i)}]^2 + 1.2\overline{C}^{(i)} + 2.833$	0	0

Table 6.1: Bid-in utility function and minimum network withdrawal/injection limits for DERAs at each bus

6.1 Running the Robust Access Allocation

The access allocation results for the 4 DERAs under different σ are illustrated in Fig. 6.1. The positive and negative segments of the left y-axis respectively represent the allocated injection and withdrawal ranges. The right y-axis shows the injection and withdrawal access prices. We show the injection access price over the positive segment of the right y-axis, and the negative range of the right y-axis shows the opposite number for the withdrawal access price. The plots reveal that cleared access limits for DERAs were smaller with higher σ. Such a trend is expected as higher σ increases the burden from distribution utility's customers on the distribution network, implying a lesser share of the pie available to the DERAs. This burden makes network access more expensive. This manifested in higher locational access prices when σ was larger.

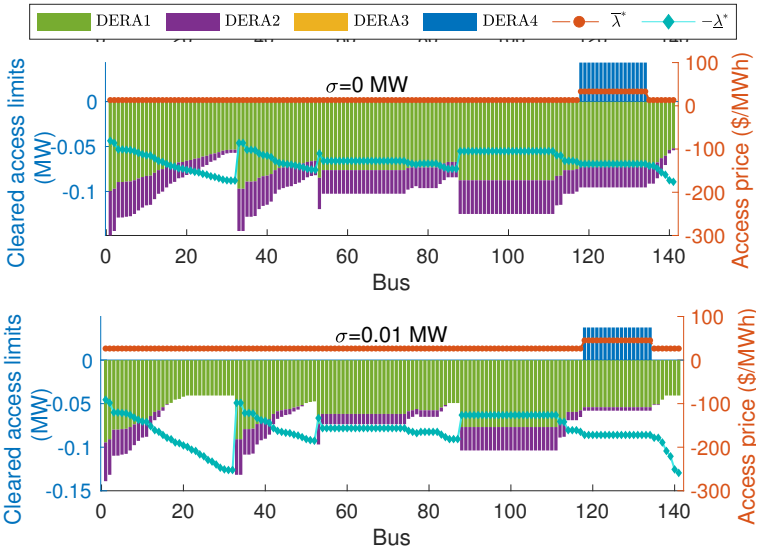

Figure 6.1: Auction results over the 141-bus distribution network. Left y-axis: cleared access limits, right y-axis: access clearing prices

DERAs 1 and 2 had lower BTM DG compared to DERAs 3 and 4. Thus, DERAs 1 and 2 behaved as net consumers, who bid for and received withdrawal access, as shown in Fig. 6.1. DERAs 3 and 4, on the other hand, largely acted as net power producers, and they purchased injection access through the auction at buses they operated. We remark that DERA 3 has a small access limit across all buses with $\sigma = 0$ MW, and it vanishes with $\sigma = 0.01$ MW. DERA 3 commands less BTM DG than DERA 4, and the surplus it can generate for its customers is lower. As a result, it bids a higher induced utility, compared to DERA 4. Consequently, its cleared access remains lower than that of DERA 4. With the highest BTM DG, DERA 4 has the largest incentive to acquire injection access at the buses it operates at, i.e., buses 118 - 134.

The access prices varied by location. As Proposition 1 reveals, prices must be uniform unless either network constraints or maximum injection/withdrawal limits are binding. Indeed, with both values of σ, voltage constraints at buses 52 and 141 were binding, leading to locationally varying access prices. Moreover, the figures suggest that prices are monotonic only over certain segments of the

DERA	$\sigma = 0$ MW	$\sigma = 0.004$ MW	$\sigma = 0.006$ MW	$\sigma = 0.008$ MW
1	599.54	488.00	431.20	369.41
2	324.07	291.43	277.58	265.01
3	1043.85	1042.54	1042.41	1042.41
4	80.18	76.74	75.09	73.49

Table 6.2: Variation of DERA surplus with σ

distribution network. However, as the network structure in [26] reveals, the price *is* monotonic along paths away from the substation. Notice that price monotonicity is only guaranteed by Proposition 3 with linear cost structures for the DSO. Our numerical results are derived with quadratic DSO costs, and yet, the conclusion of Proposition 3 holds, implying that the conditions for the result as stated are only sufficient, but not necessary.

The surpluses of the various DERAs are reported in Table 6.2. As evident, the surpluses reduce with higher σ. The larger the σ, the lower the DERAs' access to the network and consequently, their surpluses.

6.2 Comparing the Robust and Stochastic Auctions

For the stochastic access allocation models, we considered three different risk levels—$\delta = 0.99, 0.9, 0.8$. The allocation results for the withdrawal access and price are shown at the top of Fig. 6.2. Negative values indicate withdrawal access and positive values encode injection access. Compared to the robust allocation mechanism, the stochastic model had larger withdrawal accesses cleared and lower prices for those access limits. The difference in the outcomes from the robust and the stochastic models are substantial, even with a high risk parameter of $\delta = 0.99$. With more uncertainty (larger σ), the cleared withdrawal accesses were lesser and allocation prices were higher—a trend we already observed with the robust allocation model.

The DSO's surplus on the top left of Fig. 6.3 was nonnegative for all experiments. The same holds for the DERAs' surpluses, the aggregate value for which is plotted on the top right of Fig. 6.3. These verify Propositions 2-3 and 4. The surpluses are higher under the stochastic model, compared to the robust counterpart. Correspondingly, the social surplus (the sum of DERAs' and DSO's surplus) at the bottom of Fig. 6.3, is higher in the stochastic model. In fact, the conservative robust allocation had DSO and DERA surpluses around 20% lower than in the stochastic setting when $\sigma = 0.01$MW. This observation suggests that even a small $\sim$1% risk tolerance can drastically improve the surpluses of the auction participants.

The variation of DERA surpluses with σ is expected—largely, the DERAs' surpluses reduced with higher σ that burdens the distribution network with higher possible injections from the DSO's customers. As a result, DERAs got lesser access limits with lower surpluses.

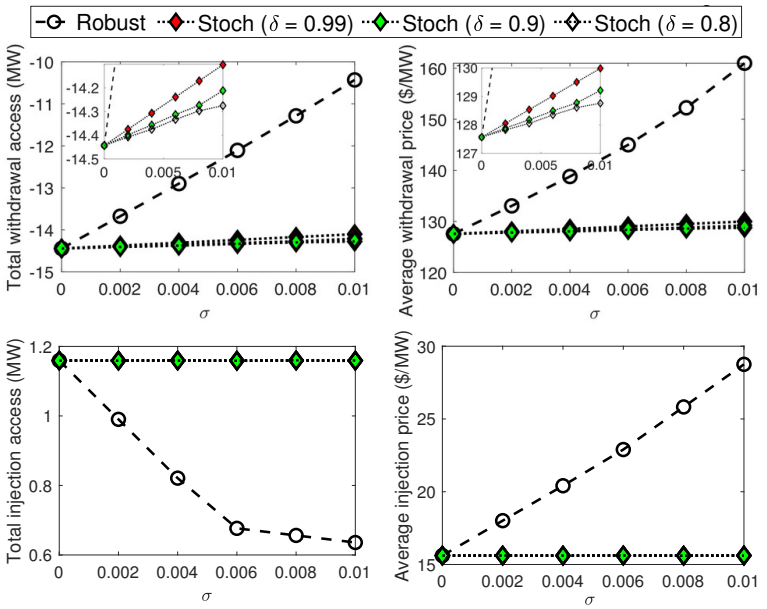

Figure 6.2: Top left: injection access, top right: injection price, bottom left: withdrawal access, bottom right: withdrawal price.

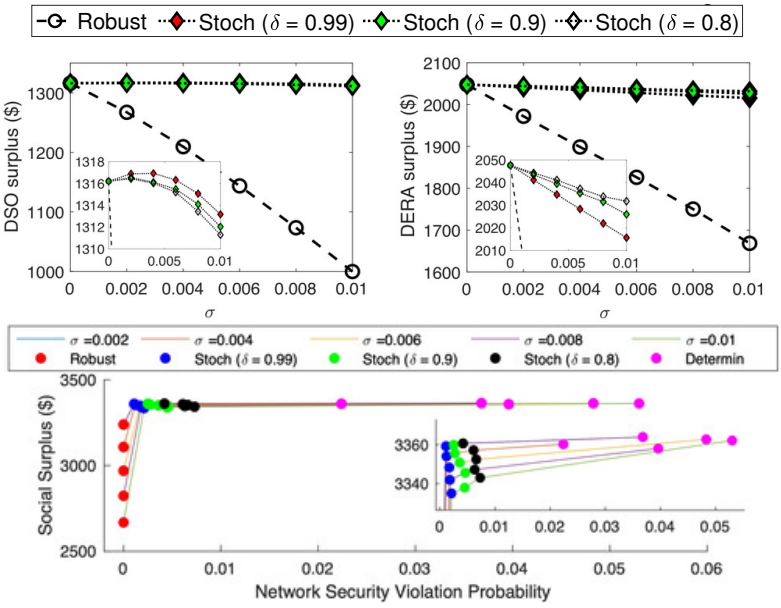

Figure 6.3: Top left: DSO surplus. Top right: DERA surplus. Bottom: Pareto front of the network security violation probability and social surplus.

We also compared our results with a *deterministic* model that computed the access against the average of all sampled scenarios by running (4.3) with that average scenario. As such an auction model ignores the uncertainty in the power injection/withdrawal scenarios, network security constraint violation probabilities were 7-30 times higher than that of the stochastic auction, as Fig. 6.3 reveals. Recall that uncertainties in operating conditions result from two sources–the first is the natural variation in the real-time DERA-ISO interactions over time, and the second is the aleatory uncertainty in possible real-time system conditions as visible at the forward auction stage. Undoubtedly, any uncertainty model that a DSO adopts, will affect the outcomes of our auctions. From practical use, a DSO must calibrate the uncertainty model, the resulting auction outcomes, and its implications for real-time DERA-ISO transactions through exhaustive simulations.

7. Conclusions

We have proposed a DSO-DERA-ISO coordination mechanism for multi-DERA participation in the wholesale market. Through a forward auction and welfare-maximizing robust and risk-sensitive market clearings, the proposed mechanism allocates network access limits to DERAs based on their willingness to pay for the access of the DSO-operated network. The key advantage of our proposed coordination mechanism is that it decouples DSO-DERA-ISO operations–the DSO-DERA forward auction in our model computes operating envelopes for real-time DERA-ISO transactions. This salient feature makes the proposed solution compatible with existing jurisdictional boundaries of DSOs and ISOs and yet, guarantees distribution network security with minimal coorindation.

Several relevant issues remain outside the scope of this work, requiring further investigation. We have not considered possible topology changes of the distribution network in our auction designs. We anticipate that a security-constrained version of our auction can be designed similarly to the security-constrained unit commitment and economic dispatch problem for wholesale market clearing. In this work, we have not addressed the question of bid/offer formation for DERAs. The overall market efficiency of our designs rests on this bid/offer formation process with price-taking and price-making DERAs. See our parallel effort in [19] for a step towards such an analysis. We have not delved into the details of the DSO's bid-in operational costs. Defining the scientific basis for a regulatory framework to calculate such costs, building on insights from [20] remains an interesting direction for future research. Admittedly, our simulations are limited in scope, designed primarily to study the properties of our design. As we have repeatedly pointed out, more realistic empirical analyses on larger systems are required to validate the practical efficacy of our designs.

References

[1] FERC. (2020) Participation of distributed energy resource aggregations in markets operated by regional transmission organizations and independent system operators, order 2222. 2020. [Online]. Available: https://www.ferc.gov/sites/default/files/2020-09/E-1_0.pdf

[2] A. Renjit, "TSO-DSO coordination frameworks, 2021 PSERC summer workshop," See also TSO-DSO Coordination Functions for DER, 2022. [Online]. Available: https://www.epri.com/research/products/000000003002016174

[3] K. Alshehri, M. Ndrio, S. Bose, and T. Başar, "Quantifying market efficiency impacts of aggregated distributed energy resources," *IEEE Transactions on Power Systems*, vol. 35, no. 5, pp. 4067–4077, 2020.

[4] Z. Gao, K. Alshehri, and J. R. Birge, "On efficient aggregation of distributed energy resources," in *2021 60th IEEE Conference on Decision and Control (CDC)*. IEEE, 2021, pp. 7064–7069.

[5] J. Bridge, "Export limits for embedded generators up to 200 kva connected at low voltage," *AusNet Services, Melbourne, Australia*, 2017.

[6] "Pushing the envelope for renewables," [Online], available 2023/07/01) at https://switchdin.com/blog/2023/3/21/pushing-the-envelope-for-renewables, March 2023.

[7] N. Nazir and M. Almassalkhi, "Grid-aware aggregation and realtime disaggregation of distributed energy resources in radial networks," *IEEE Transactions on Power Systems*, vol. 37, no. 3, pp. 1706–1717, 2021.

[8] M. Z. Liu, L. N. Ochoa, S. Riaz, P. Mancarella, T. Ting, J. San, and J. Theunissen, "Grid and market services from the edge: Using operating envelopes to unlock network-aware bottom-up flexibility," *IEEE Power and Energy Magazine*, vol. 19, no. 4, pp. 52–62, 2021.

[9] M. Z. Liu, L. F. Ochoa, P. K. Wong, and J. Theunissen, "Using opf-based operating envelopes to facilitate residential DER services," *IEEE Transactions on Smart Grid*, vol. 13, no. 6, pp. 4494–4504, 2022.

[10] A. Papalexopoulos, "The evolution of the multitier hierarchical energy market structure: The emergence of the transactive energy model," *IEEE Electrification Magazine*, vol. 9, no. 3, pp. 37–45, 2021.

[11] W. Muneer, "Dynamic operating envelopes can enable DERs in wholesale market without endangering grid reliability," [Online], available (2023/6/28) at https://utilityanalytics.com/2021/11/dynamic-operating-envelopes-can-enable-ders-in-wholesale-market-without-endangering-grid-reliability/, November 2021.

[12] "Who are controlling the DERs? increasing DER hosting capacity through targeted modeling, sensing, and control," 2022. [Online]. Available: https://documents.pserc.wisc.edu/documents/publications/reports/2022_reports/T_64_Final_Report__1_.pdf

[13] X. Chen, E. Dall'Anese, C. Zhao, and N. Li, "Aggregate power flexibility in unbalanced distribution systems," *IEEE Transactions on Smart Grid*, vol. 11, no. 1, pp. 258–269, 2019.

[14] M. Mousavi and M. Wu, "A DSO framework for market participation of DER aggregators in unbalanced distribution networks," *IEEE Transactions on Power Systems*, vol. 37, no. 3, pp. 2247–2258, 2021.
[15] K. Oikonomou, M. Parvania, and R. Khatami, "Deliverable energy flexibility scheduling for active distribution networks," *IEEE Transactions on Smart Grid*, vol. 11, no. 1, pp. 655–664, 2020.
[16] W. W. Hogan, "Contract networks for electric power transmission," *Journal of regulatory economics*, vol. 4, no. 3, pp. 211–242, 1992.
[17] M. Baran and F. F. Wu, "Optimal sizing of capacitors placed on a radial distribution system," *IEEE Transactions on power Delivery*, vol. 4, no. 1, pp. 735–743, 1989.
[18] "Power system analysis a mathematical approach," May 2022. [Online]. Available: http://netlab.caltech.edu/book/copies/Low-201909-ee135Notes-Ch1toCh12AppNoSol-20230116.pdf
[19] C. Chen, A. S. Alahmed, T. D. Mount, and L. Tong, "Wholesale market participation of DERA part II: Competitive DER aggregation," [Online], available 2023/07/06) at arXiv, July 2023.
[20] S. R. K. Yeddanapudi, Y. Li, J. D. McCalley, A. A. Chowdhury, and W. T. Jewell, "Risk-based allocation of distribution system maintenance resources," *IEEE Transactions on Power Systems*, vol. 23, no. 2, pp. 287–295, 2008.
[21] G. Still, "Lectures on parametric optimization: An introduction," *Optimization Online*, 2018.
[22] R. T. Rockafellar, S. Uryasev *et al.*, "Optimization of conditional value-at-risk," *Journal of risk*, vol. 2, pp. 21–42, 2000.
[23] R. T. Rockafellar and S. Uryasev, "Conditional value-at-risk for general loss distributions," *Journal of banking & finance*, vol. 26, no. 7, pp. 1443–1471, 2002.
[24] A. N. Madavan, N. Dahlin, S. Bose, and L. Tong, "Risk-based hosting capacity analysis in distribution systems," *IEEE Transactions on Power Systems*, pp. 1–11, 2023.
[25] A. Shapiro, D. Dentcheva, and A. Ruszczynski, *Lectures on stochastic programming: modeling and theory*. SIAM, 2021.
[26] H. Khodr, F. Olsina, P. De Oliveira-De Jesus, and J. Yusta, "Maximum savings approach for location and sizing of capacitors in distribution systems," *Electric power systems research*, vol. 78, no. 7, pp. 1192–1203, 2008.
[27] J. Löfberg, "YALMIP," 2023. [Online]. Available: https://yalmip.github.io
[28] "GUROBI Optimization," 2023. [Online]. Available: https://www.gurobi.com
[29] "MATPOWER data case141," 2020. [Online]. Available: https://github.com/MATPOWER/matpower/blob/master/data/case141.m

Part II

Wholesale Market Participation of DERAs: Competitive DER Aggregation

Lang Tong
Timothy D. Mount
Cong Chen, Graduate Student
Ahmed Alahmed, Graduate Student
Siying Li, Graduate Student

Cornell University

For information about this project, contact

Professor Lang Tong
School of Electrical and Computer Engineering
Cornell University, Ithaca, New York 14853

Power Systems Engineering Research Center

The Power Systems Engineering Research Center (PSERC) is a multi-university Center conducting research on challenges facing the electric power industry and educating the next generation of power engineers. More information about PSERC can be found at the Center's website: http://www.pserc.org.

For additional information, contact:

Power Systems Engineering Research Center
Arizona State University
527 Engineering Research Center
Tempe, Arizona 85287-5706
Phone: 480-965-1643
Fax: 480-727-2052

Notice Concerning Copyright Material

Table of Contents

List of Figures

List of Tables

1. Introduction

We address open problems in the direct participation of distributed energy resource aggregators (DERAs) in the wholesale electricity market operated by regional transmission organizations and independent system operators (RTOs/ISOs), under the general framework in FERC order 2222 [1]. We focus on the aggregation strategy of a profit-seeking DERA, whose industrial, commercial, and residential customers have competing service providers, such as their incumbent regulated utilities. The central theme of this work is to develop *profitable* and *competitive* aggregation strategies to attract and retain customers. By competitive aggregation, we mean that the benefits of the DERA customers must be no less than those offered by electricity provider benchmarks. An example of such a benchmark is the incumbent utility or a community choice aggregator (CCA) adopting net energy metering (NEM) policies, offering strong incentives to prosumers with behind-the-meter (BTM) DERs [2–4]. A major barrier to DERA's entrance to direct wholesale market participation is having an aggregation strategy and a participation model to make DER aggregation a profitable venture [5].

The technical challenge of designing a *profitable and competitive* DER aggregation is twofold. First, the DERA plays a dual role in the aggregation process: an energy supplier to its customers in retail market and a producer/demand in wholesale market. Its aggregation must consider retail competition, distribution network access limits, and its overall revenue adequacy. To this end, a DERA needs to derive profit-maximizing bids/offers from its competitive aggregation.

Second, competitive aggregation requires the DERA to offer more attractive pricing to its customers than the regulated tariff and shield them from the volatility of wholesale market prices. Examples of unstable pricing are two-part tariffs from Griddy [6] and Amber [7] defined by the wholesale spot price and a connection charge. Although Griddy's aggregation offered competitive pricing compared to regulated utility tariffs, its customers experienced a 100-fold price surge during the extreme winter storm Uri in 2021.

1.1 Related Work

FERC Order 2222 removes regulatory barriers for DERAs to participate in wholesale capacity, energy, and ancillary service markets. Prior studies have demonstrated DERs' capability to provide ancillary services both empirically [8, 9] and analytically [10]. In this report, we focus on DERA participation in energy market, where aggregators submit quantity [11] or price-quantity bids [12, 13], and the ISO clears the market and issues dispatch signals. Our analysis centers on market efficiency, DERA profitability, and how aggregators directly control DERs [14] to follow dispatch signals. While this study focuses on energy markets, the proposed framework is also extensible to capacity and ancillary service markets.

The growing literature on DER aggregation and wholesale market participation models broadly falls into two categories. One is through a retail market design operated by a distribution system operator (DSO) [15–17], an aggregation/sharing platform [18–20], or an energy coalition such as CCA [21–23]. For the most part, these works do not consider a profit-maximizing DERA's active participation in the wholesale market. In particular, in [15, 18], the DSO or an aggregation platform participates in the wholesale markets with the aggregated net demand (or possibly net production), treating the wholesale market as a balancing resource.

Our approach belongs to the second category of DER aggregations, where profit-seeking DERAs aggregate both generation and flexible demand resources, participating directly in the wholesale market with bid/offer curves. To ensure secure distribution network operation, DERA obeys the allocated distribution network access limits [24] (or operating envelopes [13]), rather than considering the computationally expensive network power flow constraints. Within the framework of FERC Order 2222, this type of DER aggregation has the potential to improve the overall system efficiency and reliability.

Although the notion of competitive DER aggregation has not been formally defined, two prior works have developed competitive aggregation solutions in [11, 21]. In [21], Chakraborty *et al.* consider DER aggregation by a CCA, where the authors provide an allocation rule that offers its customers competitive benefits with respect to the regulated utility.

Most relevant to our work is the DERA's wholesale market participation method developed by Gao *et al.* [11] where the authors consider a profit-seeking DERA aggregating BTM distributed generations (DGs) and offering its aggregated generation resources to the wholesale market. In particular, their approach achieves a social surplus equal to that achievable by customers' direct participation in the competitive wholesale market. In other words, their approach achieves the highest economic efficiency for aggregating DGs. A significant difference between [11] and this study is that we formulate a general competitive aggregation that includes the regulated utility. In achieving DERA's profit maximization, our aggregation and market participation are also different from [11].

The approach proposed in [11] follows the earlier work in [12] where a Stackelberg game-theoretic model is used. Both approaches assume that the DERA elicits prosumer participation with an optimized (one-part or two-part) tariff, and the prosumer responds with its quantity to be aggregated by the DERA. The real-time wholesale market price is reflected by the variable price in [6, 7, 11]. Such a variable price conveys low but volatile wholesale prices directly to customers. To protect customers from price spikes in real-time wholesale prices, methods like price caps [25] were proposed.

1.2 Summary of Results, Contributions, and Limitations

In this report, we substantially extend the DERA aggregation model in [26] to one that aggregates customers across multiple locations in distribution networks and incorporates security constraints

on network injection and withdrawal limits. We further investigate the competitive aggregation impact on market efficiency, price stability, and long-run equilibrium.

First, we propose a DER aggregation approach based on a constrained convex optimization that maximizes DERA surplus while providing higher customer surpluses than those offered by a competing aggregation model. In particular, we are interested in aggregation schemes that are competitive with the regulated utility rates such as various versions of regulated NEM rates,[1] with which a customer can make cost-benefit comparisons in her decision to become a customer of the DERA. We show that such a competitive DER aggregation, despite that the aggregation involving real-time wholesale locational marginal price (LMP), has an energy cost no greater than the regulated NEM tariff. This implies that the proposed DER aggregation mechanism ensures price stability regardless of the volatility of the wholesale market LMP, a property missing in Griddy's pricing model [6]. Meanwhile, we establish the profitability of DERA when competing with NEM.

Second, we propose a virtual storage model for DERA's wholesale market participation compatible with the practical continuous storage facility participation considered by ISOs under FERC order 841 [28, 29]. The DERA bidding curve is derived from the closed-form solution of the proposed DERA model. While the aggregation optimization explicitly involves wholesale market LMP, the virtual storage bidding curves do not require forecasting of LMP. We show that the proposed DERA wholesale market participation results in market efficiency equal to what is achievable when DERA's customers participate directly in the wholesale market.

Finally, we derive the benefit function of DERA over distribution network injection and withdrawal access limits. DERAs compete in the distribution network access auction proposed by [24] to acquire network access, and we empirically evaluate the number of surviving DERAs in the long-run competitive equilibrium. We also present a set of numerical results, comparing the surplus distribution of the proposed competitive aggregation solution with those of various alternatives, including the regulated utility. Among significant insights gained are the higher social surplus, customer surplus, and DERA surplus achievable in the proposed competitive DERA model, when compared to other alternatives.

A few remarks are warranted regarding the scope and limitations of this report. First, the losses in distribution systems are not considered. Second, the contingency cases where DSO rejects cleared bids and offers from DERA for reliability concerns [1] are neglected. Under the access limit allocation framework proposed in [24], reliability concerns of DER aggregation are already satisfied under normal operating conditions. Lastly, although the proposed competitive aggregation offers higher benefits to DERA customers, it does so with a non-uniform payment, which might raise equity concerns.

[1] NEM analyzed in [27] is an inclusive parametric tariff design that captures key features of the existing and proposed NEM tariffs.

1.3 Report Organization and Notations

In Chapter 2, we summarize the DER aggregation model and its main interactions. The problem of competitive DER aggregation is formulated in Chapter 3 where we derive the optimal aggregation solution. Chapter 4 and Chapter 5 consider DERA's wholesale market participation and its bidding strategies in the distribution network access auction, respectively. Numerical simulations are presented in Chapter 6.

A list of major designated symbols is shown in Table 1.1. The notations used here are standard. We use boldface letters for column vectors as in $\boldsymbol{x} = (x_1, \ldots, x_n)$. In particular, $\mathbf{1}$ is a column vector of all ones. The indicator function is denoted by $\mathbb{1}\{x_n \leq y_n\}$, which equals 1 if $x_n \leq y_n$, and 0 otherwise. $\boldsymbol{x} \preceq \boldsymbol{y}$ means $x_n \leq y_n, \forall n$. $\mathbb{R}_+$ represents the set of all nonnegative real numbers. $[x]$ represents the set of integers from 1 to x, *i.e.,* $[x] := \{1, \ldots, x\}$.

$\boldsymbol{d}$:	consumption bundle of aggregated customers.
$\overline{\boldsymbol{d}}, \underline{\boldsymbol{d}}$:	consumption bundle's upper and lower limits.
$\overline{\boldsymbol{C}}, \underline{\boldsymbol{C}}$:	distribution network injection and withdrawal access limits.
g, G:	BTM single and aggregated DG.
$\mathscr{K}$:	competitiveness constant for benchmark prosumer surplus.
N:	total number of prosumers.
M:	total number of points of aggregation (PoAs).
$\mathscr{N}_m$:	set of aggregated customers under the m-th PoA.
ω:	payment function of the aggregated customer.
π^+, π^-, π^0:	import rate, export rate, and fixed charges of NEM.
π:	wholesale locational marginal price (LMP).
Q:	aggregated net injection quantity of DERA.
S_{DERA}:	total surpluses of DERA and its aggregated prosumers.
S_{NEM}:	prosumers surplus under tariff NEM.
$\mathscr{S}(\cdot)$:	aggregated supply function.
U:	prosumer utility function for energy consumption.
V:	prosumer marginal utility function.

Table 1.1: Major symbols

2. DER Aggregation Model

A DERA aggregates flexible resources from its customers and coordinates with the DSO for power delivery to the wholesale market operated by ISO/RTO. Following the DERA interaction model proposed in [24], we focus on the DERA-DSO-ISO/RTO interfaces (a)–(c), as shown in Fig. 2.1. Since a DERA uses DSO's physical infrastructure for power delivery between its customers and the wholesale market, it is essential to delineate the financial and physical interactions at these interfaces. Below, we describe the three interfaces (a)–(c).

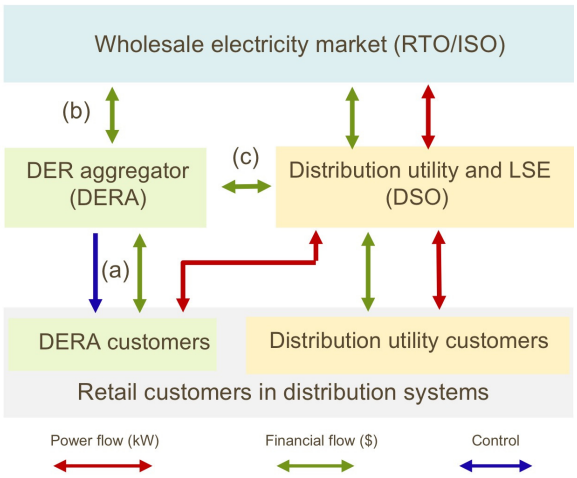

Figure 2.1: DERA model's physical and financial interactions. The red arrows show the bidirectional power flow, the green for the financial transactions, and the blue for direct control signals.

DERA and its customers at interface (a): We assume the DERA aggregates resources in a retail market from residential, commercial, and industrial customers, who have the option of being served by a regulated utility. Under a single-bill payment model, each customer settles both consumption charges and production compensation with the DERA. The DERA deploys an energy management system with *direct controls*[1] of the customer's BTM generation and flexible demand resources, such as rooftop PV, heat pumps, water heaters, and EV chargers. To remain competitive with the incumbent utility, the DERA must offer more attractive aggregation benefits; otherwise, customers will revert to the utility. Accordingly, the DERA optimizes the customer's BTM resources and provides the customer with a cost-benefit comparison with the NEM benchmark offered by the utility. See Chapter 3 for details.

[1] The direct control in [14] is implemented through cloud-based platforms.

DERA and RTO/ISO at interface (b): We focus on DERA's participation in the energy market based on a virtual storage model compatible with the continuous storage facility participation model [28]. See Chapter 4 for the construction of bid/offer curves. To this end, the DERA submits offer/bid curves or self-scheduled quantity bids. The DERA may participate in both the day-ahead and real-time markets, although here we focus only on the real-time energy market participation. The DERA may also deploy its own DG and storage capabilities to mitigate aggregation uncertainties.

DERA and DSO at interface (c): We consider the DERA-DSO coordination model in [24], where DERA acquires access limits at distribution network buses operated by DSO. DERA's willingness to pay for network access is explained in Chapter 5. Specifically, DERA secures injection and withdrawal access either through an access limit auction or a bilateral contract with the DSO. During real-time operation, DERA must aggregate DER from its customers in such a way that abides by the injection and withdrawal constraints set by the allocated access limits. That way, DERA's aggregation has no effect on the operational reliability of DSO under nominal operating conditions, avoiding DSO intervention on ISO dispatch of DERA's aggregation.

In summary, these three interactions at (a)–(c) establish our core framework for a DER aggregation model that is competitive, profit-making, and grid-aware.

3. Competitive DER Aggregation

This chapter formulates the optimal competitive aggregation and analyzes the properties of the optimal solution when competing with the incumbent utility's NEM. Our DER aggregation is built on the deregulated retail market. For example, in Texas and New York,[1] customers can choose their electricity suppliers based on electricity rate and services. We consider prosumers owning all energy consumption and DG devices. After joining a DERA, prosumers grant device access to DERA for measurements and direct controls.

3.1 Closed-Form Solution for Competitive DER Aggregation

We consider a DERA aggregating customers over multiple points of aggregation (PoAs) in the distribution network.[2] We define PoAs[3] as the main buses with higher voltages in the distribution network, which can be recognized with main substation information [30]. With the DERA-DSO coordination method in [24],[4] DERA receives injection and withdrawal access limits at all PoAs, represented respectively by

$$\overline{\boldsymbol{C}} := (\overline{C}_m, m \in [M]), \;\; \underline{\boldsymbol{C}} := (\underline{C}_m, m \in [M]),$$

where $\overline{\boldsymbol{C}}, \underline{\boldsymbol{C}} \in \mathbb{R}_+^M$ and M denotes the total number of PoAs. Thus, in the real-time operation, DERA must guarantee that its aggregated power at the m-th PoA satisfies

$$-\underline{C}_m \leq \sum_{n=1}^{\mathscr{N}_m} (g_n - \mathbf{1}^\top \boldsymbol{d}_n) \leq \overline{C}_m, \forall m \in [M], \tag{3.1}$$

where $g_n \in \mathbb{R}_+$ represents the BTM DG output of the n-th aggregated customer and $\mathscr{N}_m$ the set of aggregated customers under the m-th PoA. Denote N as the total number of DERA customers, and mapping $\rho(n) : [N] \to [M]$ such that $\rho(n)$ gives the index of PoA connecting customer n, then

$$\mathscr{N}_m := \{n \in [N] \mid \rho(n) = m\}. \tag{3.2}$$

$\boldsymbol{d}_n \in \mathbb{R}_+^K$ is the consumption bundle of all customers, *i.e.,*

$$\boldsymbol{d}_n := (d_{nk}, k \in [K]),$$

[1] For reference, we provide links to publicly available listings of retail energy providers in Texas [link] and New York [link].

[2] For simplicity, we illustrate the single time interval aggregation model here and apply it to the multi-interval aggregation empirically in Sec. 6.5.

[3] A diagram illustrating PoA is in Fig. 2 of [24].

[4] Details about how the DERA coordinates with DSO to get distribution network injection and withdrawal accesses are explained in Chapter 5.

where K denotes the total number of energy-consuming devices, including lamps, air-conditioners, washers/dryers, and heat pumps, for each customer $n \in [N]$. Customers set exogenous parameters $\underline{\boldsymbol{d}}_n, \bar{\boldsymbol{d}}_n \in \mathbb{R}_+^K$ as the minimum and maximum energy consumption limits of each device, *i.e.,*

$$\underline{\boldsymbol{d}}_n \preceq \boldsymbol{d}_n \preceq \bar{\boldsymbol{d}}_n, \forall n \in [N]. \tag{3.3}$$

Feasibility of the DER aggregation requires that the distribution network access limits (3.1) and consumption limits (3.3) have a non-empty intersection at all times. Thus, we assume DERA acquires enough injection and withdrawal accesses such that

$$\sum_{n=1}^{\mathcal{N}_m} \sum_{k=1}^{K} \underline{d}_{nk} - \underline{C}_m \leq \sum_{n=1}^{\mathcal{N}_m} g_n \leq \sum_{n=1}^{\mathcal{N}_m} \sum_{k=1}^{K} \overline{d}_{nk} + \overline{C}_m. \tag{3.4}$$

To attain customers in the energy aggregation, DERA adopts the *$\mathscr{K}$-competitive constraint* in (3.5) to ensure that the surplus of each prosumer under aggregation is higher than the benchmark surplus $\mathscr{K}_n$ (e.g. surplus under the incumbent provider), *i.e.,*

$$U_n(\boldsymbol{d}_n) - \omega_n \geq \mathscr{K}_n, \forall n \in [N]. \tag{3.5}$$

$U_n(\boldsymbol{d}_n)$ is the n-th customer's utility of consuming $\boldsymbol{d}_n$. We assume the utility function is concave, nonnegative, nondecreasing, continuously differentiable, additive (*i.e.,* across the K devices $U(\boldsymbol{d}) = \sum_{k=1}^{K} U_k(d_k)$). Here, the utility function is given; in practice, utility functions can be computed by parametric [27] or nonparametric [31] methods.

$\mathscr{K}$-competitive constraint is the criterion for a rational customer, seeking surplus maximization, to join a DERA. Otherwise, a rational prosumer has the incentive to leave DERA and switch to the benchmark service provider for a higher surplus. Details of benchmark $\mathscr{K}_n$ are in Sec. 3.2.

To summarize, in real-time, the DERA solves for the consumption bundle of all aggregated customers $\boldsymbol{D} \in \mathbb{R}_+^{N \times K}$ and their single-bill payments $\boldsymbol{\omega} \in \mathbb{R}^N$, defined by

$$\boldsymbol{D} := (\boldsymbol{d}_n, n \in [N]), \quad \boldsymbol{\omega} := (\omega_n, n \in [N])$$

from the following convex profit maximization

$$\begin{aligned} \Pi(\overline{\boldsymbol{C}}, \underline{\boldsymbol{C}}) := \quad & \underset{\boldsymbol{\omega}, \boldsymbol{D}}{\text{maximize}} \quad \sum_{n=1}^{N} (\omega_n - \pi(\mathbf{1}^\top \boldsymbol{d}_n - g_n)) \\ & \text{subject to} \quad (3.1), (3.3), (3.5). \end{aligned} \tag{3.6}$$

The optimal value $\Pi(\overline{\boldsymbol{C}}, \underline{\boldsymbol{C}})$ epresents the DERA's profit under the given distribution network access limits. In the objective function, DERA seeks profit maximization from both aggregated customer payments and the revenue from the wholesale market. Without loss of generality, all PoAs are under the same point of interconnection, facing a common LMP $\pi \in \mathbb{R}$. It is important to note that the LMP in (3.6) serves as a parameter to inform the DERA's bidding strategy in the wholesale market, rather than as a fixed operational price. Bidding details are described in (4.1) of Chapter 4. Under the feasibility assumptions in (3.4) and the specified utility function, Theorem 1 establishes a closed-form solution of (3.6) parameterized by π.

Theorem 1 (Optimal DERA scheduling and payment)**.** *Given the wholesale market LMP π, the optimal consumption bundle $\boldsymbol{d}_n^* = (d_{nk}^*)$ of prosumer n and its payment ω_n^* are given by*

$$d_{nk}^* = \begin{cases} h_{nk}(\underline{\xi}_m), & \sum_{n=1}^{\mathscr{N}_m} g_n \le \sum_{n=1}^{\mathscr{N}_m}\sum_{k=1}^{K} h_{nk}(\pi) - \underline{C}_m \\ h_{nk}(\overline{\xi}_m), & \sum_{n=1}^{\mathscr{N}_m} g_n \ge \sum_{n=1}^{\mathscr{N}_m}\sum_{k=1}^{K} h_{nk}(\pi) + \overline{C}_m \\ h_{nk}(\pi), & \textit{otherwise} \end{cases} \tag{3.7}$$

$$\omega_n^* \;\; = \;\; U_n(\boldsymbol{d}_n^*) - \mathscr{K}_n, \tag{3.8}$$

where $V(x) := \frac{d}{dx}U(x)$ is the marginal utility function and

$$h_{nk}(x) := \max\{\underline{d}_{nk}, \min\{V_{nk}^{-1}(x), \overline{d}_{nk}\}\}. \tag{3.9}$$

m is the index of PoA connecting customer n, i.e., $n \in \mathscr{N}_m$ defined by (3.2)*. Solve for $\underline{\xi}_m, \overline{\xi}_m, \forall m \in [M]$ from*

$$\sum_{n=1}^{\mathscr{N}_m}\sum_{k=1}^{K} h_{nk}(\underline{\xi}_m) = \sum_{n=1}^{\mathscr{N}_m} g_n + \underline{C}_m, \tag{3.10}$$

$$\sum_{n=1}^{\mathscr{N}_m}\sum_{k=1}^{K} h_{nk}(\overline{\xi}_m) = \sum_{n=1}^{\mathscr{N}_m} g_n - \overline{C}_m. \tag{3.11}$$

The proof is in the appendix of [32], following the convexity and Karush-Kuhn-Tucker (KKT) conditions of (3.6). This optimal solution has two noteworthy characteristics. First, the optimal consumption in (3.7) is only a function of the LMP π when DERA purchases enough network accesses at the PoA. Note also the difference between the optimal consumption schedule in (3.7) and those in [12] where the optimally scheduled consumption always depends on the anticipated LMP and forecast of BTM DG. Second, (3.6) finds a Pareto efficient allocation that maximizes the surplus of the DERA, subject to the constraint that the aggregated customer has the given level of surplus $\mathscr{K}_n$. Similar optimization and the Pareto efficient allocation are also analyzed in [33, P602]. The payment function ω_n can be realized by a two-part tariff as [11]. Overall, this closed-form solution allows DERA to apply simple dispatch and pricing policies when aggregating massive households over multiple PoAs.

3.2 Properties of DERA Competitive with NEM

We analyze the profitability of DERA and the energy consumption cost of aggregated prosumers when DERA is competitive with a regulated NEM tariff parameterized by the retail (consumption) rate π^+, the sell (production) rate π^-, and the connection charge π^0. Assume $0 \le \pi^- \le \pi^+$ and customers' surpluses under NEM are nonnegative [27]. Denote the n-th prosumer surplus under

NEM to be $S_n^{\text{NEM}}(g_n, \underline{C}_n, \overline{C}_n)$, whose computation depends on the DG generation and network access limits. Explicit formulations are in Sec. 8. DERA sets the benchmark prosumer surplus

$$\mathscr{K}_n = \zeta S_n^{\text{NEM}}(g_n, \underline{C}_n, \overline{C}_n), \;\; \zeta \geq 1, \tag{3.12}$$

which is used in (3.5) with profit ratio ζ to obtain competitive aggregation over the DSO's NEM-based aggregation with the same network access.[5] In this section, the network access limits carry the subscript n, which is equivalent to m since we set $\mathscr{N}_m = 1$ and $K = 1$ for simplicity.

The *$\mathscr{K}$-competitive constraint* in (3.5) has significant implications on pricing stability, despite that the aggregation is based on real-time LMP. Price stability means the price and payment faced by customers cannot go randomly high, for which a counterexample is the real-time LMP. Because the NEM tariff has price stability, achieving a finite customer payment regardless of the wholesale LMP fluctuation, an aggregation mechanism competitive with the NEM tariff must also be stable. The proposition below formalizes this intuition.

Proposition 1 (Average cost of consumption)**.** *The prosumer's average energy consumption cost under DERA aggregation is no higher than the NEM retail rate, i.e.,* $\omega_n^*/d_n^* \leq \pi^+$.

See proof in the appendix of [32]. Such price stability comes directly from the *$\mathscr{K}$-competitive constraint*, which enforces a lower bound for customer surplus and thus naturally limits the maximum customer payment. Note that the two-part pricing of Griddy [6] is not a stable pricing mechanism because the retail rate is tied directly to real-time LMP.

In the *$\mathscr{K}$-competitive constraint* (3.5) with (3.12), the profit ratio ζ controls surplus distribution between DERA and its aggregated prosumers. A larger ζ rebates more benefits to prosumers and incentivizes prosumers to join DERA, although it increases the deficit risk of DERA. Therefore, the DERA must carefully set ζ to balance profitability and competitiveness. In Proposition 2, we establish that the DERA can achieve nonnegative expected profit by choosing an appropriate ζ, assuming that BTM DG generation $\boldsymbol{g}$ and the LMP π are independent random variables in a competitive market.

Proposition 2 (Profitability of DERA)**.** *If* $\pi^- \leq \mathbb{E}[\pi] \leq \pi^+$*, then there exists a profit ratio* $\zeta \geq 1$ *such that the DERA's expected profit is nonnegative.*

In practice, the condition $\pi^- \leq \mathbb{E}[\pi] \leq \pi^+$ is often satisfied. For instance, in many states—including California—the export rate π^- is set near the avoided cost, which typically approximates the expected LMP $\mathbb{E}[\pi]$, as a way to mitigate cross-subsidies [3, 5, 34].

[5] Customers owning DERs switch from NEM to DERA for higher consumer surplus, granting DERs control to DERA upon joining.

4. DERA Wholesale Market Participation

The virtual storage model is adopted by ISOs to enable DERAs' participation in the wholesale market with bi-directional monetary and power flows [28, 29]. This means DERA can submit a combination of supply offers and demand bids, purchasing its aggregated consumption (as charging the virtual storage) and selling its aggregated production (as discharging).

4.1 Offer/Bid Curves of DERA in Energy Markets

As a virtual storage participant in the real-time energy market, the DERA is either self-scheduled or scheduled by ISO/RTO according to its bids and offers. This work focuses on developing price-quantity bid/offer curves that define DERA's willingness to consume/produce. In a competitive market, such curves are the marginal cost of production and the marginal benefit of consumption derived from the optimal DERA decision in Theorem 1.

Let Q be DERA's aggregated quantity to buy (when $Q < 0$) or sell (when $Q > 0$), and π be the wholesale market LMP. Let $G := \sum_{n=1}^{N} g_n$ be the BTM DG aggregated by DERA. In a competitive market, a price-taking DERA participant bids truthfully with its aggregated supply function

$$Q = \mathscr{F}(\pi), \;\; \mathscr{F}(\pi) := G - \sum_{n=1}^{N} \mathbf{1}^\top \boldsymbol{d}_n^*(\pi), \tag{4.1}$$

where $\boldsymbol{d}_n^*$ is defined in (3.7). Note that the inverse of the DERA supply function $\mathscr{F}^{-1}(Q)$ defines the offer/bid curves of the DERA. For a quantity bid, the DERA forecasts the LMP and computes the optimal net production with (4.1). In contrast, for a price-quantity bid/offer curve $\mathscr{F}^{-1}(Q)$, the DERA avoids LMP forecasting, as the ISO clears the market using the submitted curve and ensures consistency between the LMP and the resulting dispatch. More details are provided in Lemma 1, and a simulation of this offer/bid curve is presented in our previous paper [26].

Note also that the supply function depends on the aggregated BTM generation G, which is not known to the DERA at the time of the market auction. In practice, G can be approximated by using historical data or $N\mathbb{E}(g_n)$ via the Law of Large Numbers involving N independent prosumers or via the Central Limit Theorem for independent and dependent random variables [35].

4.2 Market Efficiency with DERA Participation

We now establish that the DERA's participation in the wholesale market achieves the same social welfare as that when all profit-maximizing prosumers participate in the wholesale market individually. We assume the wholesale market is competitive, where all participants are price takers with truthful bidding incentives. Prosumer notations in this section overlap with those in Chapter 3, but subscripts are modified to include the transmission network bus index.

Consider a transmission network with I buses. At each bus of the transmission network, we as-

sume M PoAs at the distribution network are connected and N prosumers are aggregated by the proposed DERA model. Denote U_{in} as the concave utility function for the n-th prosumer at the i-th transmission network bus. $\boldsymbol{g}_n := (g_{in})_{i\in[I]}$ and $\boldsymbol{d}_n := (d_{in})_{i\in[I]}$ are respectively the vectors of BTM DG generation and energy consumption for the prosumers. For simplicity, we ignore the number of energy-consuming devices for each prosumer, *i.e.,* $K = 1$, in this section. At each transmission bus, we sum up all load-serving entities and generators into one demand function and supply function. The load-serving entity at bus i purchases electricity e_i with a concave benefit function $B_i(e_i)$. The generator at bus i produces p_i with a convex cost function $C_i(p_i)$. Denote $\boldsymbol{e} := (e_i)_{i\in[I]}$, $\boldsymbol{p} := (p_i)_{i\in[I]}$. $\boldsymbol{f} \in \mathbb{R}^L$ is the line flow limit for L branches of the transmission network. $\boldsymbol{S} \in \mathbb{R}^{L\times I}$ is the network parameter for DC power flow model.

Lemma 1 (Wholesale market clearing with DERA)**.** *When prosumers participate in the wholesale market indirectly through the proposed DERA with offer/bid curve (4.1), social welfare* $\mathsf{SW}_{\text{DERA}}$ *is the optimal value of the convex problem*

$$\max_{\boldsymbol{D},\boldsymbol{p},\boldsymbol{e}\geq 0} \quad \sum_{i=1}^{I}\Big(\sum_{n=1}^{N} U_{in}(d_{in}) + B_i(e_i) - C_i(p_i)\Big) \tag{4.2a}$$

$$\textit{subject to} \quad (3.1), (3.3),$$

$$\lambda: \quad \sum_{i=1}^{I} p_i = \sum_{i=1}^{I}\Big(\sum_{n=1}^{N}(d_{in} - g_{in}) + e_i\Big), \tag{4.2b}$$

$$\mu: \quad \boldsymbol{S}\Big(\sum_{n=1}^{N}(\boldsymbol{g}_n - \boldsymbol{d}_n) + \boldsymbol{p} - \boldsymbol{e}\Big) \preceq \boldsymbol{f}. \tag{4.2c}$$

The sum of the DERA surplus and prosumers' surpluses, denoted by S_{DERA}*, can be computed by*

$$S_{DERA} = \textstyle\sum_{i=1}^{I}\sum_{n=1}^{N}(U_{in}(d_{in}^{\star}) - \pi_i(d_{in}^{\star} - g_{in})), \tag{4.3}$$

where $d_{in}^{\star}$ *is the optimal solution of* (4.2)*, which equals* (3.7)*.*

Proof of this Lemma relies on showing that pricing and dispatch results from (4.2) are at the bidding curve of DERA, *i.e.,* (4.1). With the optimal dual $\lambda^{\star} \in \mathbb{R}$ for the power balance constraint (4.2b) and $\mu^{\star} \in \mathbb{R}^L$ for the line flow limit (4.2c), LMP over I buses is defined by $\pi := \mathbf{1}\lambda^{\star} - \boldsymbol{S}^{\top}\mu^{\star}$, where $\pi := (\pi_i)_{i\in[I]}$. The prosumer utility in (4.2a), and constraints for energy consumption and distribution network access in (3.1)(3.3) come from DERA's offer/bid (4.1).

In direct wholesale market participation, a price-taking prosumer n at bus i constructs her offer/bid curves by solving the following surplus maximization with the given LMP π_i:

$$\max_{d_{in}\in\mathscr{D}_{in}} \; U_{in}(d_{in}) - \pi_i(d_{in} - g_{in}), \tag{4.4}$$

where $\mathscr{D}_{in} := [\max\{\underline{d}_{in}, g_{in} - \overline{c}_{in}\}, \min\{\bar{d}_{in}, g_{in} + \underline{c}_{in}\}]$. The access limits $\overline{c}_{in}$ and $\underline{c}_{in}$ represent the

distribution network injection and withdrawal capacities allocated to each prosumer.[1] These values match those in (3.7), enabling a fair comparison. Prosumers participating directly in the wholesale market face the same access constraints at each PoA as in the proposed DERA model. By solving (4.4), we obtain the bid/offer curve for prosumer n at bus i, *i.e.,*

$$\mathscr{S}_{in}(\pi_i) = g_{in} - d^*_{in}(\pi_i), \tag{4.5}$$

where $d^*_{in}(\pi_i)$ is defined as (3.7). Let $\mathsf{SW}_{\text{Direct}}$ and S_{PRO} be, respectively, the optimal social welfare and prosumers' surplus when all prosumers directly participate in the wholesale market. The following theorem is parallel to [11], although we use different aggregation and network settings.

Theorem 2 (Market efficiency)**.** *When all prosumers directly participate in the wholesale market, the market clearing result can be computed by* (4.2)*,* $\mathsf{SW}_{\text{Direct}} = \mathsf{SW}_{\text{DERA}}$*, and* $S_{\text{PRO}} = S_{\text{DERA}}$.

The proof is in the appendix of [32], which relies on the fact that the proposed DERA has its bidding curve (4.1) equal to the sum of the prosumer's bidding curve in (4.5). From this, we can establish that the wholesale market clearing problem with the direct participation of all prosumers has the same market-clearing results as (4.2).

Although the proposed DER aggregation model only focuses on DERA's profit maximization in the objective of (3.6), the competitive constraint (3.5) aligns the aggregated prosumer's surplus maximization with DERA's profit maximization. So, in the deregulated retail market, the competitive DERA has the incentive to maximize prosumers' surpluses and get the maximum total surplus that can be split among DERA and its aggregated prosumers. Essentially, the DERA acts as an intermediary, enabling prosumers to indirectly participate in the wholesale market. As the DERA earns a profit for providing aggregation service, each prosumer receives a lower surplus than they would under direct participation (Fig. 6.1). This is justified, since individual prosumers lack the scale required for direct participation in the wholesale market.

[1] Detail formulations are in [32].

5. DERA-DSO Coordination

All generation and consumption resources aggregated by DERA need to bypass the distribution network to participate in the wholesale market. The DERA aggregation presented in this work ensures that the aggregated DER at each distribution network PoA is bounded by access limits imposed through the distribution network access limit auction in [24]. A DERA submits a bid curve in this auction representing its willingness to acquire access at PoAs. We assume that a DERA is a price taker in the access limit auction. Therefore, the bid-in demand curve for network access from the DERA at a particular PoA is the marginal benefit (profit) from having a DER aggregation under the PoA. The maximum expected profit of DERA is

$$\varphi(\overline{\boldsymbol{C}},\underline{\boldsymbol{C}}) := \mathbb{E}_{\boldsymbol{g},\pi}[\Pi(\overline{\boldsymbol{C}},\underline{\boldsymbol{C}})], \tag{5.1}$$

where $\Pi(\overline{\boldsymbol{C}},\underline{\boldsymbol{C}})$ is the maximum DERA profit computed from (3.6), given renewable generations and LMP. Note that when participating in the forward network access auction, both the BTM DG and LMP are random.

5.1 DERA Benefit Function for Distribution Network Access

The following Proposition provides an expression for the benefit function of DERA, $\varphi(\overline{\boldsymbol{C}},\underline{\boldsymbol{C}})$, which can be used as the bid curve of access limits submitted to the auction in [24].

Proposition 3 (Benefit function for network access)**.** *With the DERA profit maximization (3.6), the expected DERA surplus is*

$$\varphi(\underline{\boldsymbol{C}},\overline{\boldsymbol{C}}) = \mathbb{E}\Big\{ \sum_{m=1}^{M} (\underline{\phi}_m(\underline{C}_m) + \overline{\phi}_m(\overline{C}_m)) + \sum_{n=1}^{N} (\rho_n - \mathscr{K}_n)\Big\}, \tag{5.2}$$

$$\underline{\phi}_m(\underline{C}_m) := \Big(\sum_{n=1}^{\mathscr{N}_m} U_n(\boldsymbol{h}_n(\underline{\xi}_m)) - \pi\underline{C}_m\Big) \mathbb{1}\{ \sum_{n=1}^{\mathscr{N}_m} g_n \le \underline{q}_m\},$$

$$\overline{\phi}_m(\overline{C}_m) := \Big(\sum_{n=1}^{\mathscr{N}_m} U_n(\boldsymbol{h}_n(\overline{\xi}_m)) + \pi\overline{C}_m\Big) \mathbb{1}\{ \overline{q}_m \le \sum_{n=1}^{\mathscr{N}_m} g_n\},$$

$$\rho_n := \big(U_n(\boldsymbol{h}_n(\pi)) - \pi(\boldsymbol{h}_n(\pi) - g_n)\big) \mathbb{1}\{ \sum_{n=1}^{\mathscr{N}_m} g_n \in (\underline{q}_m, \overline{q}_m)\}.$$

The proof is in [32] with $\boldsymbol{h}_n(x) := \sum_{k=1}^{K} h_{nk}(x)$, $U_n(\boldsymbol{h}_n(x)) = \sum_{k=1}^{K} U_{nk}(h_{nk}(x))$ from the additive property of the utility function, and

$$\overline{q}_m := \overline{C}_m + \textstyle\sum_{n=1}^{\mathscr{N}_m} \boldsymbol{h}_n(\pi),\ \underline{q}_m := -\underline{C}_m + \sum_{n=1}^{\mathscr{N}_m} \boldsymbol{h}_n(\pi).$$

The optimal DERA surplus is decomposed into three terms: one dependent on the withdrawal access $\underline{\phi}_m(\underline{C}_m)$, one dependent on the injection access $\overline{\phi}_m(\overline{C})$, and one independent of network access. $\varphi(\underline{\boldsymbol{C}}, \overline{\boldsymbol{C}})$ is separable across injection and withdrawal access over M PoAs. Therefore, DERA can bid separately for the distribution network accesses at different PoAs when coordinating with DSO. At PoA m with less BTM DG, *i.e.,* $\sum_{n=1}^{\mathcal{N}_m} g_n \leq \underline{q}_m$, DERA's benefit depends on the withdrawal access. Conversely, if there is more BTM DG, *i.e.,* $\overline{q}_m \leq \sum_{n=1}^{\mathcal{N}_m} g_n$, DERA's benefit depends on the injection access. Related simulations are in Sec. 6.4.

5.2 Long-Run Equilibrium for Competitive DERA

In a long-run competitive industry, we explore how many DERA can survive. DERAs compete to attract customers, attain distribution network access, and participate in the wholesale market. We assume all DERAs adopt the competitive DER aggregation method in (3.6). The condition for a competitive long-run equilibrium [36, P193] has two components: (i) the marginal benefit of DERA equals the marginal cost of DSO for providing the distribution network access, and (ii) all DERAs have profits equal to zero, *i.e.,* DERA's profit in conducting aggregation equals DERA's payment to acquire distribution network access. Related derivations and simulations are in Sec. 6.5 and [32].

6. Case Studies

We compared the expected surplus distribution of different DER aggregation methods under varying network access limits and BTM DG generations.[1] We also computed the benefit function of DERA to the distribution network access and empirically evaluated the long-run equilibrium of DERA with multi-interval aggregation.

6.1 Parameter Settings

Denote the utility function for the aggregated customer as

$$U(x) = \begin{cases} \alpha x - \frac{\beta}{2}x^2, & 0 \le x \le \frac{\alpha}{\beta} \\ \frac{\alpha^2}{2\beta}, & x > \frac{\alpha}{\beta} \end{cases}, \tag{6.1}$$

where $\alpha = \$0.4/\text{kWh}, \beta = \$0.1/(\text{kWh})^2$ [27]. Let the marginal utility $V^{-1} \in [\underline{d}, \bar{d}]$ for the consumption limits.[2]

We used NEMa and NEMp to represent the DER aggregation under NEM when prosumers were active and passive, respectively. Passive customers are not responsive to the retail prices, but active customers will optimize their energy consumption given the retail price and the BTM DG generations. Based on PG&E residential rate, we set $\pi^+ = \$0.3/\text{kWh}$ for the NEM. We assumed $\pi^- = \mathbb{E}[\pi]$ and the fixed cost of NEM was covered by extracting fixed payment from DERA, so we simulated with $\pi^0 = \$0$. Gao-Alshehri-Birge (GAB) represented the two-part pricing in [11], which allowed customers to sell BTM DG to the DERA while purchasing energy from its incumbent utility company. Detailed models for NEMa, NEMp, and GAB are provided in Chapter 8 and the appendix online [32]. Our DER aggregation method was simulated in Co.NEMa and Co.GAB, competitive with NEMa and GAB, respectively. For Co.NEMa, we set profit ratio ζ at the upper bound in the proof of Proposition 2. For Co.GAB, we set $\zeta = 1.05$ to provide 5% more customer surplus than the GAB competitor.

We considered the randomness of LMP and BTM DG generation using data sources from CAISO [37] and Pecan Street Dataport [38], respectively. The LMP π was modeled as a Gaussian random variable with a mean of \$0.05/kWh and a standard deviation (STD) of \$0.01/kWh. The BTM DG generation g was modeled as a Gaussian random variable with a mean ranging from 1.1 kWh to 5.1 kWh and a standard deviation of 0.2 kWh, truncated at $(0, +\infty)$. We generated 10,000 random

[1] Under the access limit allocation framework in [24], distribution network reliability concerns are resolved if DERAs obey allocated distribution network access limits. So the distribution network topology was ignored here.

[2] We simulated the case of $K = 1$ for simplicity.

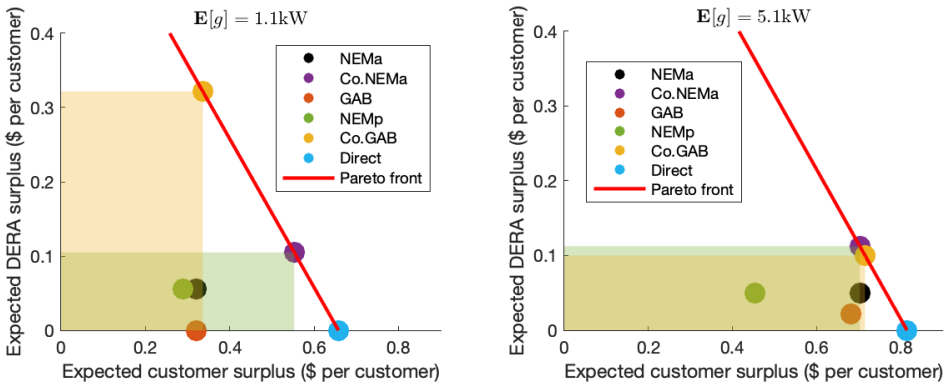

Figure 6.1: Expected surplus distribution and market efficiency with 80% DG adopter rate. Each shaded rectangle is dominated by its top right corner. (From left to right, the expected DG increases from 1.1 to 5.1 kW.)

scenarios for both the LMP and BTM DG. At a given PoA, we evaluated the expected per-customer surplus metrics based on the sample means from these scenarios.

6.2 Performances with Unlimited Distribution Network Access

Four observations below were drawn when all aggregators received plenty of distribution network accesses.

First, Co.NEMa and Co.GAB were at the Pareto front in Fig. 6.1, achieving the maximum social surplus as if all prosumers directly participated in the wholesale market. This verified Theorem 2. The Pareto front was computed by aggregating the surpluses of DERA and customers, omitting surpluses of other units. This was because we adopted the price taker assumption in the wholesale market, thus surpluses of other units stayed the same in different DERA models. The blue dot, named Direct, represented the ideal case that prosumers directly participated in the wholesale market with bidding curve (4.5). The green rectangle contained aggregation methods achieving less DERA surplus and customer surplus than Co.NEMa, thus dominated by our proposed competitive DER aggregation method. Similarly, the orange rectangle was dominated by its top right corner, Co.GAB. This was because our aggregation methods efficiently participated in the wholesale market with aggregated resources and scheduled the aggregated customers at a consumption level with a higher customer surplus. When the expected BTM DG increased from 1.1kW to 5.1kW, comparing the left and right panels in Fig. 6.1, we observed that the expected social surplus, which was the sum of DERA and customer surpluses, increased, because more BTM DG was sold to the wholesale market.

Second, customers had the highest expected surplus in Co.NEMa and Co.GAB, as shown by the top of Fig. 6.2. Passive customers in NEMp had the least surplus because their scheduling was agnostic of DG generation. Customer surpluses almost overlapped in all cases at a low DG adopter ratio with fewer producers, since most aggregation benefits came from BTM DG of producers.

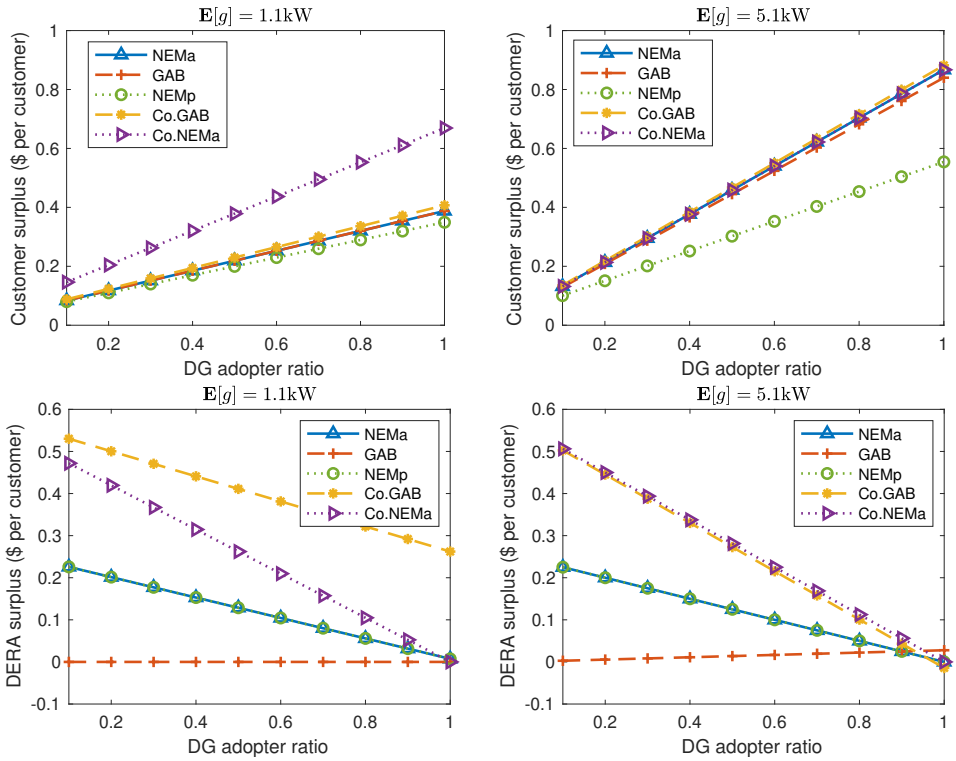

Figure 6.2: Expected surplus distributions vs. network access ratio. (Top: expected customer surplus; bottom: expected DERA surplus.)

When the DG adopter ratio increased, the expected customer surplus increased in all cases.

Third, when the DG adopter ratio or the DG generation was low, Co.NEMa and Co.GAB achieved the highest expected DERA surplus, as shown at the bottom of Fig. 6.2. When the DG adopter ratio and DG generation were high, GAB achieved the highest DERA surplus because GAB only aggregated producers.[3] Co.NEMa always had DERA profit no less than zero since we chose ζ based on Proposition 2. The DERA surpluses under NEMp and NEMa were identical, as setting $\pi^- = \pi$ ensures that aggregated DGs are compensated at the wholesale market price, eliminating any surplus gained by aggregating active prosumers' DG production.

Fourth, since NEM provided a higher surplus to customers with BTM DG, DERAs must commensurately reduce their profits and share them with the customers to remain competitive with NEM. Therefore, in most cases of Fig. 6.2, the expected DERA surplus decreased when the DG adopter ratio increased. Notably, GAB's DERA surplus increased with the DG adoption ratio, as GAB aggregated only producers.

[3] GAB achieved the Pareto front when all prosumers were producers, e.g., DG adopter ratio equal 100% and $\mathbb{E}[g] =$ 5.1kW.

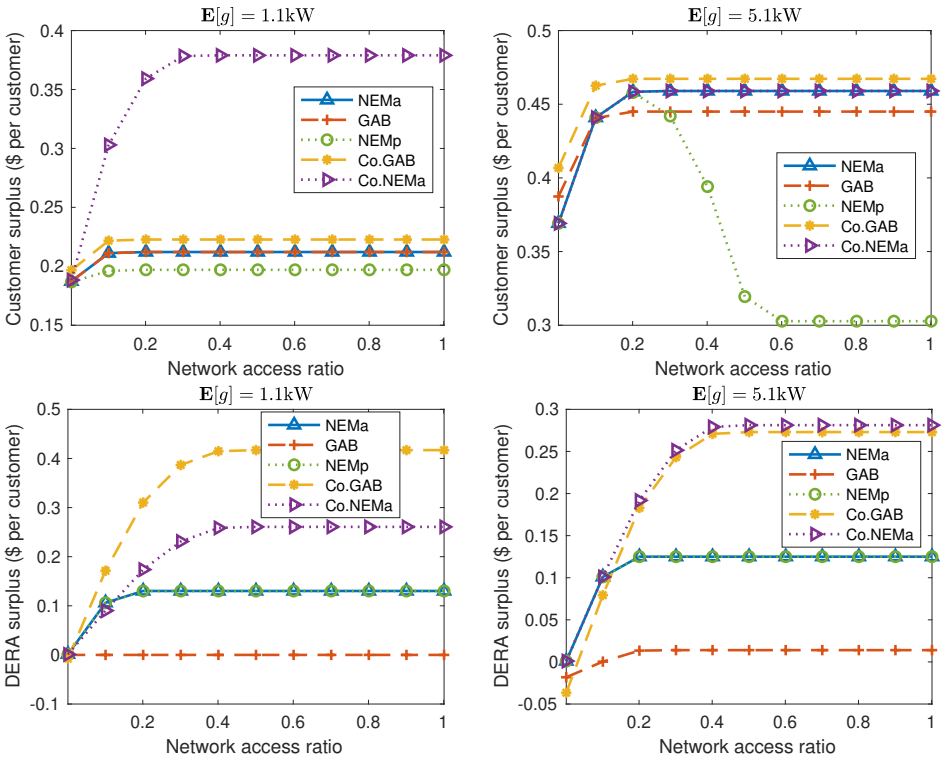

Figure 6.3: Expected surplus distributions vs. network access ratio with 50% DG adopter rate. (Top: expected customer surplus; bottom: expected DERA surplus when $\mathbb{E}[g] = 1.1$ kW and 5.1 kW, respectively.)

6.3 Performances with Limited Distribution Network Access

Here, we set distribution network access limits for each prosumer by $\overline{C} = \underline{C} = 8\delta$ kW and varied the *network access ratio* δ from 0 to 1 to analyze the influence of limited distribution network access. First, as is shown in Fig. 6.3, either Co.NEMa or Co.GAB achieved the highest customer surplus or DERA surplus under a limited network access ratio. Second, when the network access ratio increased, customer surplus increased in most cases except NEMp, which passively controlled DG. Third, the DERA surplus in all cases increased when the network access ratio increased. This was intuitive because DERAs needed distribution network access to deliver the aggregated DER and participate in the wholesale market.

6.4 Benefit Function of DERA for Distribution Network Access

We computed the bid-in benefit function of the proposed DERA model, *i.e.,* (5.2), with $\zeta = 1.01$ and 50 prosumers aggregated at a certain PoA. DERA was competing with NEM, and prosumers were passive. Figure 6.4 shows the expected benefit φ of the DERA as a function of injection and withdrawal access, under varying levels of expected BTM DG generations.

In Fig.6.4 (left), DERAs with lower expected DG generation exhibited higher benefits and submitted higher bid prices for withdrawal access, as indicated by the steeper slope of the benefit function.

This is because, with less BTM generation, DERAs rely more on electricity withdrawn from the network. In Fig.6.4 (right), the benefit function decreased with higher DG generation—a counter-intuitive result. This occurred because NEM offers greater surplus to customers with higher DG output, forcing DERAs to reduce their profit margins and share more benefits with customers to remain competitive.

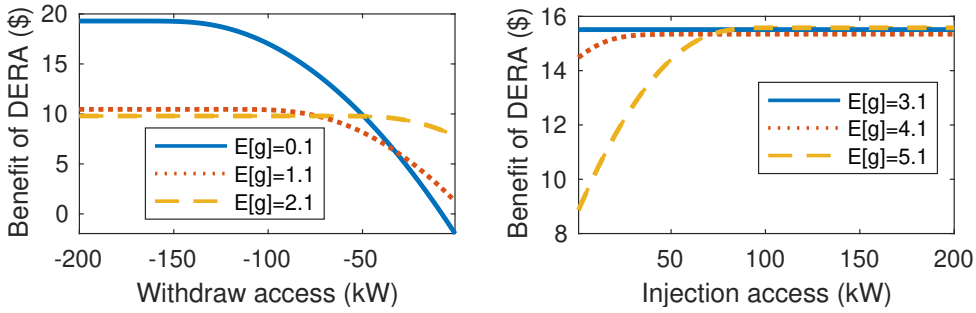

Figure 6.4: DERA benefit function φ. (Left: withdrawal access $-\underline{C}$; right: injection access $\overline{C}$.)

6.5 Long-Run Competitive Equilibrium of DERAs

In the long-run competitive equilibrium analysis with multi-interval aggregation of DERs, we assumed that 200 DERAs initially existed and computed the expected number of surviving DERAs in the long run. For simplicity, we assumed DERAs were homogeneous and had the same setting as Sec. 6.4. Prosumers had the same expected DG generation created from the 24-hour rooftop solar data in Pecan Street [38].[4] We multiplied the mean of 24-hour DG by the factor $\varepsilon_1 \in \mathbb{R}_+$ to simulate different DG installation capacities and sampled 10,000 random DG scenarios. DERA submitted the benefit function, as in Fig. 6.4, to acquire hourly distribution network access. Same as [24], the DSO cost function for providing distribution network access was assumed to be the sum of quadratics, $J(x) = \frac{1}{2}bx^2 + ax$ with $a = \$0.009/\text{kWh}, b = \$0.0005/(\text{kWh})^2$ for both the injection and withdrawal access. We multiplied DSO's cost J by $\varepsilon_2 \in \mathbb{R}_+$ to simulate different levels of DSO's costs.

Two observations were drawn from the results in Fig. 6.5. First, when the DG capacity ratio ε_1 was between 0.4 and 1.4, all initial 200 DERAs survived because DERAs were able to internally balance customer demands with their aggregated DG, thus relying less on and paying less to the network access. This was validated by the yellow dot curve from Fig. 6.5 (right), which required almost zero network access over 24 hours. Second, when the DG capacity ratio decreased from 0.4 to 0 in Fig. 6.5 (left), the number of surviving DERA decreased. In this case, DG was lower than the aggregated customers' consumption, and not all DERAs can survive when competing and paying for network withdrawal access over 24 hours, as shown by the blue solid curve in Fig. 6.5

[4] Detail DG trajectories and the long-run equilibrium results for single-interval aggregation are shown in the appendix [32], providing intuitions about long-run equilibrium for multi-interval aggregation here.

(right). In the green dashed curve of Fig. 6.5 (left), DSO's cost for providing network access was lower, so more DERAs survived than in other curves. Similar reasons applied when DG capacity ratio increased beyond 1.4.

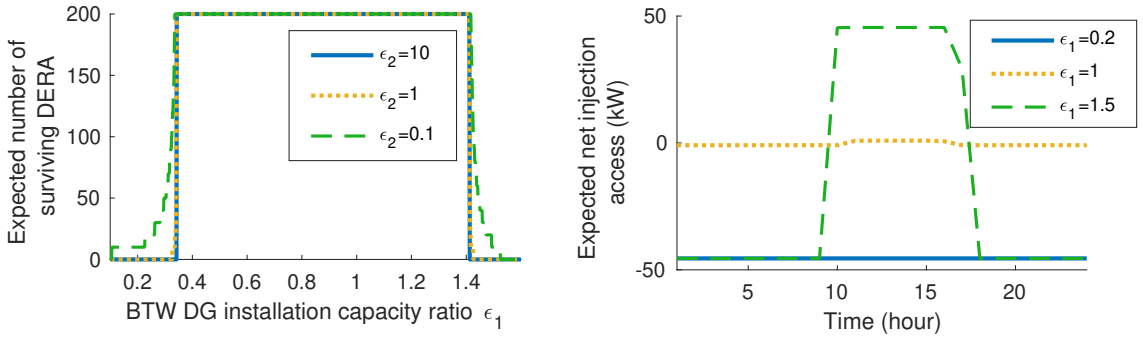

Figure 6.5: Long-run competitive equilibrium for multi-interval aggregation. (Left: expected number of surviving DERA vs. DG installation capacity ratio ε_1; right: expected distribution network net injection access of DERA over 24-hour, whose negativity represents withdrawal access.)

7. Conclusions

A major challenge to realizing the goals of FERC Order 2222 is enabling profit-maximizing DERAs to effectively compete with the retail programs offered by distribution utilities. To this end, this report considers the *competitive DER aggregation* of a profit-seeking DERA in the wholesale electricity market. As a wholesale market participant, DERA can both inject and withdraw power from the wholesale market. It is shown that the proposed DERA model maximizes its profit while providing competitive services to its customers with higher surpluses than those offered by the distribution utilities. We also establish that the resulting social welfare from DERA's participation on behalf of its prosumers is the same as that gained by the direct participation of price-taking prosumers, making the proposed DERA aggregation model optimal in achieving wholesale market efficiency. Additionally, we derive two significant optimal price-quantity bids of DERA, of which one is submitted to the wholesale market, and the other to the distribution network access allocation [24].

An open issue of the proposed aggregation solution is that the payment functions for prosumers are nonlinear and non-uniform. Although each customer is guaranteed to be better off than the competing scheme, two customers producing the same amount may be paid and compensated differently. In other words, the total charge/credits depend not only on the quantity but also on the flexibility of the demand and constraints imposed by the prosumer. Note that a profit-seeking DERA participating in the wholesale electricity market is not subject to the same regulations as a regulated utility. Such non-uniform pricing may be acceptable and has also been proposed in the form of non-uniform fixed charges [5, 11].

References

[1] FERC. (2020) Participation of distributed energy resource aggregations in markets operated by regional transmission organizations and independent system operators, order 2222. 2020. [Online]. Available: https://www.ferc.gov/sites/default/files/2020-09/E-1_0.pdf

[2] M. Birk, J. P. Chaves-Ávila, T. Gómez, and R. Tabors, "TSO/DSO coordination in a context of distributed energy resource penetration," *Proceedings of the EEIC, MIT Energy Initiative Reports, Cambridge, MA, USA*, pp. 2–3, 2017.

[3] A. S. Alahmed and L. Tong, "Integrating distributed energy resources: Optimal prosumer decisions and impacts of net metering tariffs," *SIGENERGY Energy Inform. Rev.*, vol. 2, no. 2, p. 13–31, Aug. 2022.

[4] J. Nelson, "Order 2222: Observations from a Distribution Utility," Southern California Edison (SCE), Tech. Rep., 10 2021.

[5] S. Borenstein, M. Fowlie, and J. Sallee, "Designing electricity rates for an equitable energy transition," *Energy Institute at Haas working paper*, vol. 314, 2021.

[6] "Real-time wholesale electricity pricing in Griddy," Accessed: June 23, 2025. [Online]. https://www.energyogre.com/is-realtime-wholesale-pricing-risky, February 2025.

[7] "Amber wholesale energy price explained," Accessed: June 23, 2025. [Online]. https://www.youtube.com/watch?app=desktop&v=DckQbwwWPWA and https://www.amber.com.au/electricity, June 2021.

[8] C. Loutan, "Operating challenges integrating higher levels of inverter-based resources," Presented at the NYU–Princeton Workshop on Future Electricity Grids and Energy Markets with Decarbonization, jan 2025, brooklyn, NY, Jan. 22–23. [Online]. Available: https://nyup.orfe.princeton.edu/sites/g/files/toruqf7271/files/documents/Day%202%20-%2003%20-%20Loutan%20-%20Operating%20Challenges%20Integrating%20Higher%20Levels%20of%20Inverter%20Based%20Resources.pdf

[9] W. Wu, Z. Guo, H. Liu, G. Wu, S. Li, and Y. Cheng, "A 100% pv powered microgrid operates independently and stably," *Energy Internet*, vol. 1, no. 2, pp. 113–115, 2024. [Online]. Available: https://ietresearch.onlinelibrary.wiley.com/doi/abs/10.1049/ein2.12021

[10] Z. Guo, W. Wu, and G. Wu, "Full-state virtual oscillator control for grid-forming pvs to endure solar radiation and grid disturbances," *IEEE Transactions on Energy Conversion*, pp. 1–11, 2024.

[11] Z. Gao, K. Alshehri, and J. R. Birge, "Aggregating distributed energy resources: efficiency and market power," *Manufacturing & Service Operations Management*, 2024.

[12] K. Alshehri, M. Ndrio, S. Bose, and T. Başar, "Quantifying market efficiency impacts of aggregated distributed energy resources," *IEEE Transactions on Power Systems*, vol. 35, no. 5, pp. 4067–4077, 2020.

[13] A. Attarha, M. Mahmoodi, S. M. N. RA, P. Scott, J. Iria, and S. Thiébaux, "Adjustable price-sensitive DER bidding within network envelopes," *IEEE Transactions on Energy Markets, Policy and Regulation*, vol. 1, no. 4, pp. 248–258, 2023.

[14] "Turnkey VPPs: Streamlining DER management for the decarbonized grid of the future," Accessed: June 23, 2025. [Online]. https://uplight.com/resources/turnkey-vpps-streamlining-der-management-decarbonized-grid-of-the-future/, March 2023.

[15] S. D. Manshadi and M. E. Khodayar, "A hierarchical electricity market structure for the smart grid paradigm," *IEEE Transactions on Smart Grid*, vol. 7, no. 4, pp. 1866–1875, 2015.

[16] C. M. Jeong, H. S. Moon, and S. W. Kim, "Probabilistic prequalification scheme of a distribution system operator for supporting market participation of multiple distributed energy resource aggregators," *IEEE Transactions on Energy Markets, Policy and Regulation*, vol. 2, no. 4, pp. 465–475, 2024.

[17] Y. Zhou, J. Wang, Y. Zhang, J. Wei, W. Sun, and J. Wang, "A fully-decentralized transactive energy management under distribution network constraints via peer-to-peer energy trading," *IEEE Transactions on Energy Markets, Policy and Regulation*, vol. 1, no. 4, pp. 297–309, 2023.

[18] T. Morstyn and M. D. McCulloch, "Multiclass energy management for peer-to-peer energy trading driven by prosumer preferences," *IEEE Transactions on Power Systems*, vol. 34, no. 5, pp. 4005–4014, 2018.

[19] Y. Chen and C. Zhao, "Review of energy sharing: Business models, mechanisms, and prospects," *IET Renewable Power Generation*, 2022.

[20] L. He and J. Zhang, "Energy trading in local electricity markets with behind-the-meter solar and energy storage," *IEEE Transactions on Energy Markets, Policy and Regulation*, vol. 1, no. 2, pp. 107–117, 2023.

[21] P. Chakraborty, E. Baeyens, P. P. Khargonekar, K. Poolla, and P. Varaiya, "Analysis of solar energy aggregation under various billing mechanisms," *IEEE Transactions on Smart Grid*, vol. 10, no. 4, pp. 4175–4187, 2018.

[22] L. Han, T. Morstyn, and M. McCulloch, "Incentivizing prosumer coalitions with energy management using cooperative game theory," *IEEE Transactions on Power Systems*, vol. 34, no. 1, pp. 303–313, 2018.

[23] J. Faraji, F. Vallée, and Z. De Grève, "A preference-informed energy sharing framework for a renewable energy community," *IEEE Transactions on Energy Markets, Policy and Regulation*, vol. 2, no. 4, pp. 503–518, 2024.

[24] C. Chen, S. Bose, T. D. Mount, and L. Tong, "Wholesale market participation of deras: DSO-DERA-ISO coordination," *IEEE Transactions on Power Systems*, vol. 39, no. 5, pp. 6605–6614, 2024.

[25] "How does the energy price cap work?" Accessed: June 23, 2025. [Online]. https://www.nerdwallet.com/uk/personal-finance/what-is-the-energy-price-cap/, April 2025.

[26] C. Chen, A. S. Alahmed, T. D. Mount, and L. Tong, "Competitive DER aggregation for participation in wholesale markets," *in Proceedings of the 56th Hawaii International Conference on System Sciences.*, 2023.

[27] A. S. Alahmed and L. Tong, "On net energy metering X: Optimal prosumer decisions, social welfare, and cross-subsidies," *IEEE Transactions on Smart Grid*, 2022.

[28] ISO-NE. (2019) Continuous storage facility participation. Accessed: June 9, 2024. [Online]. https://www.iso-ne.com/static-assets/documents/2019/02/20190221-csf.pdf.
[29] ——. (2021) Order no. 2222: Participation of distributed energy resource aggregations in wholesale markets. Accessed: June 9, 2024. [Online]. https://www.iso-ne.com/static-assets/documents/2021/07/a7_order_2222.pdf.
[30] "Italy publishes interactive map of substations for energy communities," Accessed: June 23, 2025. [Online]. https://www.pv-magazine.com/2023/10/06/italy-publishes-interactive-map-of-substations-for-energy-communities/, October 2023.
[31] H. R. Varian, "The nonparametric approach to demand analysis," *Econometrica: Journal of the Econometric Society*, pp. 945–973, 1982.
[32] C. Chen, A. S. Alahmed, T. D. Mount, and L. Tong, "Appendix: Wholesale market participation of DERA: Competitive DER aggregation," Accessed: June 29, 2025. [Online]. http://arxiv.org/abs/2307.02004, June 2024.
[33] H. R. Varian, *Price discrimination*. Elsevier, 1989, vol. 1.
[34] "Solar power in california," Accessed: July 4, 2025. [Online]. https://en.wikipedia.org/wiki/Solar_power_in_California, April 2023.
[35] P. Billingsley, *Probability and measure*. John Wiley & Sons, 2008.
[36] G. A. Jehle and P. J. Reny, *Advanced microeconomic theory*. Pearson, 2011.
[37] "CAISO price map," Accessed: July 3, 2025. [Online]. https://www.caiso.com/todays-outlook/prices.
[38] "Pecan street dataport," Accessed: July 3, 2025. [Online]. https://www.pecanstreet.org/dataport/, 2024.

8. NEM Benchmarks

Considering the benchmark performance of a regulated utility offering the NEM tariff, we extend the results in [3, 27] and present closed-form characterizations of consumer/prosumer surpluses. For simplicity, we consider one representative prosumer by setting $\mathscr{N}_m = 1, K = 1$ and dropping the prosumer index n and PoA index m. The prosumer's net consumption is $z := d - g$, where $g \in [0, \infty)$ is the BTM distributed generation (DG). The prosumer is a producer if $z < 0$ and a consumer if $z \geq 0$.

In evaluating the benchmark prosumer surplus under a regulated utility, we assume that the prosumer maximizes its surplus under the utility's NEM tariff, where π^+ is the retail (consumption) rate, π^- the sell (production) rate, and π^0 the connection charge. In general $\pi^- \leq \pi^+$ under NEM tariff, and the prosumer's energy bill $P(z)$ for the net consumption z is given by the convex function $P(z) := \max\{\pi^+ z, \pi^- z\} + \pi^0$. The prosumer surplus under NEM is $S(d) := U(d) - P(z)$.

For an *active prosumer* whose consumption is a function of the available DG output g, the optimal consumption can be obtained by $d_{\text{NEM-a}} := \arg\max_{d \in \mathscr{D}} (U(d) - P(d - g))$. For the fairness of comparison, we assume the aggregated customer is subject to the same distribution network injection and withdrawal access limits, *i.e.,* $-\underline{C} \leq g - d \leq \overline{C}$, which is the same as that applied to the proposed DERA optimization (3.6). So, for the above optimization, the domain is $\mathscr{D} := [\max\{\underline{d}, g - \overline{C}\}, \min\{\bar{d}, g + \underline{C}\}]$.

The surplus $S_{\text{NEM-a}}$ and the consumption $d_{\text{NEM-a}}$ of an active prosumer are given by the following equations.

$$\begin{aligned} S_{\text{NEM-a}}(g, \underline{C}, \overline{C}) &= U(d_{\text{NEM-a}}) - P(d_{\text{NEM-a}} - g) \\ &= \begin{cases} U(d^-) - \pi^-(d^- - g) - \pi^0, & g \geq d^- \\ U(d^+) - \pi^+(d^+ - g) - \pi^0, & g \leq d^+ \\ U(d^0) - \pi^0, & \text{otherwise} \end{cases} \\ d_{\text{NEM-a}} &= \max\{d^+, \min\{g, d^-\}\}, \end{aligned} \tag{8.1}$$

where $d^+ := f(\pi^+)$, $d^- := f(\pi^-)$, $d^0 := f(\mu^*(g))$ with

$$f(x) := \max\{\underline{d}, g - \overline{C}, \min\{V^{-1}(x), \bar{d}, g + \underline{C}\}\}, \tag{8.2}$$

and, by solving $f(\mu) = g$, we have $\mu^*(g) \in [\pi^-, \pi^+]$.

A prosumer is called passive if it decides energy consumption without the awareness of its DG output and the influence brought by NEM X switching among π^- and π^+. The optimal consumption bundle of such a *passive prosumer* under the NEM X tariff is given by $d_{\text{NEM-p}} :=$

$\arg\max_{d\in\mathscr{D}}(U(d)-\pi^+ d)$. The total consumption $d_{\text{NEM-p}}$ and the surplus $S_{\text{NEM-p}}$ of a *passive prosumer* are given by

$$\begin{aligned} S_{\text{NEM-p}}(g,\underline{C},\overline{C}) &= U(d_{\text{NEM-p}}) - P(d_{\text{NEM-p}}-g) \qquad (8.3)\\ &= \begin{cases} U(d^+)-\pi^-(d^+-g)-\pi^0, & g\geq d^+ \\ U(d^+)-\pi^+(d^+-g)-\pi^0, & g<d^+ \end{cases} \\ d_{\text{NEM-p}} &= d^+. \qquad (8.4) \end{aligned}$$

In summary, the prosumer surplus under NEM, $S_{\text{NEM}}(g,\underline{C},\overline{C})$ is given by

$$S_{\text{NEM}}(g,\underline{C},\overline{C}) = \begin{cases} S_{\text{NEM-a}}(g,\underline{C},\overline{C}), & \text{active prosumer,} \\ S_{\text{NEM-p}}(g,\underline{C},\overline{C}), & \text{passive prosumer.} \end{cases} \qquad (8.5)$$

Part III

Coordinating Transmission and Distribution System Operations for Intensive DER Integration: A Parametric Programming Approach

Meng Wu
Mohammad Mousavi, Graduate Student

Arizona State University

For information about this project, contact:

Meng Wu
Arizona State University
mwu@asu.edu

Power Systems Engineering Research Center

The Power Systems Engineering Research Center (PSERC) is a multi-university Center conducting research on challenges facing the electric power industry and educating the next generation of power engineers. More information about PSERC can be found at the Center's website: http://www.pserc.org.

For additional information, contact:

Power Systems Engineering Research Center
Arizona State University
527 Engineering Research Center
Tempe, Arizona 85287-5706
Phone: 480-965-1643
Fax: 480-727-2052

Table of Contents

List of Figures

List of Tables

1. Introduction

The ever-growing penetration of distributed energy resources (DERs) and electrified transportation to achieve 100% clean electricity in US by 2035 conveys a profound paradigm shift for electricity markets, and renders the existing paradigm of electricity market design and operation inadequate to address imminent system reliability and economic efficiency challenges in future DER-rich markets. Specifically, DER-rich wholesale market operation requires online transmission and distribution (T&D) coordination, since DERs are located down the distribution feeders, while independent system operators (ISOs) only model, observe, and dispatch transmission networks and resources. However, T&D coordination is extremely limited in today's industry practice, which will significantly challenge the operational reliability and economic efficiency of future DER-rich systems [1], as 1) DER aggregators in ISO markets can control numerous DERs across the distribution grids without knowing distribution operating constraints, causing distribution-level voltage/thermal violations and even outages; and 2) integrating numerous DER aggregators into ISO markets can cause significant computation burden, divergence, and price oscillations to ISO's unit commitment (UC) and economic dispatch (ED), damaging ISO market efficiency.

Part III of this report establishes full-scale online T&D coordination in future DER-rich markets, by developing theoretical coordination frameworks, low-time-complexity algorithms, and distribution system pricing designs. To ensure real-world applicability, we will strictly follow several design requirements for DER-rich T&D-coordinated markets. 1) Under extremely limited communications between T&D systems, T&D operation should be coordinated with minimal T&D communications. 2) To respect data ownership and model confidentiality, exchanging T&D system models should be avoided. 3) To enable smooth transition from today's established ISO markets, T&D coordination should minimize the changes to ISO's existing market operations. 4) T&D-coordinated markets should guarantee optimal operation while satisfying all the operating constraints for the entire T&D systems. 5) To enable online operations, computations of large-scale T&D-coordinated markets should be fast. The above requirements call for fast online coordination of a large-scale decentralized network optimization problem under extremely limited communications and zero model exchange, which is theoretically and computationally challenging.

To address the above technical challenges, three chapters are presented in Part III of this report.

- Chapter 1: Theoretical frameworks for the T&D-coordinated market operation with guaranteed real-world applicability, by leveraging parametric-programming-based multilevel system decomposition.
- Chapter 2: Distribution system pricing designs which can efficiently and economically support the T&D-coordinated economic dispatch based on parametric programming.
- Chapter 3: Low-time-complexity algorithms for the online T&D-coordinated market operation, by developing minimum cost flow algorithms and cutting plane methods.

2. TSO-DSO Coordination - A Parametric Programming Framework

2.1 Introduction

The Federal Energy Regulatory Commission (FERC) issued Order No. 2222 which requires all the US independent system operators (ISOs) to open their wholesale energy and ancillary service markets to the distributed energy resources (DER) aggregators market participation [2]. However, the uncontrolled participation of DER aggregators in the wholesale market may cause security and reliability issues in the distribution system. To overcome this issue, designing a distribution system operator (DSO) for coordinating the DER aggregators has been proposed [3]. However, the operation of the DSO should be compatible with the current practice of the wholesale markets operated by independent system operators (ISOs). Hence, the operation of the DSO and ISO should be coordinated.

Recently, several works have studied the coordination of the ISO and DSO [4–24]. They fall into three categories based on the modeling and solution method. The first category proposed bi-level models with the ISO and DSO markets modeled at two levels. The problem is transformed to single level optimization [4–9]. In [4], a bi-level optimization model is proposed for DSO market clearing and pricing considering ISO-DSO coordination. The clearing conditions for the DSO and ISO markets are proposed in the upper-level and lower-level problems, respectively. The problem is converted to mixed-integer linear programming via an equilibrium problem with equilibrium constraints (EPEC) approach. In [5], a bi-level optimization model is proposed for the energy storage sizing and siting problem in the DSO-ISO coordination framework. In [6], a bi-level optimization model is proposed for the energy and flexibility market in which, the upper-level models the clearing conditions of the transmission level market while, in the lower level, clearing conditions of the distribution level market are modeled. In [7], a coordination scheme is proposed for energy service providers, transmission system operator (TSO), and DSO for DER planning while coordinating the operation of the TSO and DSO based on bi-level optimization. In the upper-level problem, the DSO cost is minimized and the profit of the energy service providers is ensured while the lower-level problem models the transmission level constraints and wholesale market. In [8], a bi-level optimization model is proposed for the coordinated operation of active distribution networks with multiple virtual power plants in joint energy and reserve markets operated by the DSO. At the upper level, the DSO minimizes the total operational cost of the distribution system while in the lower level problem, virtual power plants maximize their profit. In [9] a tri-level coordinated scheme for transmission and distribution (T&D) systems expansion planning is proposed. In the first and second levels, the expansion planning of T&D systems operated by the TSO and DSO are proposed, respectively. The third level is the economic dispatch problem performed by the ISO. The multi-parametric programming approach is used to convert the multi-level optimization problem into a single-level optimization problem. Bi-level optimization models are computationally expensive and hard to solve especially for large systems. These approaches place a high computation burden on the wholesale market and is not compatible with the current practice of the wholesale market.

The second category of works uses decentralized models and some of them use decomposition algorithms to decouple the ISO and DSO markets [10–20]. In [10], an extension of the decentralized

market framework is proposed to consider loss allocation and its impact on the market outcome. However, the decentralized market framework is not compatible with the current market structures. In [11], a transactive market framework starting from the ISO to the DSO is proposed. The DSO runs the transactive market using an iterative method. However, the convergence of the proposed method is not guaranteed. In [12], a Nash bargaining-based method is proposed for the market-clearing process and the ISO-DSO coordination. The proposed model requires high ISO-DSO communication burden within each wholesale market clearing interval. In [13], a three-stage unit commitment (UC) is proposed for transmission-distribution coordination based on stochastic programming. A convex AC branch flow model is proposed to handle the distribution grid's physical constraints. However, stochastic programming is not compatible with the current practice of the wholesale market. In [14], a distributed optimization algorithm is proposed for modeling the DSO retail market considering energy and ancillary services. However, the DSO's impact on wholesale market clearing is not considered. In [15], the optimal operation and coordination of the ISO-DSO are proposed. A decomposition algorithm is proposed and the original problem is decomposed into ISO and DSO sub-problems. In [16], a non-cooperative game approach is proposed for ISO-DSO coordination in which they optimize their operational costs. The approaches in [15, 16] are hard to solve for large systems. In [17], a coordination framework for coordinating the economic dispatch of the TSO and DSO is proposed. Benders' decomposition is used for solving the proposed problem. In [18], a coordination framework is proposed for the dynamic economic dispatch problem of the ISO and DSO. A decentralized approach is proposed to solve this problem. Nevertheless, References [17, 18] do not propose any market framework or settlement. In [19], an economic dispatch for co-optimization of T&D systems is proposed. Primal-dual gradient algorithm based on the Lagrangian function is proposed to solve the co-optimization problem. However, the proposed method is not appropriate for a large number of DERs in the distribution system as it places so much computation burden on the economic dispatch of the wholesale market.

The third group of works proposed equivalent models for T&D coordination [21–24]. In [21], a feasible region-based approach is proposed for the integration of DERs into the wholesale market considering the physical constraints of the distribution system operated by the DSO. In [22], a multi-port power exchange model is proposed to integrate the high penetration of the DERs into the wholesale market considering the physical constraints of the distribution network. The approaches in [21] and [22] require modeling a transformed version of the distribution level constraints in the ISO market clearing problem, which significantly increases the modeling and computational complexity for the ISO. In [23], a unified equivalent model for external power networks based on multi-parametric programming is proposed for determining the transfer capacity of tie lines. However, they have not considered the distribution system and the market settlement of these external power networks. In [24], a coordinated economic dispatch is proposed for a multi-area power system based on parametric programming. However, no market framework is proposed. Besides, this approach requires iterative communications between the coordinator and each economic dispatch sub-area before reaching convergence for the overall coordinated problem. This places very high communication burden between the market operators which is difficult to be implemented in real world applications.

Ideally speaking, the ISO-DSO coordination for DER integration in the wholesale market should satisfy the following requirements: 1) There should be no exchange of grid models between

T&D systems, in order to eliminate data confidentiality/privacy issues and avoid additional modeling/computational burden for ISO or DSO. 2) The coordination procedure should introduce no or minimal change to existing ISO wholesale market clearing procedure. 3) The coordination procedure should minimize the communication burden between ISO and DSO, by exchanging the minimal amount of public data and also by avoiding iterative T&D communications within each wholesale market clearing interval.

So far, there is no existing ISO-DSO coordination which fully satisfies the above requirements. Existing works either 1) exchange T&D grid models [4–9]; 2) introduce significant changes to existing ISO market clearing [10, 11, 13, 15–19]; or 3) introduce high ISO-DSO communication burden and iterative ISO-DSO communications within each wholesale market clearing interval [12, 14, 19–22].

This chapter proposes an ISO-DSO coordination framework which satisfies all the above requirements. The proposed framework coordinates the operation of ISO and DSO to leverage the wholesale market participation of DER aggregators while ensuring the secure operation of distribution grids. The proposed coordination framework is based on parametric programming. The DSO builds the bid-in cost function based on the distribution system market considering its market participants' constraints and distribution system physical constraints including the power balance equations and voltage limitation constraints. The DSO submits the resulting bid-in cost function to the wholesale market operated by the ISO. After the clearance of the wholesale market, the DSO determines the share of its DSO market participants (i.e., aggregators). Case studies are performed to verify the effectiveness of the proposed method.

This chapter extends our prior works in [3, 25–27]. To the best of our knowledge, this is the first ISO-DSO coordination framework which fully satisfies all the above performance requirements for ideal and practical ISO-DSO coordination. This is achieved by the following major contributions:

- A framework is proposed to coordinate the operation of the DSO and ISO which is compatible with the current structure of the wholesale market without introducing additional changes to existing wholesale market clearing procedure.
- In this coordination framework, the DER aggregators participate in the wholesale market through the coordination of the DSO, which ensures the secure operation of the distribution grid. A parametric programming approach is proposed to construct the bid-in cost function of the DSO (to be submitted to the ISO) and run the DSO-level market clearing procedure, which is built upon the offers collected from the DER aggregators.
- A market settlement approach is proposed for the DSO, which coordinates with the wholesale market clearing process and ensures the DSO's non-profit characteristic. It is proved that under the proposed ISO-DSO coordination framework, each DER aggregator will receive identical dispatch signals and payments when they participate in the wholesale market through the coordination of the DSO and when they participate in the wholesale market directly with the ISO overseeing all the transmission-level and distribution-level operating constraints.
- The parametric-programming-based ISO-DSO coordination enables complete decoupling

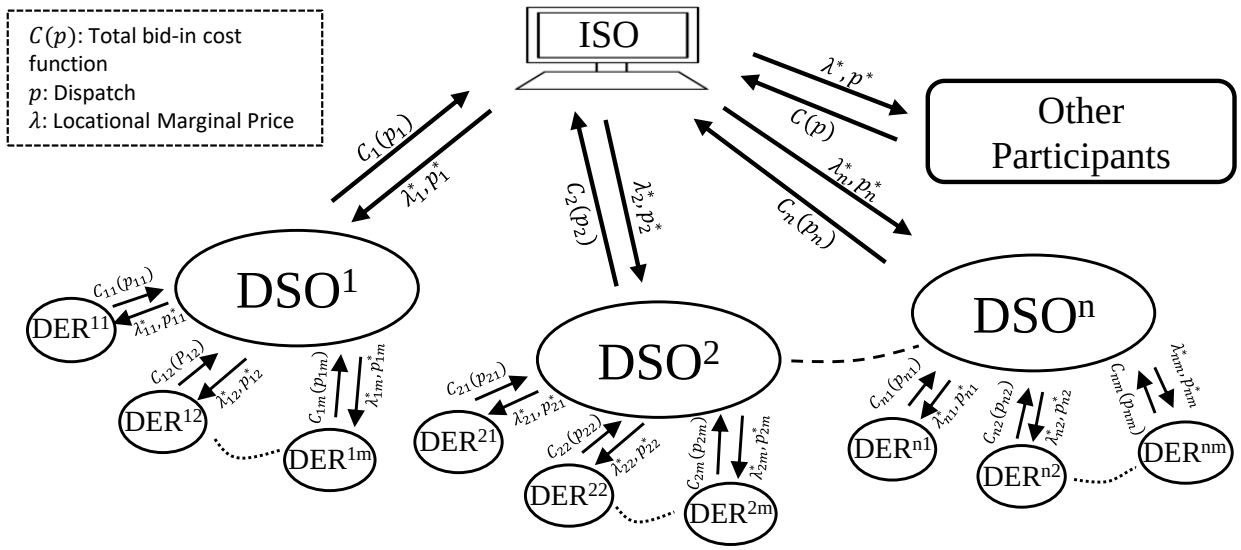

Figure 2.1: The framework of the ISO-DSO coordination.

between the solution process of the ISO and DSO optimization sub-problems. This avoids iterative ISO-DSO communications within each wholesale market clearing interval and allows the ISO and DSO to exchange the minimal amount of public data only after each entity reaches its optimal solution. The proposed approach requires no exchange of private/confidential ISO or DSO grid model data.

- The DSO's market outcomes and market settlement process are investigated through case studies on the modified IEEE 33-node and 240-node distribution test systems.

The rest of the chapter is organized as follows. Section 2.2 presents general idea of the DSO and ISO coordination framework. Section 2.3 presents the mathematical formulation of ISO-DSO coordination framework. Section 2.4 proposes the market settlement approach for the ISO-DSO coordination framework. Section 2.5 discusses the case studies. Section 2.6 presents the concluding remarks.

2.2 The ISO-DSO Coordination Framework

In this section, the proposed ISO-DSO coordination framework, which is shown in Fig. 2.1, is explained. In this work, the DSO is defined as a non-profit entity [28] that deals with the wholesale market on one side and coordinates the DER aggregators on the other side. The DER aggregators participate in the wholesale market through the coordination of the DSO, instead of directly participating in the wholesale market. The DER aggregators submit their offers to the DSO. The DSO gathers all these aggregated DER offers and runs the DSO market at the distribution level to construct the bid-in cost function of the DSO using a parametric programming approach. Then, the DSO submits that bid-in cost function to the wholesale market operated by the ISO. The ISO gathers the bid-in cost functions from all the DSOs as well as from other market participants and clears the wholesale market. Then, the ISO sends the dispatches and loactional

marginal prices (LMPs) to the DSOs and other market participants. Once each DSO receives the wholesale-level dispatch and LMP from the ISO, the DSO will determine the optimal operating point of the DSO market and determine the optimal dispatches of the DER aggregators in the DSO territory. Then, each DSO will determine the distribution LMPs (D-LMPs) in the distribution system based on the wholesale-level dispatch and LMP received by the DSO from the ISO at the coupling substation. The DSO will also settle the DSO market participants (i.e., DER aggregators) based on these D-LMPs. Following this procedure, the optimal dispatches and LMPs for all the ISO-level and DSO-level market participants determined by this ISO-DSO coordination framework will be identical to those determined by the ideal case in which the ISO oversees all the T&D-level operating constraints. This procedure eliminates the ISO's modeling/computation burden since it avoids sending the distribution grid model data to the ISO by allowing the distribution-level operating constraints and computations to be handled by each DSOs (instead of the ISO).

2.3 ISO-DSO Coordination Formulation

In this section, the mathematical formulation of the proposed ISO-DSO coordination framework is presented. In order to evaluate the proposed ISO-DSO coordination, an ideal case in which the ISO can oversee all the T&D-level operating constraints and the DER aggregators can participate in the wholesale market directly is defined and formulated. Then, the formulation of the ISO-DSO coordination is proposed.

2.3.1 Ideal Case

To perform market clearing computations for generating resources in both transmission-level and distribution-level systems (i.e., the conventional generators and DERs), as well as ensuring the secure operation of both T&D systems, an ideal market framework will be letting one single entity (the ISO) 1) collect both T&D-level offers/bids (i.e., the bid-in cost functions) from all the conventional generators and DER aggregators; 2) oversee both T&D-level operating constraints; and 3) optimally dispatch both T&D-level resources (conventional generators and DER aggregators). However, this ideal case is not implementable with the current practice of the wholesale market since 1) the distribution system is not observable to the ISO 2) considering all these small DER aggregators and all the distribution-level constraints in the wholesale market increases the computation burden of the ISO problem. This chapter addresses this implementability issue by decomposing this ideal case into one ISO and multiple DSO sub-problems. This decomposition allows the distribution-level modeling and computation burden to be handled by each DSO, such that the ISO only needs to handle transmission-level modeling and computation while coordinating with the DSOs. The following sections prove that the proposed ISO-DSO coordination framework and this ideal case achieve identical optimal dispatches and LMPs for all the T&D-level market participants (generators and DER aggregators).

This ideal case is formulated as follows.

$$\text{Min}_{\boldsymbol{p}} \quad \sum_{i\in\mathcal{N}_{gen}} c_i^g p_i^g + \sum_{j\in\mathcal{N}_{dis}} \sum_{i\in\mathcal{N}_{agg}} c_{i,j}^{agg} p_{i,j}^{agg} \tag{2.1a}$$

s.t.

$$\sum_{i\in\mathcal{N}_{gen_n}} p_i^g + \sum_{k\in\mathcal{N}_{\cdot,n}} F_k - \sum_{k\in\mathcal{N}_{n,\cdot}} F_k - L_n = 0;\ \forall n \in \mathcal{N}_{tra} \tag{2.1b}$$

$$\underline{p_i^g} \le p_i^g \le \overline{p_i^g};\ \forall i \in \mathcal{N}_{gen} \tag{2.1c}$$

$$-\overline{F_k} \le F_k \le \overline{F_k}; \forall k \in \mathcal{N}_l \tag{2.1d}$$

$$\sum_{i\in\mathcal{N}_{aggn}} p_{i,j}^{agg} + \sum_{k\in\mathcal{N}_{jn,\cdot}^d} f_{k,j} - \sum_{k\in\mathcal{N}_{jn,\cdot}^d} f_{k,j} - l_{n,j} = 0 \tag{2.1e}$$

$$\forall n \in \mathcal{N}_j^d, \forall j \in \mathcal{N}_{dis}$$

$$\sum_{i\in\mathcal{N}_{aggn}} q_{i,j}^{agg} + \sum_{k\in\mathcal{N}_{jn,\cdot}^d} q_{k,j} - \sum_{k\in\mathcal{N}_{jn,\cdot}^d} q_{k,j} - q_{n,j} = 0 \tag{2.1f}$$

$$\forall n \in \mathcal{N}_j^d, \forall j \in \mathcal{N}_{dis}$$

$$\underline{p_{i,j}^{agg}} \le p_{i,j}^{agg} \le \overline{p_{i,j}^{agg}};\ i \in \mathcal{N}_{agg}, j \in \mathcal{N}_{dis} \tag{2.1g}$$

$$-\overline{f_{k,j}} \le f_{k,j} \le \overline{f_{k,j}};\ k \in \mathcal{N}_j^l, j \in \mathcal{N}_{dis} \tag{2.1h}$$

$$U_{m,j} = U_{n,j} - 2(r_{k,j} f_{k,j} + x_{k,j} q_{k,j}) \tag{2.1i}$$

$$\forall n \in \mathcal{N}_j^d, j \in \mathcal{N}_{dis}, (m,n,k) \in \mathcal{N}_C$$

$$\underline{U} \le U_{n,j} \le \overline{U}; \forall n \in \mathcal{N}_j^d, j \in \mathcal{N}_{dis} \tag{2.1j}$$

$$-\overline{q_{k,j}} \le q_{k,j} \le \overline{q_{k,j}};\ k \in \mathcal{N}_j^l, j \in \mathcal{N}_{dis} \tag{2.1k}$$

where i and j represent indices for market participants (generators/aggregators) and distribution grids in the ISO territory, respectively. p_i^g and $p_{i,j}^{agg}$ denote the dispatched power, while $c_i^g(p_i^g)$ and $c_{i,j}^{agg}(p_{i,j}^{agg})$ are the bid-in cost functions of generators in the transmission system and aggregators in distribution systems under the ISO territory, respectively. The sets $\mathcal{N}_{gen}$, $\mathcal{N}_{dis}$, and $\mathcal{N}_{agg}$ represent all generators in the transmission systems, all distribution systems, and all aggregators in the corresponding distribution systems, respectively. F_k denotes the active line flow in transmission lines, while L_n represents the active power load at each bus in the transmission system. The sets $\mathcal{N}_{gen_n}$, $\mathcal{N}_{\cdot,n}$, and $\mathcal{N}_{n,\cdot}$ include all generators connected to bus n, all lines coming to bus n, and all lines leaving bus n, respectively. $\underline{p_i^g}$ and $\overline{p_i^g}$ denote the minimum and maximum generating power of each generator in the transmission system, respectively, and $\overline{F_k}$ represents the transmission line capacity. Additionally, $f_{k,j}$ denotes the DSO level branch active power flow, and $l_{n,j}$ represents the active power load at each node in the DSO. The sets $\mathcal{N}_{agg_n}$, $\mathcal{N}_{jn,\cdot}^d$, $\mathcal{N}_{jn,\cdot}^d$, and $\mathcal{N}_j^d$ represent all aggregators connected to node n, all branches coming to node n, all branches leaving node n, and all nodes in the distribution systems, respectively. qk, j and $q_{n,j}$ denote the reactive power flow in the distribution systems branches and the reactive power load at each node in the distribution systems, respectively. $\underline{p_{i,j}^{agg}}$ and $\overline{p_{i,j}^{agg}}$ represent the minimum and maximum generation of the aggregators, respectively.

$\overline{f_{k,j}}$ denotes the capacity of distribution systems branches. $U_{m,j}$ represents the square of the voltage of nodes. $r_{k,j}$ and $x_{k,j}$ denote the resistance and reactance of branches in the distribution systems, respectively. The set $\mathcal{N}_C$ includes all lines and their corresponding start and end nodes. $\underline{U}$ and $\overline{U}$ represent the minimum and maximum permitted voltage, respectively. Lastly, $\overline{q_{k,j}}$ denotes the reactive power capacity of branches in the distribution systems.

Equation (2.1a) minimizes the total cost function of the wholesale market, taking into account all generators and DER aggregators. Equation (2.1b) presents the power balance equations in the transmission system. Equation (2.1c) imposes limits on the generating output of transmission system generators. Equation (2.1d) represents the limits on the transmission lines. Equations (2.1e) and (2.1f) represent the active and reactive power balance in distribution systems, respectively. Equation (2.1g) limits the power of aggregators. Equation (2.1h) sets the limits on distribution level branches. Equation (2.1i) defines the voltage in distribution systems. Equation (2.1j) restricts the voltage of distribution nodes within the permitted range. Lastly, Equation (2.1k) limits the reactive power flow on the distribution system branches.

2.3.2 ISO-DSO Coordination

In this section, the mathematical formulation of the proposed ISO-DSO coordination framework is presented. This framework decomposes the above ideal case into one ISO sub-problem and multiple DSO sub-problems. Each DSO sub-problem can be solved independently. This framework and the ideal case will result in identical optimal dispatch and payment/LMP to each of the T&D-level market participants. However, the decomposition in this framework reduces the computation and modeling burden of the ISO by moving all the distribution-level decision variables and constraints to each DSO's sub-problem.

The ISO sub-problem is formulated as follows:

$$\text{Min}_{\boldsymbol{p}} \quad \sum_{i\in\mathcal{N}_{gen}} c_i^g p_i^g + \sum_{j\in\mathcal{N}_{dis}} \sum_{a\in\mathcal{D}_j} c_{j,a}^{dso} p_{j,a}^{dso} \tag{2.2a}$$

s.t.

$$\sum_{i\in\mathcal{N}_{gen_n}} p^g + \sum_{k\in\mathcal{N}_{\cdot,n}} F_k - \sum_{k\in\mathcal{N}_{n,\cdot}} F_k - L_n = 0;\ \forall n \in \mathcal{N}_{tra} \tag{2.2b}$$

$$\underline{p_i^g} \le p_i^g \le \overline{p_i^g};\ \forall i \in \mathcal{N}_{gen} \tag{2.2c}$$

$$-\overline{F_k} \le F_k \le \overline{F_k}; \forall k \in \mathcal{N}_l \tag{2.2d}$$

$$0 \le p_{j,a}^{dso} \le \overline{p_{j,a}^{dso}};\ j \in \mathcal{N}_{dis}, a \in \mathcal{D}_j \tag{2.2e}$$

Equation (2.2a) minimizes the total cost in the wholesale market, after collecting the bid-in cost functions from all the wholesale market participants (including conventional generators and DSOs). Other equations has been explained in the ideal case formulation.

Each DSO j needs to determine its bid-in cost function $c_j^{dso}(p_j^{dso})$ and the corresponding DSO

operating constraints S_j^{dso} to be submitted to the wholesale market (the above ISO sub-problem). The bid-in cost function $c_j^{dso}(p_j^{dso})$ is dependent on the parameter p_j^{dso}, which is derived from minimizing the total cost in the distribution system while satisfying all system constraints. An optimization problem in which data depends on one or multiple parameters is known as parametric programming [29]. We propose the following parametric programming approach for each DSO j to determine these data.

$$c_j^{dso}(p_j^{dso}) = \text{Min}_{\boldsymbol{p}^{agg}} \sum_{i \in \mathcal{N}_{agg}} c_{i,j}^{agg} p_{i,j}^{agg} \tag{2.3a}$$

$$s.t.$$

$$\sum_{i \in \mathcal{N}_{agg_n}} p_{i,j}^{agg} + \sum_{k \in \mathcal{N}_{jn,.}^{d}} f_{k,j} - \sum_{k \in \mathcal{N}_{jn,.}^{d}} f_{k,j} - l_{n,j} = 0 \tag{2.3b}$$

$$\forall n \in \mathcal{N}_j^d, \forall j \in \mathcal{N}_{dis}$$

$$\sum_{i \in \mathcal{N}_{agg_n}} q_{i,j}^{agg} + \sum_{k \in \mathcal{N}_{jn,.}^{d}} q_{k,j} - \sum_{k \in \mathcal{N}_{jn,.}^{d}} q_{k,j} - q_{n,j} = 0 \tag{2.3c}$$

$$\forall n \in \mathcal{N}_j^d, \forall j \in \mathcal{N}_{dis}$$

$$\underline{p_{i,j}^{agg}} \leq p_{i,j}^{agg} \leq \overline{p_{i,j}^{agg}};\ i \in \mathcal{N}_{agg}, j \in \mathcal{N}_{dis} \tag{2.3d}$$

$$-\overline{f_{k,j}} \leq f_{k,j} \leq \overline{f_{k,j}};\ k \in \mathcal{N}_j^l, j \in \mathcal{N}_{dis} \tag{2.3e}$$

$$U_{m,j} = U_{n,j} - 2(r_{k,j} f_{k,j} + x_{k,j} q_{k,j}) \tag{2.3f}$$

$$\forall n \in \mathcal{N}_j^d, j \in \mathcal{N}_{dis}, (m,n,k) \in \mathcal{N}_C$$

$$\underline{U} \leq U_n \leq \overline{U}; \forall n \in \mathcal{N}_j^d, j \in \mathcal{N}_{dis} \tag{2.3g}$$

$$-\overline{q_{k,j}} \leq q_{k,j} \leq \overline{q_{k,j}};\ k \in \mathcal{N}_j^l, j \in \mathcal{N}_{dis} \tag{2.3h}$$

where k is the substation node of DSO j; l is the index for branches; $\mathcal{N}_{f_k}$ is the set of all branches connected to node k; $f_{l,j}$ is the flow on branch l of DSO j; $L_{k,j}$ is the firm load of node k in DSO j.

Equation (3.3) defines a parametric programming problem, where p_j^{dso} is treated as a parameter in the minimization problem. Note that while the power balance equation at the substation is explicitly presented as the equality constraint, the power balance constraints in other nodes are incorporated in S_j^{Dis}. After collecting bid-in cost functions from all the DSO-level market participants (i.e., DER aggregators), for every possible p_j^{dso} value, this problem minimizes the total generation cost in the DSO-level market while satisfying the following constraints: 1) power balance constraint at each node; 2) the operating constraints of DER aggregators; and 3) the system-wide distribution grid constraints. Linearized three-phase power flow is considered which ignores losses [30]. Please note that in the objective function (3.3), both generating and demand response aggregators are defined. For the demand response aggregator, the corresponding price $c_{i,j}^{agg}$ is negative. The energy storage aggregator can be considered either as a demand response aggregator or as a generating aggregator, as this is a single interval formulation.

Before the ISO market clearing run, each DSO collects the bid-in cost functions from all the DSO-level market participants (i.e., the DER aggregators) in its territory and solves (3.3) to determine its DSO bid-in cost function $c_j^{dso}(p_j^{dso})$ and the corresponding DSO operating constraints S_j^{dso} (i.e., the upper/lower limits for the DSO bid-in cost function) to be submitted to the wholesale market in the ISO sub-problem. The ISO collects the bid-in cost functions from all the DSOs and other ISO-level market participants (such as conventional generators), which allows the ISO to clear the wholesale market by solving problem (3.2).

Lemma 1. *The optimal bid-in cost function from DSO to ISO, $c_j^{dso}(p_j^{dso})$, is a convex function of parameter p_j^{dso}, if the following conditions are all satisfied: 1) the bid-in cost function submitted by each aggregator $c_{i,j}^{agg}(p_{i,j}^{agg})$ is a convex function; 2) the operating constraints of each DER aggregator define a convex set $S_{i,j}^{agg}$; and 3) the system-wide distribution grid constraints define a convex set S_j^{Dis}.*

The convexity of the optimal DSO bid-in cost function $c_j^{dso}(p_j^{dso})$ ensures that our proposed ISO-DSO coordination is compatible with the current wholesale market structure, by allowing each DSO to always submit a convex bid-in cost function to the ISO. The ISO can then directly clear the wholesale market following its current market clearing procedure without introducing any additional change.

After the ISO clears the wholesale market, the dispatch and LMP data is distributed to all the DSOs. Each DSO utilizes the LMP of the coupling substation, as determined by the ISO, and employs it as the wholesale market price in the subsequent proceedings.

$$\mathrm{Min}_{\boldsymbol{p}^{agg}} \sum_{i\in\mathcal{N}_{agg}} c_{i,j}^{agg} p_{i,j}^{agg} - LMP_j^* p_j^{dso} \tag{2.4a}$$

$s.t.$

$$\sum_{i\in\mathcal{N}_{agg_n}} p_{i,j}^{agg} + \sum_{k\in\mathcal{N}_{jn,\cdot}^d} f_{k,j} - \sum_{k\in\mathcal{N}_{jn,\cdot}^d} f_{k,j} - l_{n,j} = 0 \tag{2.4b}$$

$\forall n \in \mathcal{N}_j^d, \forall j \in \mathcal{N}_{dis}$

$$\sum_{i\in\mathcal{N}_{agg_n}} q_{i,j}^{agg} + \sum_{k\in\mathcal{N}_{jn,\cdot}^d} q_{k,j} - \sum_{k\in\mathcal{N}_{jn,\cdot}^d} q_{k,j} - q_{n,j} = 0 \tag{2.4c}$$

$\forall n \in \mathcal{N}_j^d, \forall j \in \mathcal{N}_{dis}$

$$\underline{p_{i,j}^{agg}} \le p_{i,j}^{agg} \le \overline{p_{i,j}^{agg}};\ i \in \mathcal{N}_{agg}, j \in \mathcal{N}_{dis} \tag{2.4d}$$

$$-\overline{f_{k,j}} \le f_{k,j} \le \overline{f_{k,j}};\ k \in \mathcal{N}_j^l, j \in \mathcal{N}_{dis} \tag{2.4e}$$

$$U_{m,j} = U_{n,j} - 2(r_{k,j} f_{k,j} + x_{k,j} q_{k,j}) \tag{2.4f}$$

$\forall n \in \mathcal{N}_j^d, j \in \mathcal{N}_{dis}, (m,n,k) \in \mathcal{N}_C$

$$\underline{U} \le U_n \le \overline{U}; \forall n \in \mathcal{N}_j^d, j \in \mathcal{N}_{dis} \tag{2.4g}$$

$$-\overline{q_{k,j}} \le q_{k,j} \le \overline{q_{k,j}};\ k \in \mathcal{N}_j^l, j \in \mathcal{N}_{dis} \tag{2.4h}$$

where LMP_j^* is the optimal wholesale LMP determined by ISO market clearing at the bus where the DSO j is located.

Section 2.4 presents the detailed DSO market settlement procedure for each DSO to utilize (3.3) and (3.4) to determine the optimal dispatch and distribution LMPs (D-LMPs) for all the aggregators in the DSO territory.

A detailed formulation for the above DSO sub-problem in (3.3)-(3.4) which considers the real/reactive power flow limits and voltage limits using the linearized three-phase distribution power flow [30] is presented below.

$$c^{dso}(P^{dso}) = Min \sum_{g\in G}\sum_{b\in B} P_{g,b}\pi_{g,b} - \sum_{d\in D}\sum_{b\in B} P_{d,b}\pi_{d,b} \tag{2.5a}$$

s.t.

$$\begin{aligned}&\sum_{d\in D}\sum_{b\in B} H_{n,d}P_{d,b} + H_n^{sub}P^{dso} + L_n^P \\ &- \sum_{g\in G}\sum_{b\in B} H_{n,g}P_{g,b} + \sum_{j\in J} Pl_j A_{j,n} = 0; \quad \forall n \in N\end{aligned} \tag{2.5b}$$

$$\begin{aligned}&\sum_{d\in D}\sum_{b\in B} H_{n,d}P_{d,b}tan\phi_d + H_n^{sub}Q^{dso} + L_n^Q \\ &- \sum_{g\in G}\sum_{b\in B} H_{n,g}P_{g,b}tan\phi_g + \sum_{j\in J} Ql_j A_{j,n} = 0; \forall n \in N\end{aligned} \tag{2.5c}$$

$$0 \le P_{g,b} \le P_{b,g}^{max}; \quad \forall b \in B, \forall g \in G \tag{2.5d}$$

$$0 \le P_{d,b} \le P_{d,g}^{max}; \quad \forall b \in B, \forall d \in D \tag{2.5e}$$

$$\begin{aligned}&U_m = U_n - 2(r_j Pl_j + x_j Ql_j); \quad \forall m \in N, \\ &\qquad \forall n \in N,\ C(m,n) = 1,\ A(j,n) = 1\end{aligned} \tag{2.5f}$$

$$\underline{U} \le U_n \le \overline{U}; \quad \forall n \in N \tag{2.5g}$$

$$-Pl^{max} \le Pl_j \le Pl^{max}; \quad \forall j \in J \tag{2.5h}$$

$$-Ql^{max} \le Ql_j \le Ql^{max}; \quad \forall j \in J \tag{2.5i}$$

where g and G represent the index and set of all generating aggregators; d and D represent the index and set of all demand response aggregators; b and B represent the index and set of all production/demand blocks; j and J represent the index and set of all lines; n and N represent the index and set of all nodes; P^{dso} represents the DSO's aggregated offers to the ISO market; $P_{g,b}$ and $P_{d,b}$ represent the energy offers submitted by the generating aggregators and demand response aggregators, respectively, with corresponding prices $\pi_{g,b}$ and $\pi_{d,b}$; $H_{n,d}$, $H_{n,g}$, and H_n^{sub} represent the mapping matrices of generating aggregators, demand response aggregators, and substations to node n, respectively; Pl_j and Ql_j represent the active and reactive power of branch j, respectively; $A_{j,n}$ represents the incidence matrix of branches and nodes; ϕ_g and ϕ_d represent the phase angle of the generating aggregators and demand response aggregators, respectively; Q_n^D represents the

reactive power of the firm load at each node; L_n^P and L_n^Q represent the active and reactive power load at each node; $P_{g,b}^{max}$ and $P_{d,b}^{max}$ represent the maximum production/consumption at each block of the generating aggregators and demand response aggregators, respectively; U represents the square of the voltage of each node; $\underline{U}$ and $\overline{U}$ represent the square of the minimum and maximum permitted voltage values, respectively; r_j and x_j represent the resistance and reactance of the branches; Pl^{max} and Ql^{max} represent the maximum active and reactive power of the branches.

The objective function of the DSO which minimizes the total cost over the system is defined in (2.5a). Equations (2.5b) and (2.5c) define active and reactive power balances, respectively. The generating power of each DDG is limited by (2.5d). The power consumption by the demand response is limited with respect to the maximum value in (2.5e). The voltage of each branch is defined in (4.2) and is limited with respect to the allowed voltage range in (4.3). The active and reactive flow of each branch is limited in (2.5h) and (2.5i), respectively.

2.4 Market Settlement

In our proposed ISO-DSO coordination framework, the DSO is a nonprofit mediator that deals with the DER aggregators on one hand and trades with the wholesale market on the other hand. The DSO gathers the offers from all the DER aggregators and constructs the DSO bid-in cost function and submits it to the ISO based on the parametric programming procedure in (3.3). Once the ISO receives the bid-in cost functions from all the DSOs and other wholesale market participants, the ISO clears the wholesale market by solving (3.2) and determines the power dispatch p_j^{dso*} and LMP at the ISO-DSO coupling substation for each DSO. The DSO then needs to clear the DSO-level market with p_j^{dso*} and the wholesale-level LMP it receives at the ISO-DSO coupling substation. Each DSO performs this market settlement procedure by 1) letting $p_j^{dso} = p_j^{dso*}$ in (3.3) and solving (3.3) for the optimal dispatch of all the aggregators in the DSO territory when $p_j^{dso} = p_j^{dso*}$; 2) solving (3.4) and obtaining the dual variables of (3.4) as the optimal D-LMPs of all the aggregators in the DSO territory. We prove the theorems below which guarantees that following the above market settlement procedure, the optimal dispatches, LMPs (or D-LMPs), and payments received by all the ISO-level and DSO-level market participants under the proposed ISO-DSO coordination framework will be identical to those under the ideal case where the ISO serves as the single entity overseeing all the T&D-level market participants and operating constraints.

Theorem 1. *The optimal dispatches for all the ISO-level and DSO-level market participants under the ISO-DSO coordination framework in (3.2)-(3.3) are identical to those under the ideal case in (3.1).*

Theorem 2. *The optimal payments and LMPs (or D-LMPs) for all the ISO-level and DSO-level market participants under the ISO-DSO coordination framework in (3.2)-(3.4) are identical to those under the ideal case in (3.1).*

The above theorems further guarantee: 1) Our proposed ISO-DSO coordination framework completely decouples the optimization problem in the ideal case into one ISO and multiple DSO sub-problems. 2) After this decoupling, at each market clearing run, each DSO only needs to submit its convex bid-in cost function $c_j^{dso}(p_j^{dso})$ and the corresponding DSO operating constraints

(upper/lower limits) of this cost function S_j^{Dis} to the ISO, and the ISO only needs to send the optimal wholesale-level dispatch p_j^{dso*} and wholesale LMP back to each DSO. There is no data exchange between different DSOs and no exchange of confidential ISO or DSO grid models. This data exchange procedure is compatible with the current wholesale market clearing practice. It will result in the minimal amount of ISO-DSO data exchange without changing the existing wholesale market clearing procedure. Besides, this data exchange procedure also allows the ISO and DSO to exchange data only after each entity reaches its optimal solution. There is no iterative ISO-DSO data exchange during the iterative solution process of the ISO and DSO sub-problems. This ensures a complete decouple between the iterative solution process of the ISO and DSO sub-problems and eliminates the need for iterative ISO-DSO communications within each market clearing run.

2.5 Case Studies

In this section, case studies have been implemented to verify the effectiveness of the proposed ISO-DSO coordination model. First, a small illustrative example is studied to clearly describe our proposed approach. Then, a large system is studied which includes an IEEE 118-bus test system in the wholesale market and two distribution systems - the IEEE 33-node balanced and 240-node unbalanced distribution systems.

2.5.1 Illustrative Example

In this section, in order to understand the proposed ISO-DSO coordination clearly, a small illustrative example is given. The system consists of a generating unit (G) and a firm load (L) on the transmission side, as well as two dispatchable distributed generations (DDGs) on the distribution side. The system and its corresponding data are provided in Figure 2.2. The DSO parametric programming problem is as follows:

$$
\begin{aligned}
c^{dso}(P_{dso}) = \ \mathrm{Min}_{\boldsymbol{P}_{ddg}} \quad & 25P_{ddg_1} + 15P_{ddg_2} && \text{(2.6a)}\\
\text{s.t.} \quad & P_{ddg_1} + F_{ds} = P_{dso} && \text{(2.6b)}\\
& P_{ddg_2} - F_{ds} = 0 && \text{(2.6c)}\\
& 0 \le P_{ddg_1} \le 0.5 && \text{(2.6d)}\\
& 0 \le P_{ddg_2} \le 0.5 && \text{(2.6e)}\\
& -0.1 \le F_{ds} \le 0.1 && \text{(2.6f)}
\end{aligned}
$$

where $c^{dso}(P_{dso})$ is the bid-in cost function of the DSO; P_{dso} is the output power of the DSO injected; P_{ddg_1} is the active power provided by DDG 1; P_{ddg_2} is the active power provided by DDG 2; F_{ds} is the distribution line flow.

The problem described above is simple enough that we can determine the bid-in cost function by the following straightforward approach. We simply need to increase the P_{dso} and determine which DDG will provide power and at what cost. As we begin to increase P_{dso}, DDG 2 will be the cheaper option, so we can continue to increase P_{dso} until DDG 2 reaches its maximum output or until line

F_{ds} becomes congested. Since the capacity of F_{ds} is 0.1 MW, which is lower than the capacity of DDG 2, we can increase P_{dso} up to 0.1 MW, and the cost function would be $c^{dso}(P_{dso}) = 15P_{dso}$, which is determined by DDG 2. If we need to increase P_{dso} beyond 0.1 MW, we must use DDG 1. We can increase P_{dso} until DDG 1 reaches its maximum output of 0.5 MW. Thus, we can increase P_{dso} up to 0.6 MW, and the total cost function would be $c^{dso}(P_{dso}) = 15 \times 0.1 + 25(P_{dso} - 0.1)$. Therefore, the total cost function is as follows:

$$c^{dso}(P_{dso}) = \begin{cases} 15P_{dso}, & P_{dso} \in [0, 0.1) \\ 15 \times 0.1 + 25(P_{dso} - 0.1), & P_{dso} \in [0.1, 0.6] \end{cases}$$

Hence, the bid-in total cost function and marginal cost function which is derivative of the total cost function are determined as shown in Fig. 2.3(a) and Fig. 2.3(b), respectively.

The DSO submits this marginal cost function in Fig. 2.3(b) to the wholesale market and then, the wholesale market runs the following ISO-level economic dispatch problem:

$$\begin{aligned}
\text{Min}_{\boldsymbol{P}} \quad & 20P_g + 15P_{dso,1} + 25P_{dso,2} && && \text{(2.7a)} \\
s.t. \quad & P_g - F_{tr} = 0 && [\lambda_1^{WM}] && \text{(2.7b)} \\
& F_{tr} + P_{dso,1} + P_{dso,2} = 5.2 && [\lambda_2^{WM}] && \text{(2.7c)} \\
& 0 \le P_g \le 5 && && \text{(2.7d)} \\
& 0 \le P_{dso,1} \le 0.1 && && \text{(2.7e)} \\
& 0 \le P_{dso,2} \le 0.5 && && \text{(2.7f)}
\end{aligned}$$

where P_g is the power provision from the transmission side unit; $P_{dso,1}$ and $P_{dso,2}$ are the power provision of the first and second segments of the DSO bid-in cost function shown in Fig. 2.3(b), respectively; F_{tr} is the transmission line flow; λ_1^{WM} and λ_2^{WM} are the dual variables corresponding to the transmission-level power balance constraints, respectively.

The optimal solution to the above ISO problem is: $P_g = 5$ MW, $P_{dso,1} = 0.1$ MW, $P_{dso,2} = 0.1$ MW, and the DSO has dispatched $0.1 + 0.1 = 0.2$ MW and the wholesale LMP at the ISO-DSO coupling bus is 25 \$/MWh. The DSO substitutes the parameter $P_{dso} = 0.2$ in (3.14) and determines the DDGs' optimal dispatches, $P_{ddg_1} = 0.1$ MW, $P_{ddg_2} = 0.1$ MW. Then, the DSO solves the following problem to determine optimal D-LMPs:

$$\begin{aligned}
\text{Min}_{\boldsymbol{P}} \quad & 25P_{ddg_1} + 15P_{ddg_2} + 25P_{dso} && && \text{(2.8a)} \\
\text{s.t.} \quad & P_{ddg_1} + F_{ds} = P_{dso} && [\lambda_1] && \text{(2.8b)} \\
& P_{ddg_2} - F_{ds} = 0 && [\lambda_2] && \text{(2.8c)} \\
& 0 \le P_{ddg_1} \le 0.5 && && \text{(2.8d)} \\
& 0 \le P_{ddg_2} \le 0.5 && && \text{(2.8e)} \\
& -0.1 \le F_{ds} \le 0.1 && && \text{(2.8f)}
\end{aligned}$$

where λ_1, λ_2 are the dual variables corresponding to the distribution-level power balance constraints (i.e., the D-LMPs). The solution to this DSO problem determines the following D-LMPs: $\lambda_1 = 25$ \$/MWh, and $\lambda_2 = 15$ \$/MWh.

The following equations describe the ideal case in which the ISO can oversee both T&D-level operations and DER aggregators directly participate in the ISO market:

$$\begin{aligned}
\text{Min}_{\boldsymbol{P}} \quad & 20P_g + 15P_{ddg1} + 25P_{ddg2} && && \text{(2.9a)}\\
s.t. \quad & P_g - F_{tr} = 0 && [\lambda_1^{WM}] && \text{(2.9b)}\\
& F_{tr} + P_{dso} = 5.2 && [\lambda_2^{WM}] && \text{(2.9c)}\\
& P_{ddg_1} + F_{ds} = P_{dso} && [\lambda_1] && \text{(2.9d)}\\
& P_{ddg_2} - F_{ds} = 0 && [\lambda_2] && \text{(2.9e)}\\
& 0 \le P_g \le 5 && && \text{(2.9f)}\\
& 0 \le P_{ddg1} \le 0.5 && && \text{(2.9g)}\\
& 0 \le P_{ddg2} \le 0.5 && && \text{(2.9h)}\\
& -6 \le F_{tr} \le 6 && && \text{(2.9i)}\\
& -0.1 \le F_{ds} \le 0.1 && && \text{(2.9j)}
\end{aligned}$$

The solution (including optimal dispatch and prices for all the T&D-level resources) to the above ideal case is the same as the ISO-DSO coordination framework. However, upon comparing formulations (3.15) and (3.13), it can be observed that constraints (3.13e), (3.13f), and (3.13o) are no longer necessary, which reduces the problem size and computational burden for the ISO, as well as avoids sending DSO-level modeling details to the ISO.

2.5.2 Large Test System

In this section, simulation studies are implemented in a large test system containing ISO running the wholesale-level economic dispatch on an IEEE 118-bus test system. We have also considered two DSOs running the DSO-level market in the IEEE 33-node balanced and 240-node unbalanced distribution systems, respectively. YALMIP [31] is utilized to solve parametric programming problems for DSOs.

118-bus Test System Data

The IEEE 118-bus test system is considered as the transmission system operated by the ISO. The system data is given in [32]. The system contains 118 buses, 186 transmission lines, and 54 generators.

33-node Test System Data and Results

The 33-node test system is a balanced radial network which is shown in Fig. 2.4. The system contains 33 nodes, 32 branches, a demand response aggregator (DRAG), four dispatchable dis-

Table 2.1: DSO market participants data for the 33-node test system

Participant	Pmin (MW)	Pmax (MW)	Offering price ($/MWh)
DDGAG 1	0	0.5	20
DDGAG 2	0	1	10
DDGAG 3	0	1.2	15
DDGAG 4	0	2	24
DRAG	0	2	28

Table 2.2: 33-node test system breakpoints and marginal costs data

Breakpoint index	Breakpoint coordinate value (MW,$/h)	Marginal cost index	Marginal cost value ($/MWh)
P_1	(-1.18654,1.54166)	C_1	-69.6072
P_2	(-1.12498, -2.74336)	C_2	10.9555
P_3	(-0.961451, -0.951813)	C_3	14.1388
P_4	(-0.504623, 5.50717)	C_4	20.5587
P_5	(-0.495727, 5.69006)	C_5	22.8007
P_6	(-0.233645, 11.6657)	C_6	24.1164
P_7	(1.66269, 57.3985)	C_7	30.3739
P_8	(2.4175, 80.325)		

tributed generation aggregators (DDGAGs), and two renewable energy aggregators (REAGs). The test system data and load data are given in [33]. The two REAGs are considered to have identical energy production profiles of 1 MW. The other aggregators' data is given in Table. 2.1. Pmin and Pmax are the minimum and maximum generating power, respectively. It is assumed that the 33-node test system is connected to the 118-bus test system trough bus 87 on the transmission side.

The total cost function of the DSO is determined based on (2.5). The DSO's total (minimal) operating costs at different output power levels are shown in Fig. 2.5. This is a piecewise linear function with eight breakpoints separating the seven linear segments. The breakpoints in Fig. 2.5 are determined by the DSO-level market participants' minimum and maximum output power considering the network's physical constraints. The bid-in marginal cost function which is the derivative of the total bid-in cost function in Fig. 2.5 is shown in Fig. 2.6. This marginal cost function consists of seven levels of marginal costs corresponding to the seven linear segments in the piecewise linear total cost function in Fig. 2.5.

The coordinates of the breakpoints in Fig. 2.5 and the values of the marginal costs in Fig. 2.6 are given in Table 2.2.

The bid-in marginal cost function starts with the output power of -1.18654 MW which means that DSO can consume the energy of -1.18654 MW due to the capability of the DRAG and inelastic load to consume power in the distribution system. The bid-in price of this consumption is -69.6072 $/MWh. The negative value indicates that if the wholesale market dispatches this consumption value to the DSO, the DSO should be paid at this price. This indicates the DSO prefer not purchasing

Table 2.3: DSO market participants information for 240-node test system

Participant	Capacity (MW)	Price ($/MWh)	Participant	Capacity (MW)	Price ($/MWh)
DDGAG 1	0.25 A	20	DRAG 1	0.15 A	28
DDGAG 2	0.25 A	10	DRAG 2	0.15 A	29
DDGAG 3	0.25 B	15	DRAG 3	0.15 B	30
DDGAG 4	0.25 B	24	DRAG 4	0.15 B	27
DDGAG 5	0.25 C	14	DRAG 5	0.15 C	26
DDGAG 6	0.25 C	15	DRAG 6	0.15 C	25
DDGAG 7	0.25 A	16	DRAG 7	0.15 A	24
DDGAG 8	0.25 B	17	DRAG 8	0.15 B	22
DDGAG 9	0.25 C	18	DRAG 9	0.15 C	22
DDGAG 10	0.25 A	19	DRAG 10	0.15 A	23

energy from the ISO at this segment, since this may increase the total DSO-level generation cost. This is because it may violate certain voltage constraints that require the DSO to provide energy from its costly units. When the price of the wholesale market increases, the DSO starts selling energy to the wholesale market because the price in the wholesale market is higher than the offering prices of the DDGAGs in the distribution system. In the end, the DSO sells energy to the wholesale market at the price of 30.3739 $/MWh. This is due to the fact that if the offering price of the wholesale market is greater than 30.3739 $/MWh, the DSO sells the energy to the ISO instead of to the DRAG. The DSO submits its marginal cost function, shown in Fig. 2.6, to the ISO and waits for the ISO to clear the wholesale market.

240-node Distribution System Data and Results

The 240-node distribution test system is an unbalanced radial network in Midwest U.S. The data of the system is given in [34]. The system contains 240 nodes and 239 branches. Multiple aggregators are considered as follows: ten DRAGs, ten DDGAGs, and four REAGs. The data of the DER aggregators are given in Table 2.3. It is assumed that the 240-node system is connected to the 118-bus system through bus 27 of the transmission system.

The bid-in cost function of the DSO is determined based on (2.5). The formulation is extended to handle the single-phase aggregators and unbalanced distribution system physical constraints based on our prior work in [25].

The DSO's total bid-in cost function of the 240-node test system is shown in Fig. 2.7. The breakpoints in Fig. 2.7 are determined by the DSO market participants' minimum and maximum output power as well as the physical constraints of the distribution system. There are 18 breakpoints including the beginning and ending points. The bid-in marginal cost function of the DSO which is the derivative of the total bid-in cost function in Fig. 2.7 is given in Fig. 2.8. The data of the breakpoints and the marginal costs are given in Table 2.4.

Table 2.4: 240 node breakpoints and marginal costs data

Breakpoint index	Breakpoint coordinate value (MW,$/h)	Marginal cost index	Marginal cost value ($/MWh)
P_1	(-2.142,-34.538)	C_1	15
P_2	(-1.587, -26.213)	C_2	15.333
P_3	(-1.461, -24.281)	C_3	15.667
P_4	(-1.392, -23.2)	C_4	16.667
P_5	(-0.837, -13.95)	C_5	17.667
P_6	(-0.711, -11.724)	C_6	19
P_7	(-0.642, -10.413)	C_7	20.333
P_8	(-0.192,-1.263)	C_8	21
P_9	(-0.087, 0.942)	C_9	21.667
P_{10}	(0.039, 3.672)	C_{10}	23
P_{11}	(0.363, 11.124)	C_{11}	23.667
P_{12}	(0.489, 14.106)	C_{12}	24.333
P_{13}	(0.558, 15.785)	C_{13}	25.333
P_{14}	(0.813, 22.245)	C_{14}	26.667
P_{15}	(.939,25.605)	C_{15}	27
P_{16}	(1.008, 27.468)	C_{16}	28
P_{17}	(1.263, 34.608)	C_{17}	28.333
P_{18}	(1.389, 38.178)		

In Fig. 2.8, the bid-in marginal cost function starts with -2.14 MW with the price of 15 $/MWh which means that if the price of the wholesale market is lower than or equal to this value the DSO operating the 240-node test system buys energy from the wholesale market for consumption in the distribution system. As the wholesale market price increases, the energy consumption in the DSO decreases until it reaches 23 $/MWh at which the DSO sells energy to the wholesale market for any price greater than this value. The amount of energy provision of the DSO for the ISO increases as the price in the wholesale market increases until it reaches its maximum capacity which is 1.39 MW.

Market Clearing Results

This section compares the market clearing results of the ideal case in (3.1) and our proposed ISO-DSO coordination case. In the ideal case, the ISO is the single entity which oversees all the market participants and operating constraints in the transmission system and in both distribution systems. In our proposed ISO-DSO coordination case, both 33-node and 240-node DSOs submit their marginal bid-in cost functions in Figs. 2.6 and 2.8 to the ISO. Then, ISO clears the wholesale market based on (3.2). Table 2.5 shows the market dispatch results of the ideal case and the ISO-DSO coordination case for this large test system. Since these two cases share identical market dispatch results for all the T&D-level market participants (generators and DER aggregators), we only used one table to present these identical results for both cases. Table 2.5 shows the total

Table 2.5: Ideal case and ISO-DSO coordination case dispatch

Total wholesale market generators' dispatch			
6601.1 MW			
33 node test system dispatches			
Participant	Dispatch (MW)	Participant	Dispatch (MW)
DDGAG 1	0	DDGAG 3	1.2
DDGAG 2	0.7102	DDGAG 4	0
DRAG	0.6998		
240 node test system dispatches			
Participant	Dispatch (MW)	Participant	Dispatch (MW)
DDGAG 1	0.065 A	DRAG 1	0.15 A
DDGAG 2	0.25 A	DRAG 2	0.15 A
DDGAG 3	0.25 B	DRAG 3	0.15 B
DDGAG 4	0 B	DRAG 4	0.15 B
DDGAG 5	0.25 C	DRAG 5	0.15 C
DDGAG 6	0.25 C	DRAG 6	0.15 C
DDGAG 7	0.25 A	DRAG 7	0.15 A
DDGAG 8	0.25 A	DRAG 8	0.15 A
DDGAG 9	0.25 B	DRAG 9	0.15 B
DDGAG 10	0.023 C	DRAG 10	0.15 C

dispatch in the wholesale market and the individual DER aggregators' dispatches in both 33-node and 240-node distribution systems. In the ISO-DSO coordination case, the total dispatches for the 33-node and 240-node DSOs are -0.5046 MW and -0.642 MW, respectively.

Market Settlements

In this section, we compare the market settlements of the ideal case and ISO-DSO coordination case. In the ideal case, the LMP on the transmission side is 20.24 \$/MWh, which remains the same throughout the transmission system, as there is no transmission-level congestion. Therefore, the LMPs at the coupling points of the 33 node system and 240-node system are also 20.24 \$/MWh. The 240-node system is unbalanced, resulting in different D-LMPs for each phase, namely 20 \$/MWh, 21.71 \$/MWh, and 19 \$/MWh for phase A, phase B, and phase C, respectively. The average of the three-phase D-LMPs is 20.24 \$/MWh. More detailed information on determining LMP in an unbalanced system can be found in our previous work [3].

In the ISO-DSO coordination case, the LMP on the transmission side is obtained by (3.2) and remains identical to the ideal case (20.24 \$/MWh). Each DSO then determines its own D-LMPs based on (3.4), by letting $LMP_j^* = 20.24$ \$/MWh. The D-LMPs of the 33 node test system and 240-node system obtained from the ISO-DSO coordination case are identical to those obtained from the ideal case.

2.6 Conclusion

In this chapter, an ISO-DSO coordination framework is proposed based on parametric programming, which ensures distribution grid operating security while allowing wholesale market participation of DER aggregators. Each DSO runs the DSO-level market in the distribution system and gathers offers from all the market participants (DER aggregators) in its territory and build the bid-in cost function for submission to the ISO. Then, the ISO gathers all these bid-in cost functions from all the DSOs and from other wholesale market participants to clear the wholesale market. Once the ISO clears the wholesale market, the dispatch and payment of each DSO are determined. Then, DSOs determine the DSO-level dispatch and D-LMPs in their territories based on the ISO-cleared market. A market settlement approach is presented and proved that each market participant (generator or aggregator) will receive identical compensation and dispatch under the proposed ISO-DSO coordination framework and under the ideal case where the DER aggregators can participate in the wholesale market directly and the ISO is the single entity overseeing both T&D-level operating constraints. This ISO-DSO coordination framework is compatible with today's wholesale market structure without introducing additional changes to existing wholesale market clearing procedure. It only exchanges minimal amount of public data between the ISO and DSO without exchanging any confidential grid models between the T&D operations. It also completely decouples the solution process of the ISO and DSO optimization sub-problems, which allows the ISO and DSO to exchange data only after each entity converges to its optimal solution.

Case studies were implemented on a small illustrative example and a large system to investigate the proposed ISO-DSO coordination framework. The small illustrative example shows that, compared to the ideal case, the proposed model significantly removes the variables and constraints for the wholesale market while resulting in the same market clearing outcomes. The large system contains the IEEE 118-bus transmission system connected to two DSO operated distribution systems including the 33-node balanced 240-node unbalanced distribution systems. The bid-in cost functions of the DSOs were developed based on parametric programming and submitted to the ISO. The dispatches and payments to the DER aggregators are identical under the ISO-DSO coordination framework and under the ideal case.

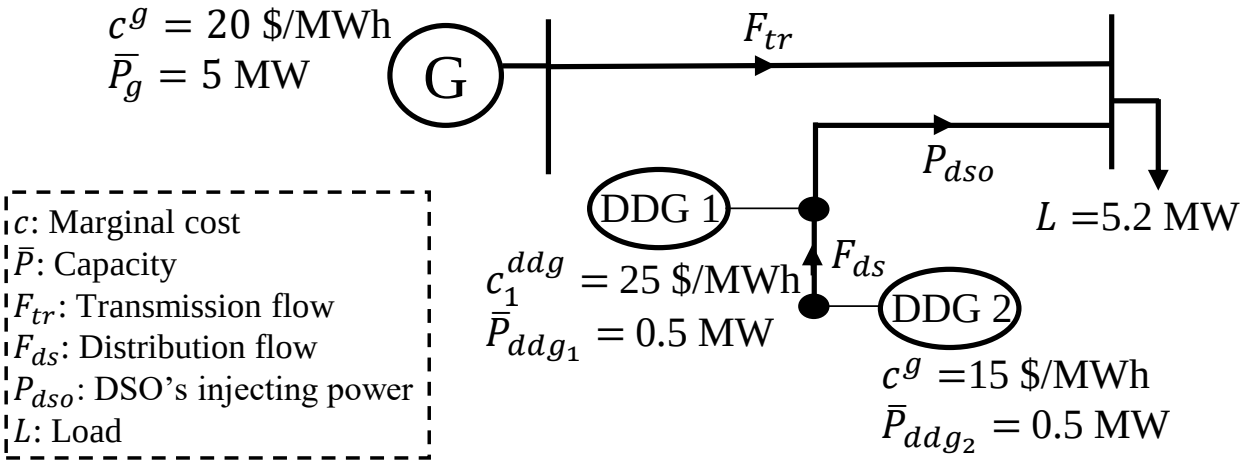

Figure 2.2: Illustrative example system. The minimum active power for all units is zero.

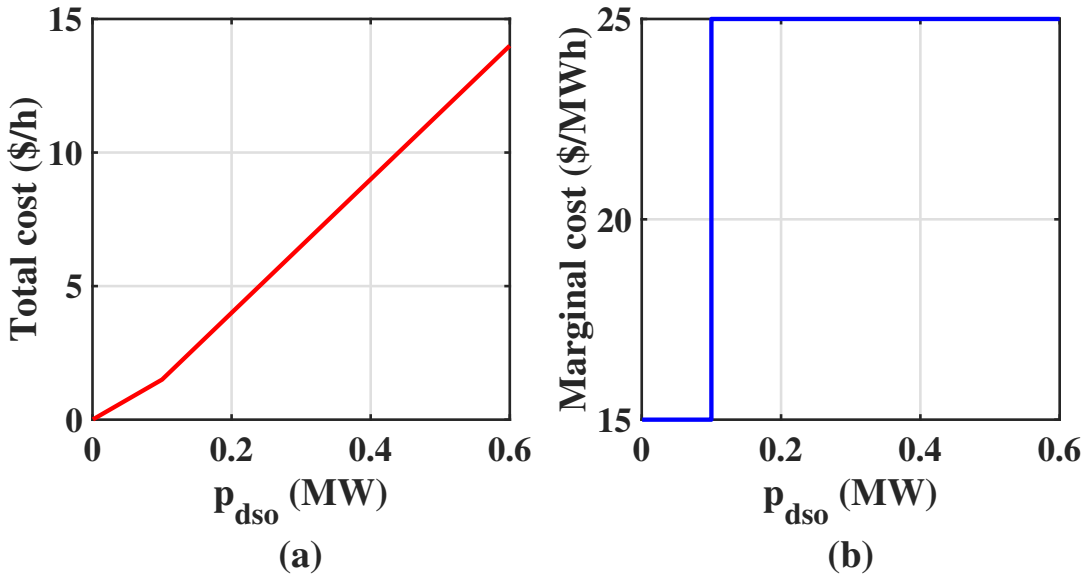

Figure 2.3: DSO bid-in total (left) and marginal (right) cost functions in the illustrative example.

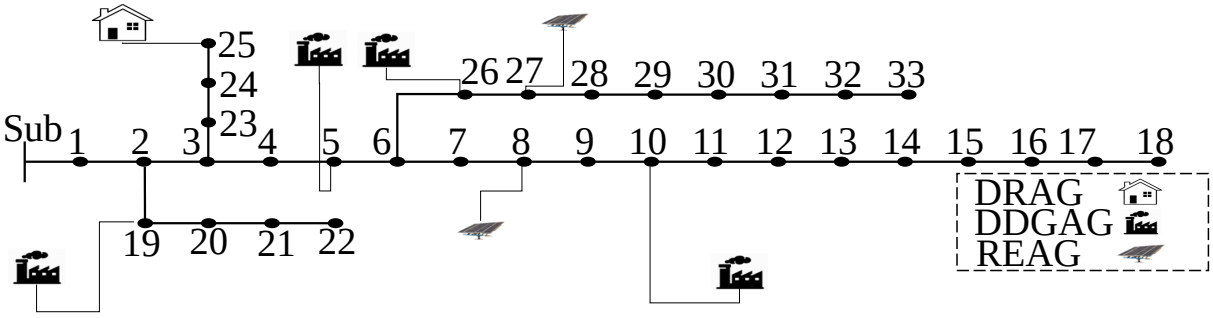

Figure 2.4: 33-node test system.

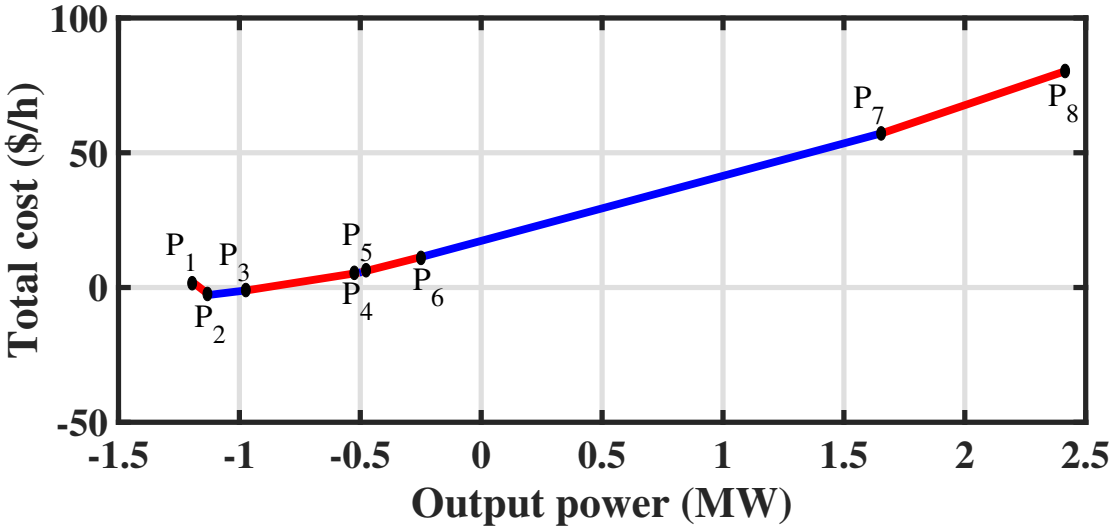

Figure 2.5: Total cost function of the 33 node test system.

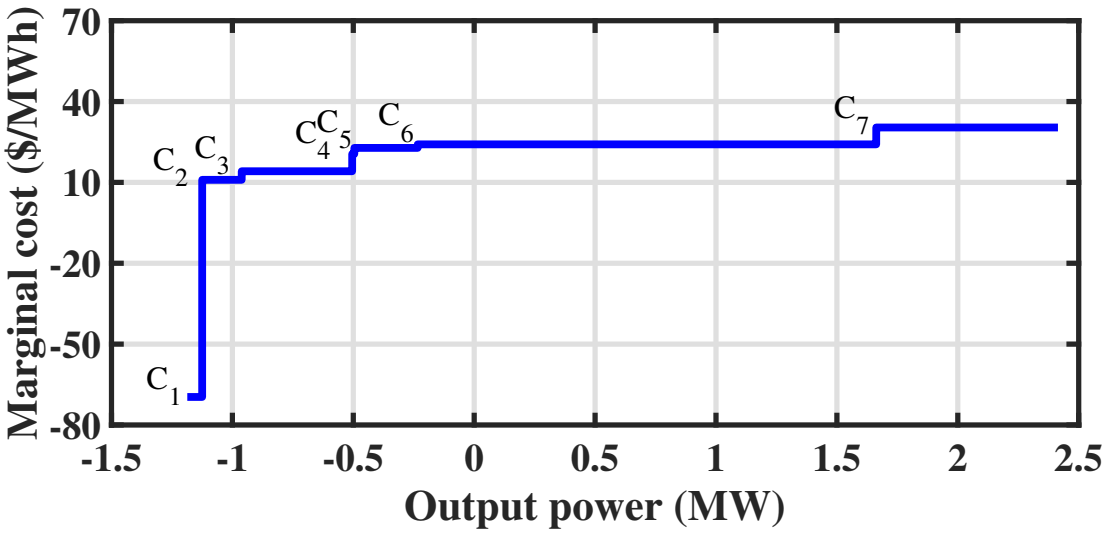

Figure 2.6: Bid-in marginal cost function of the 33 node test system.

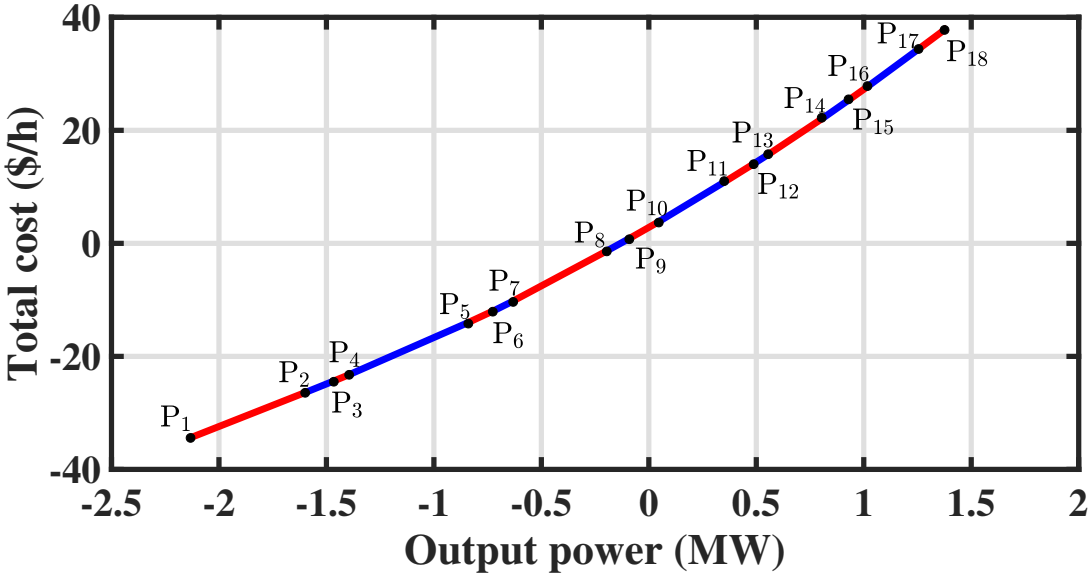

Figure 2.7: Total cost function of the 240 node test system.

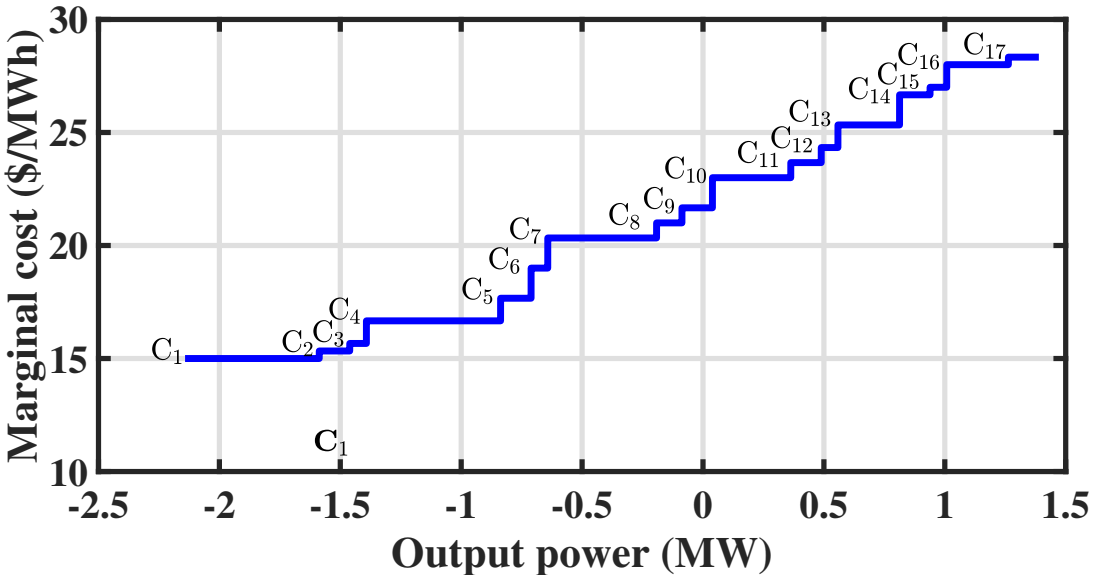

Figure 2.8: Bid in marginal cost function of the 240 node test system.

3. TSO-DSO Coordination - Optimal Pricing in Distribution Systems

3.1 Introduction

In 2020, Federal Energy Regulation Commission (FERC) Order No. 2222 [2] required all the independent system operators (ISOs) to fully unlock their wholesale markets for the aggregated distributed energy resources (DERs). This paves the path toward operating future electricity markets with significant DER participation. Ideally speaking, operating the wholesale markets with massive DERs requires coordinated operations between the transmission and distribution (T&D) systems, since the ISOs can only model, observe, and dispatch transmission-level networks and resources, while the DERs are physically located across the distribution feeders and cannot be directly monitored by the ISOs. However, T&D coordination is very limited in today's power industry practice. Without effective T&D coordination, many industry practitioners have expressed excessive concerns on both operational reliability and economic efficiency of the T&D systems when significant number of DERs are being aggregated and integrated into the wholesale markets. There is a growing industry need for enabling effective T&D coordination for reliably and economically integrating massive DERs into the wholesale markets.

The objective of this chapter is to extend the T&D coordination framework in Chapter 1 by developing theoretical justifications and thorough discussions for the T&D-coordinated pricing problem. Specifically, we prove and discuss 1) the relationship between the T&D-coordinated dispatch model and T&D-coordinated pricing model, which together guarantee the T&D operation optimality for both dispatch and pricing process; and 2) the non-profit characteristics of the DSO under the proposed T&D-coordinated pricing model. One interesting finding is that, in order to ensure zero T&D model exchange and minimal T&D communication for the parametric programming based T&D coordination framework in [35], the optimal prices for aggregated DERs in the distribution systems cannot be directly obtained from the dual problem of the DSO economic dispatch problem. Instead, a separate DSO pricing model is needed to derive the correct price signals for DSO-level resources and coordinate with the ISO-level pricing and dispatch process.

3.2 Mathematical Formulation

In this section, we first present an ideal case formulation where the ISO oversees both the transmission and distribution systems, as described in [35]. This ideal case formulation serves as a benchmark to compare the results of the proposed ISO-DSO coordination problem. Next, we present the formulation of the ISO-DSO coordination framework proposed in [35]. Finally, we formulate and discuss the pricing problem for the proposed ISO-DSO coordination.

3.2.1 Ideal Case

The ideal case refers to a scenario where DER aggregators can directly participate in the wholesale market, even if they are located within the distribution system. In this case, the ISO oversees both the distribution system constraints and transmission system constraints. However, it is important to note that the ideal case is not currently implementable within the existing practices of the wholesale

market. The purpose of considering the ideal case is to compare its results with the outcomes of our proposed ISO-DSO coordination problem. The general formulation of the ideal case is presented in the following formulation:

$$\text{Min}_{\boldsymbol{p}} \quad \sum_{i \in \mathcal{N}_{gen}} c_i^g(p_i^g) + \sum_{j \in \mathcal{N}_{dis}} \sum_{i \in \mathcal{N}_{agg}} c_{i,j}^{agg}(p_{i,j}^{agg}) \tag{3.1a}$$

$$\begin{aligned} \text{s.t.} \quad & \boldsymbol{p}^g \in S^{Tra} \\ & \boldsymbol{p}_j^{agg} \in S_j^{Dis}, \forall j \in \mathcal{N}_{dis} \\ & p_i^g \in S_i^{gen}, \forall i \in \mathcal{N}_{gen} \\ & p_{i,j}^{agg} \in S_{i,j}^{agg}, \forall i \in \mathcal{N}_{agg}, j \in \mathcal{N}_{dis} \end{aligned} \tag{3.1b}$$

where $\boldsymbol{p}$ is the vector of all decision variables (generating powers of all conventional generators and DER aggregators), i is the index for generating units, j is the index for distribution systems, $\mathcal{N}_{gen}$ is the set of conventional generating units in the transmission system, $c_i^g(p_i^g)$ is the bid-in cost function of the conventional generating units in the transmission system, $\boldsymbol{p}^g$ is the generating power of the conventional generating units in the transmission system, $\mathcal{N}_{dis}$ is the set of all distribution systems, $\mathcal{N}_{agg}$ is the set of all aggregators in the distribution system, $c_{i,j}^{agg}(p_{i,j}^{agg})$ is the bid-in cost function of the DER aggregators, $p_{i,j}^{agg}$ is the generating power of the DER aggregator in the distribution system, $\boldsymbol{p}^g$ is the vector of all generating powers provided by the conventional generating units in the transmission system, S^{Tra} is the search space defined by system-wide transmission constraints, $\boldsymbol{p}_j^{agg}$ is the vector of all generating powers of the DER aggregator in the distribution system, S_j^{Dis} is the search space defined by system-wide distribution system constraints, S_i^{gen} is the search space defined by operating constraints of the conventional generating units in the transmission system, and $S_{i,j}^{agg}$ is the search space defined by operating constraints of the DER aggregators in the transmission system.

In this ideal case, one single entity (i.e., the ISO) minimizes the total generation cost of all the T&D-level resources (conventional generators and DER aggregators), by determining the real power dispatch of all the T&D-level resources, while satisfying all the T&D-level system operating constraints.

3.2.2 ISO-DSO Coordination Dispatch Problem

In this section, we present the ISO-DSO coordination dispatch problem proposed in [35]. The process begins with all DER aggregators submitting their bid-in cost functions to the DSO. The DSO collects these bid-in cost functions and conducts a market operation at the distribution level. Using parametric programming, the DSO constructs its bid-in cost function, which is then submitted to the ISO. Subsequently, the ISO clears the wholesale market and transmits the dispatch signals to the DSO. The DSO utilizes these dispatch signals in the parametric programming problem to determine the dispatch for each DER aggregator. The general formulation of the ISO dispatch

problem in the ISO-DSO coordination framework is as follows:

$$\text{Min}_{\boldsymbol{p}} \quad \sum_{i \in \mathcal{N}_{gen}} c_i^g(p_i^g) + \sum_{j \in \mathcal{N}_{dis}} c_j^{dso}(p_j^{dso}) \tag{3.2a}$$

$$\text{s.t.} \quad \boldsymbol{p} \in S^{Tra}$$

$$p_i \in S_i^{gen}, \forall i \in \mathcal{N}_{gen} \tag{3.2b}$$

$$p_j \in S_j^{dso}, \forall j \in \mathcal{N}_{dis}$$

where $c_j^{dso}(p_j^{dso})$ denotes the bid-in cost function submitted by the DSO to the ISO; p_j^{dso} corresponds to the generating power injected by the DSO to the ISO at the ISO-DSO coupling point; S_j^{dso} defines the search space determined by the minimum and maximum allowable power generation levels of the DSO at each section of the DSO multi-segment bid-in cost function.

In the above ISO dispatch problem, the ISO only determines the optimal dispatch of transmission-level resources (conventional generators and DSOs) which will minimize the transmission-level total generation cost, while satisfying all the transmission-level system operating constraints. Since there is no distribution-level operating constraints or distribution-level resources (DER aggregators) involved in this ISO problem, there is no need to submit confidential distribution system models to the ISO. The only data submitted from the DSO to the ISO is the DSO's multi-segment bid-in cost function $c_j^{dso}(p_j^{dso})$ and its corresponding multi-segment upper/lower generation limits, which, as defined in today's wholesale market clearing rules, has to be reported to the ISO by each market participant.

The DSO constructs its bid-in cost function $c_j^{dso}(p_j^{dso})$ for participating in the ISO market by formulating the following parametric programming problem:

$$\begin{aligned} c_j^{dso}(p_j^{dso}) = & \\ & \text{Min}_{\boldsymbol{p}^{agg}} \sum_{i \in \mathcal{N}_{agg}} c_{i,j}^{agg}(p_{i,j}^{agg}) \\ & \text{s.t.} \quad p_j^{dso} = \sum_{i \in \mathcal{N}_{agg_k}} p_{i,j}^{agg} + \sum_{l \in \mathcal{N}_{f_k}} f_{l,j} - L_{k,j} \\ & \quad\; p_{i,j}^{agg} \in S_{i,j}^{agg}, \forall i \in \mathcal{N}_{agg} \\ & \quad\; \boldsymbol{p}_j^{agg} \in S_j^{Dis} \end{aligned} \tag{3.3}$$

where $\mathcal{N}_{agg_k}$ denotes the set of all DER aggregators located at node k; $\mathcal{N}_{f_k}$ denotes the set of all branches connected to node k; $f_{l,j}$ denotes the flow of branch l; $L_{k,j}$ denotes the firm load situated at node k.

In equation (3.3), the parameter p_j^{dso} introduces a parametric aspect to the formulation. The solution to this problem yields the lowest generation costs for the DSO at all possible generation levels $c_j^{dso}(p_j^{dso})$, by optimally dispatching all the DSO-level resources (DER aggregators), while satisfying all the DSO-level system operating constraints (including distribution load balancing constraints, voltage/thermal constraints, etc.). Assuming the DSO is a non-profit entity, this lowest generation cost function is the bid-in cost function of the DSO, which is a piecewise linear function

if (3.3) is a linear parametric programming problem with linearized distribution load flow as the operating constraints and piecewise linear bid-in cost functions from the DER aggregators. The DSO then submits this bid-in cost function to the ISO. Once the ISO clears the wholesale market, the dispatch of the DSO (p_j^{dso}) in the wholesale market is determined. Subsequently, the DSO incorporates this dispatch into (3.3), transforming it into a regular linear optimization problem. By solving this resulting problem, the DSO determines the dispatch for each individual DER aggregator within its territory. It has been mathematically proven in [35] that following the ISO-DSO coordination dispatch problem in (3.2)-(3.3), the dispatch of each individual aggregator or conventional generator is equivalent to the ideal case where the DER aggregator directly participates in the wholesale market and the ISO oversees all the T&D-level system operating constraints.

In the above DSO bidding and dispatch problem defined by (3.3), the DSO only determines the optimal dispatch of distribution-level resources (DER aggregators) which will minimize the distribution-level total generation cost at all possible generation levels, while satisfying all the distribution-level system operating constraints. Since there is no transmission-level operating constraints or transmission-level resources (conventional generators) involved in this DSO problem, there is no need to submit confidential transmission system models to the DSO. The only data submitted from the ISO to the DSO is the DSO's wholesale dispatch cleared by the ISO, which fully complies with today's wholesale market clearing rules. Moreover, the solution process of the ISO and DSO optimization problems in (3.2) and (3.3) is completely decoupled. The ISO and DSO only exchange data with each other once its own optimal dispatch solution is obtained. There is no exchange of intermediate solution data between ISO and DSO during the ISO and DSO optimization process.

3.2.3 ISO-DSO Coordination Pricing Problem

In the ISO-DSO coordination framework, after the ISO clears the wholesale market, the Locational Marginal Price (LMP) is determined at the bus where the DSO is located, in addition to the dispatches of all DSOs. The DSO then determines the dispatch of each DER aggregator by incorporating the total dispatch determined by the ISO into the dispatch problem proposed in equation (3.3). However, using the dual variables of this problem does not accurately reflect the true cost of the system in the wholesale market, particularly when the marginal unit is in the wholesale market. This is because the share of the wholesale market is modeled as a parameter p_j^{dso}. Under this parametric modeling, if the marginal unit is in the wholesale market, which means p_j^{dso} provides the next megawatt in the DSO, the dual variable of this node balance constraint will not reflect the corresponding price for that marginal unit in the wholesale market (out of the DSO territory). further discussion on this is provided in the simulation results section. Consequently, the DSO requires a pricing problem to clear the distribution market, ensuring price consistency with the ideal case and maintaining non-profitability. The following problem is proposed to facilitate

market clearance in the distribution system.

$$\begin{aligned} \text{Min}_{\boldsymbol{p}^{agg}, p_j^{dso}} \quad & \sum_{i \in \mathcal{N}_{agg}} c_{i,j}^{agg}(p_{i,j}^{agg}) - LMP_j^* p_j^{dso} \\ \text{s.t.} \quad & p_j^{dso} = \sum_{i \in \mathcal{N}_{agg_k}} p_{i,j}^{agg} + \sum_{l \in \mathcal{N}_{f_k}} f_{l,j} - L_{k,j} \\ & p_{i,j}^{agg} \in S_{i,j}^{agg}, \forall i \in \mathcal{N}_{agg} \\ & \boldsymbol{p}_j^{agg} \in S_j^{Dis} \end{aligned} \tag{3.4}$$

where p_j^{dso} represents the total generating power of the DSO and is a decision variable in this case (not a parameter), and LMP_j^* corresponds to the LMP at the bus where the DSO is located in the wholesale market, as determined by the ISO's market clearing process.

Lemma 3. *The price cleared by the DSO (i.e., the D-LMP) at the ISO-DSO coupling substation node in the distribution system (dual variable corresponding to substation node balance constraint) will always be equal to the price at the same node in the wholesale market cleared by the ISO (LMP_j^*). This equality implies that the DSO is always revenue adequate.*

Proof. Let $\mathbf{p}$ denote the vector of all decision variables, $f(\mathbf{p})$ denote the objective function, and $\mathbf{g}(\mathbf{p})$ represent the constraints, along with their corresponding dual variables $\boldsymbol{\lambda}$ in equation (3.4). The Lagrangian function for equation (3.4) can be formulated as follows:

$$\mathcal{L} = f(\mathbf{p}) + (\boldsymbol{\lambda})^{\mathsf{T}}(\mathbf{g}(\mathbf{p})) \tag{3.5}$$

Based on the Karush-Kuhn-Tucker (KKT) conditions, the partial derivative of the Lagrangian function with respect to p_j^{dso} must be zero at the optimal point:

$$\frac{\partial \mathcal{L}}{\partial p_j^{dso}} = \frac{\partial f(\mathbf{p})}{\partial p_j^{dso}} + \frac{\partial (\boldsymbol{\lambda})^{\mathsf{T}}(\mathbf{g}(\mathbf{p}))}{\partial p_j^{dso}} = 0 \tag{3.6}$$

Let λ^s represent the dual variable corresponding to the node balance equation at the substation, which is the D-LMP at the ISO-DSO coupling substation node. Then, we can further simplify equation (4.8) as follows:

$$\frac{\partial \mathcal{L}}{\partial p_j^{dso}} = LMP_j^* - \lambda^s = 0 \tag{3.7}$$

Therefore, D-LMP at the substation node in the distribution system is always equal to the LMP cleared in the wholesale market. Following Lemma 1 in our previous work [35], it can also be concluded that such pricing characteristics will also imply revenue adequacy for the DSO.

Lemma 4. *If the marginal unit is located within the distribution system, at the ISO-DSO coupling substation, the DSO dispatch problem in (3.3) results in the same D-LMP as the wholesale LMP determined by the ISO, which is also the same D-LMP determined by the DSO pricing problem in (3.4). However, if the marginal unit is located in the transmission system, at the ISO-DSO coupling substation, the D-LMP determined by the DSO dispatch problem in (3.3) could be different from the wholesale LMP determined by the ISO, and also could be different from the D-LMP determined by the DSO pricing problem in (3.4).*

Proof. This proof is built upon our previous work in [35], where we proved in the above ISO-DSO coordination dispatch problem, the optimal dispatches of all the T&D-level resources are identical to those in the ideal case. Also, in Lemma 1, we proved the wholesale LMP determined by the ISO problem and the D-LMP determined by the DSO pricing problem in (3.4) are always the same at the ISO-DSO coupling substation.

For the sake of simplicity and without sacrificing generality, let us consider a scenario where there are no congestion or voltage issues in the system. We will assume that the marginal unit, which is the unit that provides the last MW, is located in the transmission system. We will denote this generating unit as generator z. In the ISO problem, the LMP is $LMP_j^* = c_z^g$ (bid-in generation cost of marginal unit z at the ISO-dispatched generation level), and $p^{dso} = p^{dso*}$ (optimal wholesale dispatch of the DSO).

In the ISO-DSO coordination problem, when the DSO substitutes p^{dso*} into the DSO dispatch problem in (3.3), all the DER aggregators in the distribution system that are not more expensive than the marginal unit are dispatched fully, since the marginal unit is located in the transmission system. The D-LMP at the substation node in the distribution system can be expressed as follows:

$$DLMP_k = \frac{\partial L}{\partial L_{k,j}} = \frac{\partial L}{\partial p_j^{dso}} = \lambda^k \tag{3.8}$$

Let us consider the cheapest yet un-dispatched generating unit in the distribution system, which will provide the next MW, as aggregator m. We can then express the derivative of the Lagrangian function with respect to p_{ddg_m} as:

$$\frac{\partial L}{\partial p_{ddg_m}} = \alpha_m^+ - \alpha_m^- - \lambda^m = 0 \tag{3.9}$$

In the DSO dispatch problem in (3.3), aggregator m becomes the marginal unit, we have $\alpha_m^+ = \alpha_m^- = 0$. Therefore, $\lambda^m = c_{ddg_m}$ (bid-in generation cost of aggregator m at the DSO-dispatched generation level). Since there is no congestion, the D-LMP at node k is equal to $\lambda^k = c_{ddg_m}$, which is different from the price in the transmission side.

Now, if we assume that the marginal unit lies in the distribution system, both the generating unit z and aggregator m will be the same unit. In this scenario, the D-LMP and the LMP of the wholesale market will be the same. □

Lemma 5. *If the marginal unit is located in the transmission system, at the ISO-DSO coupling substation, the DSO pricing problem in (3.4) results in the same dispatch as the wholesale dispatch determined by the ISO problem, which is also the same dispatch determined by the DSO dispatch problem in (3.3). However, if the marginal unit is located in the distribution system, at the ISO-DSO coupling substation, the dispatch determined by the DSO pricing problem in (3.4) could be different from the wholesale dispatch determined by the ISO problem, and also could be different from the dispatch determined by the DSO dispatch problem in (3.3).*

Proof. This proof is built upon our previous work in [35], where we proved in the above ISO-DSO coordination problem, the optimal dispatches, prices and payments of all the T&D-level resources are identical to those in the ideal case.

To simplify the analysis and without loss of generality, let us consider a scenario where there are no congestion and voltage issues in the system. let us assume that the marginal unit is located in the distribution system. Specifically, let aggregator m be the marginal unit and it's dispatch level is $p_m^{ddg^*}$ MW. let us assume that the wholesale dispatch of the DSO determined by the ISO problem is p_{dso}^* MW. Since there are no active constraints related to congestion or voltage in the distribution system, we can rewrite the power balance constraint as follows:

$$p^{dso} = \sum_{i \in \mathcal{N}_{agg}} p_i^{ddg} - L \tag{3.10}$$

where L represents the total firm load in the system.

Considering that aggregator m is the marginal unit and there are no congestion or voltage issues, we can further simplify Equation (3.10) as:

$$p^{dso} = \sum_{i \in \mathcal{N}_{aggm}} \overline{p_i^{ddg}} + p_m^{agg} - L \tag{3.11}$$

where $\mathcal{N}_{agg_m}$ represents the set of all aggregators that are cheaper than aggregator m, and $\overline{p_i^{ddg}}$ denotes the maximum generation output of the aggregators.

Then we can say that ISO problem yields $p_{dso}^* = \sum_{i \in \mathcal{N}_{aggm}} \overline{p_i^{ddg}} + p_m^{ddg^*} - L$.

Now, let us determine the optimal value of p^{dso} for the DSO pricing problem in (3.4). Equation (3.11) is also valid in the DSO pricing problem. The only variable that needs to be determined in (3.11) is p_m^{agg}. To find the optimal value of p_m^{agg}, let us examine the objective function of the DSO pricing problem, which is formulated as follows:

$$\text{Min} \sum_{i \in \mathcal{N}_{agg}} c_i^{ddg} p_i^{ddg} - c_m^{ddg} p^{dso} \tag{3.12}$$

Note that we know that aggregator m is the marginal unit. Hence, $LMP_j^* = c_m^{ddg}$ in the DSO pricing problem. The term $-c_m^{ddg} p^{dso}$ in the objective function indicates that there is a demand response with a price equal to the price of aggregator m. Consequently, all aggregators cheaper than aggregator m will be dispatched at their maximum output. However, for aggregator m, it

can be dispatched at any dispatch level, and its actual dispatch level does not affect the objective function. This leads to a problem of degeneracy, where the solution for p^{dso} can have any value within the range $[\sum_{i\in\mathcal{N}_{agg_m}} \overline{p_i^{ddg}} - L, \sum_{i\in\mathcal{N}_{agg_m}} \overline{p_i^{ddg}} + \overline{p_m^{agg}} - L]$, which means it is not necessarily equal to the dispatch obtained from the wholesale market.

Now, let us suppose that the marginal unit is in the transmission side. In this case, there is no partially-dispatched unit in the distribution system. Each aggregator is either fully dispatched or not dispatched. Then aggregator m becomes the cheapest un-dispatched unit. Any unit that is cheaper than aggregator m (i.e., within set $\mathcal{N}_{agg_m}$) should be fully dispatched, and $p^{dso} = \sum_{i\in\mathcal{N}_{agg_m}} \overline{p_i^{ddg}} - L$, which is equal to the value obtained from the ISO problem. □

Lemma 2 and Lemma 3 demonstrate the following observations: 1) When coupled with the ISO dispatch/pricing model in (3.2), the DSO dispatch model in (3.3) consistently generates the correct dispatch signals for DSO-level resources; 2) The DSO pricing model in (3.4), also in conjunction with the ISO dispatch/pricing model, consistently produces the accurate price signals for DSO-level resources. However: 1) The dual variables of the DSO dispatch model do not always yield the correct D-LMPs; 2) Similarly, the primal solutions of the DSO pricing model do not always result in the correct DSO-level dispatches. In order to reserve the desired features of minimal T&D communications and zero T&D confidential model exchange in the parametric-programming-based ISO-DSO coordination framework, the DSO-level optimal dispatch and pricing need to be achieved through two separated models. This is different from the ISO market clearing which utilizes one economic dispatch model to obtain both the optimal dispatch and pricing results.

3.3 Case Studies

In this section, case studies are conducted on a small illustrative example to validate the results of the proposed ISO-DSO pricing problem. The system, as depicted in Figure 3.1, consists of a three-node distribution system connected to a three-bus transmission system. The wholesale market is operated by the ISO in the transmission side, while the distribution-level market is managed by the DSO in the distribution side. The distribution system includes two dispatchable distributed generations (DDGs), while the transmission system comprises two conventional generating units.

In Case 1, the bidding data for the conventional generators and DDGs is provided in Table 3.1, and there is a firm load of 15 MW. This case has been designed in a manner where the marginal unit is located in the wholesale market.

On the other hand, Case 2 has been designed with the marginal unit located in the distribution system. The bidding data for the conventional generators and DDGs in this case can be found in Table 3.2, and there is a firm load of 11.5 MW.

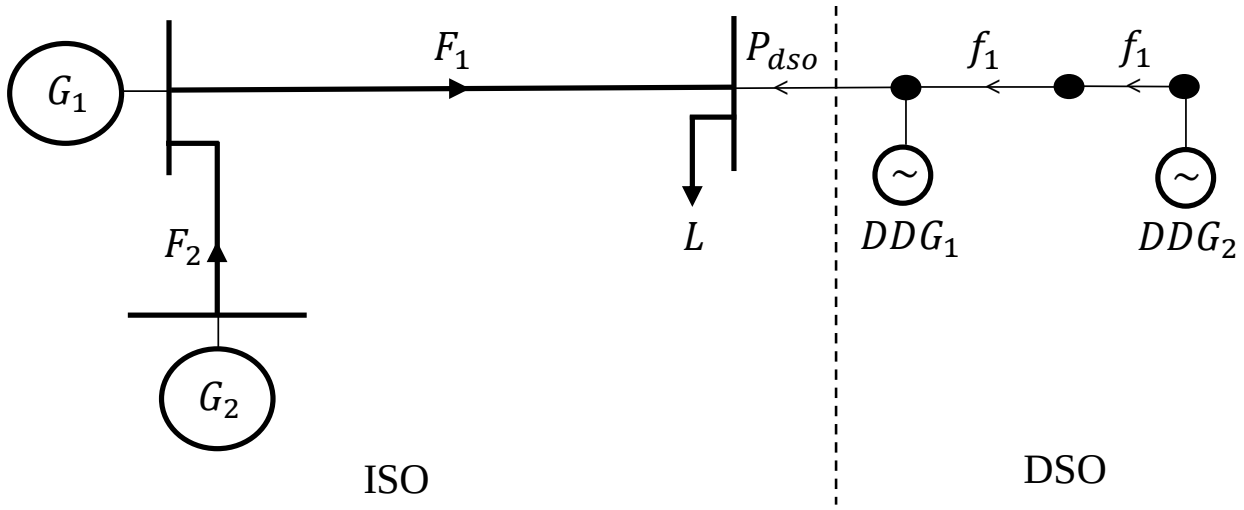

Figure 3.1: Illustrative example system.

Table 3.1: Bidding data for the conventional generators and DDGs in the illustrative example: Case 1

Participant	Pmin (MW)	Pmax (MW)	Offering price ($/MWh)
G_1	0	10	10
G_2	0	10	12
DDG_1	0	1	15
DDG_2	0	1	5

Table 3.2: Bidding data for the conventional generators and DDGs in the illustrative example: Case 2

Participant	Pmin (MW)	Pmax (MW)	Offering price ($/MWh)
G_1	0	10	10
G_2	0	10	20
DDG_1	0	1	15
DDG_2	0	1	5

3.3.1 Ideal Case

As mentioned previously, in the ideal case, it is assumed that DERs can directly participate in the wholesale market, and the ISO oversees both the transmission and distribution systems. The economic dispatch problem of the ISO in the ideal case can be formulated as follows:

$$\text{Min}_{\boldsymbol{P}} \quad c_1^g p_1^g + c_2^g p_2^g + c_1^{ddg} p_2^{ddg} + c_2^{ddg} p_2^{ddg} \tag{3.13a}$$

$$s.t. \quad p_1^g - F_1 + F_2 = 0 \qquad [\lambda_1^{WM}] \tag{3.13b}$$

$$p_2^g - F_2 = 0 \qquad [\lambda_2^{WM}] \tag{3.13c}$$

$$p^{dso} + F_1 - L = 0 \qquad [\lambda_3^{WM}] \tag{3.13d}$$

$$p_1^{ddg} + f_1 - p^{dso} = 0 \qquad [\lambda_1^{D}] \tag{3.13e}$$

$$f_1 - f_2 = 0 \qquad [\lambda_2^{D}] \tag{3.13f}$$

$$p_2^{ddg} - f_2 = 0 \qquad [\lambda_3^{D}] \tag{3.13g}$$

$$0 \le p_1^g \le 10 \tag{3.13h}$$

$$0 \le p_2^g \le 10 \tag{3.13i}$$

$$0 \le p_1^{ddg} \le 1 \tag{3.13j}$$

$$0 \le p_2^{ddg} \le 1 \tag{3.13k}$$

$$-20 \le F_1 \le 20 \tag{3.13l}$$

$$-20 \le F_2 \le 20 \tag{3.13m}$$

$$-2 \le f_1 \le 2 \tag{3.13n}$$

$$-2 \le f_2 \le 2 \tag{3.13o}$$

where p_1^g and p_2^g represent the power dispatched to the conventional units in the transmission system with corresponding prices c_1^g and c_2^g, respectively; p_1^{ddg} and p_2^{ddg} represent the power dispatched to the DDGs in the distribution system with corresponding prices c_1^{ddg} and c_2^{ddg}, respectively; F represents the transmission system line flow, f represents the distribution system line flow, $\lambda_{\cdot}^{WM}$ denotes the LMPs in the transmission system, and $\lambda_{\cdot}^{D}$ denotes the D-LMPs in the distribution system.

By substituting the values of c_1^g, c_2^g, c_1^{ddg}, and c_2^{ddg} from Table 3.1, we can construct the ideal case formulation for Case 1. The above problem is a simple linear programming that can be solved using power system insights and the solution is as follows: $p_1^g = 10$ MW, $p_2^g = 4$ MW, $p_1^{ddg} = 0$ MW, $p_2^{ddg} = 1$ MW,$\lambda_1^{WM} = \lambda_2^{WM} = \lambda_3^{WM} = \lambda_1^D = \lambda_2^D = \lambda_3^D = 12$ \$/MWh.

With the same procedure, by substituting the values of c_1^g, c_2^g, c_1^{ddg}, and c_2^{ddg} from Table 3.2, we can construct the ideal case formulation for Case 2, and the solution is as follows: $p_1^g = 10$ MW, $p_2^g = 0$ MW, $p_1^{ddg} = 0.5$ MW, $p_2^{ddg} = 1$ MW, $\lambda_1^{WM} = \lambda_2^{WM} = \lambda_3^{WM} = \lambda_1^D = \lambda_2^D = \lambda_3^D = 15$ \$/MWh.

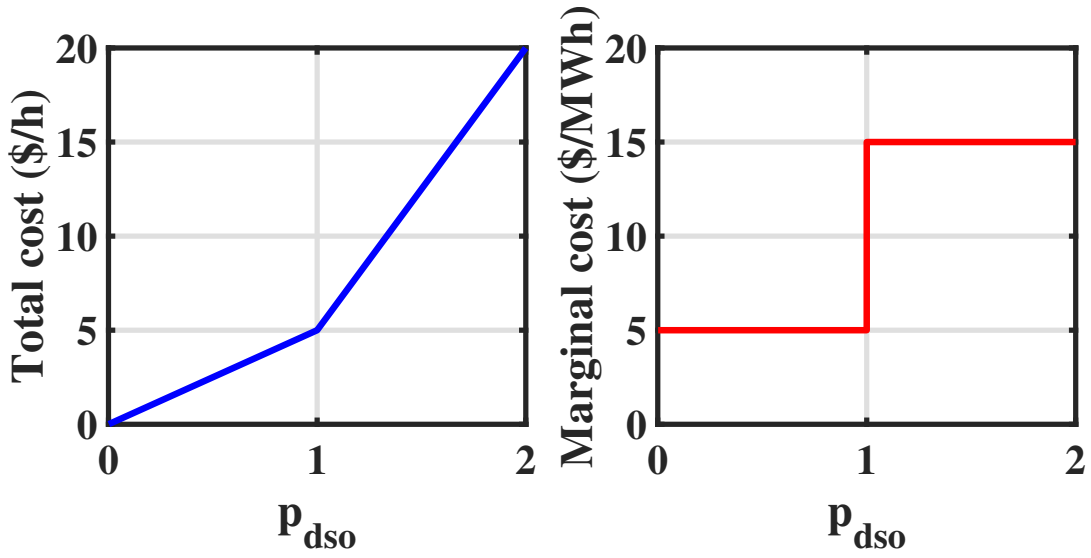

Figure 3.2: DSO bid-in total (left) and marginal (right) cost functions in the illustrative example.

3.3.2 ISO-DSO Coordination Framework

In this section, ISO-DSO coordination framework for the above example is formulated and investigated.

DSO's bid-in cost function.

In this framework, the DSO collects the offering prices of the DDGs and formulates the parametric programming dispatch problem in (3.3).

$$
\begin{aligned}
c^{dso}(p^{dso}) = \ \text{Min}_{\boldsymbol{p}^{ddg}} \quad & 15p_1^{ddg} + 5p_2^{ddg} && \text{(3.14a)}\\
\text{s.t.} \quad & p_1^{ddg} + f_1 - p^{dso} = 0 && \text{(3.14b)}\\
& f_1 - f_2 = 0 && \text{(3.14c)}\\
& p_2^{ddg} - f_2 = 0 && \text{(3.14d)}\\
& 0 \le p_1^{ddg} \le 1 && \text{(3.14e)}\\
& 0 \le p_2^{ddg} \le 1 && \text{(3.14f)}\\
& -2 \le f_1 \le 2 && \text{(3.14g)}\\
& -2 \le f_2 \le 2 && \text{(3.14h)}
\end{aligned}
$$

Both Case 1 and Case 2 have the same DDG offering prices, resulting in the DSO's bid-in cost function formulation being identical. The above formulation considers p^{dso} as a parameter, making it a parametric programming problem. This problem can be solved by varying p^{dso} from 0 to its

maximum possible value. The DSO's bid-in total and marginal cost functions for both Case 1 and Case 2 are depicted in Figure 3.2.

ISO problem.

The DSO submits its bid-in cost function to the ISO, and then the ISO proceeds to run and clear the wholesale market. The wholesale market problem can be formulated as follows:

$$\begin{aligned}
\text{Min}_{\boldsymbol{P}} \quad & c_1^g p_1^g + c_2^g p_2^g + 5p_1^{dso} + 15p_2^{dso} && \text{(3.15a)}\\
s.t. \quad & p_1^g - F_1 + F_2 = 0 \qquad [\lambda_1^{WM}] && \text{(3.15b)}\\
& p_2^g - F_2 = 0 \qquad [\lambda_2^{WM}] && \text{(3.15c)}\\
& p_1^{dso} + p_2^{dso} + F_1 - L = 0 \quad [\lambda_3^{WM}] && \text{(3.15d)}\\
& 0 \le p_1^g \le 10 && \text{(3.15e)}\\
& 0 \le p_2^g \le 10 && \text{(3.15f)}\\
& -20 \le F_1 \le 20 && \text{(3.15g)}\\
& -20 \le F_2 \le 20 && \text{(3.15h)}\\
& 0 \le p_1^{dso} \le 1 && \text{(3.15i)}\\
& 0 \le p_2^{dso} \le 1 && \text{(3.15j)}
\end{aligned}$$

where p_1^{dso}, p_2^{dso} are the variables used to model the two-segment bid-in cost function of the DSO shown in Figure 3.2.

By substituting the values of c_1^g, c_2^g from Table 3.1, we can construct the ISO problem formulation for Case 1, and the solution is as follows: $p_1^g = 10$ MW, $p_2^g = 4$ MW, $p_1^{dso} = 1$ MW, $p_2^{dso} = 0$ MW,$\lambda_1^{WM} = \lambda_2^{WM} = \lambda_3^{WM} = 12$ \$/MWh.

With the same procedure, by substituting the values of c_1^g, c_2^g from Table 3.2, we can construct the ISO problem formulation for Case 2, and the solution is as follows: $p_1^g = 10$ MW, $p_2^g = 0$ MW, $p_1^{dso} = 1$ MW, $p_2^{dso} = 0.5$ MW,$\lambda_1^{WM} = \lambda_2^{WM} = \lambda_3^{WM} = 15$ \$/MWh.

DSO's dispatch problem.

We can construct the DSO dispatch problem by substituting the value of p^{dso} determined in the ISO problem above into equation (3.14). The dispatch problem for Case 1 can be derived by substituting $p^{dso} = 1$ MW, and similarly, the dispatch problem for Case 2 can be determined by setting $p^{dso} = 1.5$ MW.

Once the dispatch problem is constructed, the dual variable (3.14b) gives the D-LMP using the dispatch problem. Since there is no congestion, the D-LMP will be the same for all nodes. The

resulting D-LMP for Case 1 is 15 $/MWh, which is different from the price determined in the ISO problem since the marginal unit is not in the distribution system. On the other hand, for Case 2, the resulting D-LMP is 15 $/MWh, which is the same as the LMP determined in the ISO problem since the marginal unit is in the distribution system.

DSO's Pricing Problem

Once the wholesale market is cleared by the ISO, the dispatch of the DSO is determined. The DSO then substitutes this dispatch into its dispatch problem to determine the dispatch of each DER aggregator in the distribution system.

The DSO utilizes the LMP at the corresponding bus to construct the pricing problem as follows:

$$\begin{aligned}
\text{Min}_{\boldsymbol{P}} \quad & 15p_1^{ddg} + 5p_2^{ddg} - LMP^* p^{dso} && \text{(3.16a)}\\
\text{s.t.} \quad & p_1^{ddg} + f_1 - p^{dso} = 0 && \text{(3.16b)}\\
& f_1 - f_2 = 0 && \text{(3.16c)}\\
& p_2^{ddg} - f_2 = 0 && \text{(3.16d)}\\
& 0 \le p_1^{ddg} \le 1 && \text{(3.16e)}\\
& 0 \le p_2^{ddg} \le 1 && \text{(3.16f)}\\
& -2 \le f_1 \le 2 && \text{(3.16g)}\\
& -2 \le f_2 \le 2 && \text{(3.16h)}
\end{aligned}$$

By substituting LMP^* from the ISO problem, we can construct the pricing problem for Case 1 and Case 2. It should be noted that in the pricing problem, p^{dso} is a decision variable that is determined by solving the optimization problem.

Pricing problem for Case 1 is constructed by substituting LMP^* with 12 $/MWh. By solving the constructed pricing problem, the value of p^{dso} for Case 1 is determined to be 1 MW, which is the same as the dispatch of the DSO determined in the ISO problem since the marginal unit is in the transmission system.

With the same procedure, the pricing problem for Case 2 can be constructed by substituting LMP^* with 15 $/MWh. However, the resulting problem exhibits degeneracy, and p^{dso} can have any value in the range of [1 MW, 2 MW] since the marginal unit is in the distribution system.

3.4 Conclusion

In this chapter, we further discuss the pricing and dispatch problem within the ISO-DSO coordination framework proposed in [35]. Specifically, we focus on the ISO-DSO coordination pricing problem, where the ISO clears the wholesale market and communicates the LMPs to the DSOs.

The DSOs then utilize these LMPs to construct the pricing problem, enabling them to determine the distribution LMPs (D-LMPs) in the distribution system market. It is mathematically proven that the D-LMP at the substation node is always equal to the LMP determined in the wholesale market, ensuring consistency in pricing across the system. We also proved the relationship between the DSO dispatch and pricing problems in the ISO-DSO coordination framework, which shows the necessity of having a dedicated DSO pricing model for the determining the D-LMPs instead of obtaining the D-LMPs directly from the DSO dispatch model. Specifically, our studies show that, under the proposed ISO-DSO coordination framework which can guarantee optimal T&D-level dispatches and prices by only requiring minimal T&D communications and zero T&D confidential model exchange, each DSO needs a dedicated dispatch model and a dedicated pricing model toward obtaining the optimal DSO-level dispatches and prices, respectively. The DSO dispatch model will not always generate the correct D-LMPs, and the DSO pricing model will not always generate the correct DSO-level dispatch signals.

To validate our findings, we conducted case studies on a small illustrative example. The results demonstrate that the DSO is revenue adequate in the ISO-DSO coordination framework. DSO's dispatch follows the ISO's dispatch by substituting ISO's dispatch signal in the dispatch problem and there will be no physical conflict. Moreover, the DSO employs LMPs determined by the ISO to formulate the DSO-level pricing problem. We have demonstrated through mathematical derivation that this pricing problem ensures no financial conflict between the ISO's market clearing and the DSO's clearing process. Specifically, we observed that when the marginal unit is located in the transmission system, the dispatch of the pricing problem consistently matches the dispatch determined by the ISO problem. On the other hand, when the marginal unit is located in the distribution system, the dispatch problem consistently yields the same D-LMP as the LMP determined in the ISO problem. These findings further support the effectiveness of the coordination between the ISO and DSO in achieving efficient and consistent outcomes.

4. ISO-DSO Coordination - An Efficient Algorithm

4.1 Introduction

The coordination of independent system operators and distribution system operators, as proposed in Chapter 1, relies on parametric programming. However, the solution of parametric programming is typically time consuming and challenging, especially for large-scale systems. Consequently, there is a need for an efficient algorithm capable of solving the parametric programming ISO-DSO coordination problem and identifying critical regions.

Many researchers have utilized parametric programming to address various issues within the field of power systems [36–43]. In [36], a modified critical region projection approach was introduced to address the multi-area economic dispatch problem. The research presented an iterative algorithm designed to solve the decomposed problem, focusing on the optimal value function within critical regions. However, no specific algorithm was provided for the identification of critical regions, and as a result, solving the parametric programming problem was not addressed. In [37], a multi-parametric programming approach was introduced to examine the influence of energy storage systems on the economic dispatch of distribution systems. The research presented an approximate algorithm designed to identify critical regions within the multi-parametric programming problem, relying on a heuristic method. However, it's important to note that the proposed algorithm does not ensure the discovery of all critical regions and could potentially be computationally inefficient, particularly when applied to large test systems. In [38], the authors employed parametric optimization techniques to investigate the effects of energy storage systems on renewable energy curtailment and system flexibility for addressing uncertainty. They introduced a ranking algorithm to identify critical regions, assuming the existence of predefined critical regions, which may not be generally accurate. In [39], a parametric programming approach is suggested for energy management in microgrids. However, it's worth noting that the paper does not present a specific algorithm to solve the parametric programming problem. In [40], a multi-parametric programming approach is employed to define the unified power trading region. The paper introduces an algorithm for identifying the solution for parameters. Nevertheless, it's important to note that there's no guarantee that this algorithm can discover all the critical regions, and computational time might be a concern with this method as well. In [41], the impact of the transmission constraints penalty factor on the market solution is explored through parametric programming. Nevertheless, the paper does not put forward an algorithm for identifying critical regions. In [42], parametric programming is employed for energy management in coordinating Distributed Energy Resources (DERs) within a microgrid. Nevertheless, the paper does not introduce an algorithm to find the critical regions associated with the solution of the parametric programming problem. In [43], a dispatch optimization model is presented for coordinating the main grid and virtual power plants, and multi-parametric programming is applied to enhance convergence speed. Nevertheless, the paper does not introduce any algorithms to identify critical regions.

To the best of our knowledge, no prior work has proposed an efficient algorithm for solving the ISO-DSO coordination problem. In this chapter, we introduce two algorithms for addressing the ISO-DSO coordination problem, as initially presented in Chapter 1. The first algorithm focuses on solving the ISO-DSO coordination parametric programming problem without accounting for

voltage constraints. The second algorithm builds upon the first by dynamically incorporating voltage constraints to determine a solution that adheres to all voltage constraints. We provide mathematical proofs to demonstrate the optimality of both algorithms. Furthermore, we extend the algorithms to accommodate unbalanced three-phase systems. To validate their effectiveness, we conduct case studies on two small illustrative examples, one balanced and one unbalanced. Additionally, we apply the algorithms to a 33-node test system, representing a balanced system, and a 240-node test system, reflecting an unbalanced system. The computational performance of both algorithms illustrates their efficiency.

4.2 ISO-DSO Coordination Problem Formulation

In this section, we introduced a general formulation of the ISO-DSO coordination problem. In the ISO-DSO coordination framework introduced in Chapter 1, the DSO needs to determine its bid in cost function to submit to the ISO. The general formulation for the DSO j to determine the bid in cost function is as follows:

$$c_j^{dso}(p_j^{dso}) = \text{Min}_{\boldsymbol{p}^{agg}} \sum_{i \in \mathcal{N}_{agg}} c_{i,j}^{agg} p_{i,j}^{agg} \tag{4.1a}$$

$$s.t.$$

$$\sum_{k \in \mathcal{N}_{jn,.}^{d}} f_{k,j}^{p} - \sum_{k \in \mathcal{N}_{jn,.}^{d}} f_{k,j}^{p} - p_j^{dso} = 0 \tag{4.1b}$$

$$\sum_{i \in \mathcal{N}_{aggn}} p_{i,j}^{agg} + \sum_{k \in \mathcal{N}_{jn,.}^{d}} f_{k,j}^{p} - \sum_{k \in \mathcal{N}_{j.,n}^{d}} f_{k,j}^{p} - l_{n,j}^{p} = 0 \tag{4.1c}$$

$$\sum_{i \in \mathcal{N}_{aggn}} q_{i,j}^{agg} + \sum_{k \in \mathcal{N}_{jn,.}^{d}} f_{k,j}^{q} - \sum_{k \in \mathcal{N}_{j.,n}^{d}} f_{k,j}^{q} - l_{n,j}^{q} = 0 \tag{4.1d}$$

$$\underline{p_{i,j}^{agg}} \leq p_{i,j}^{agg} \leq \overline{p_{i,j}^{agg}} \tag{4.1e}$$

$$\overline{-f_{k,j}^{p}} \leq f_{k,j}^{p} \leq \overline{f_{k,j}^{p}} \tag{4.1f}$$

$$U_{m,j} = U_{n,j} - 2(r_{k,j} f_{k,j} + x_{k,j} q_{k,j}) \tag{4.1g}$$

$$\underline{U} \leq U_n \leq \overline{U} \tag{4.1h}$$

where j is the index for each DSO; $\mathcal{N}_{agg}$ is the set of all aggregators; p_j^{dso} is the injected power of the DSO j to the substation which is a parameter for this parametric programming DSO problem; $\mathcal{N}_{jn,.}^{d}$ / $\mathcal{N}_{j.,n}^{d}$ are the set of lines leaving/coming node n in DSO j; $\boldsymbol{p}^{agg}$ is the vector of all decision variables; $p_{i,j}^{agg}$ is the power provided/consumed by aggregator i in DSO j with the offering cost of $c_{i,j}^{agg}$; $f_{k,j}^{p}$/$f_{k,j}^{q}$ is the active/reactive power flow of branch k in DSO j; $l_{k,j}^{p}$/$l_{k,j}^{q}$ is the active/reactive power load at node n in DSO j; $q_{i,j}^{agg}$ is the reactive power provided/consumed by aggregator i in DSO j;

Equation (4.1a) represents the objective function aimed at minimizing the total cost within the distribution system. Equation (4.1b) establishes the node balance constraint at the substation node. Equations (4.1c) and (4.1d) stand as the active and reactive power node balance constraints.

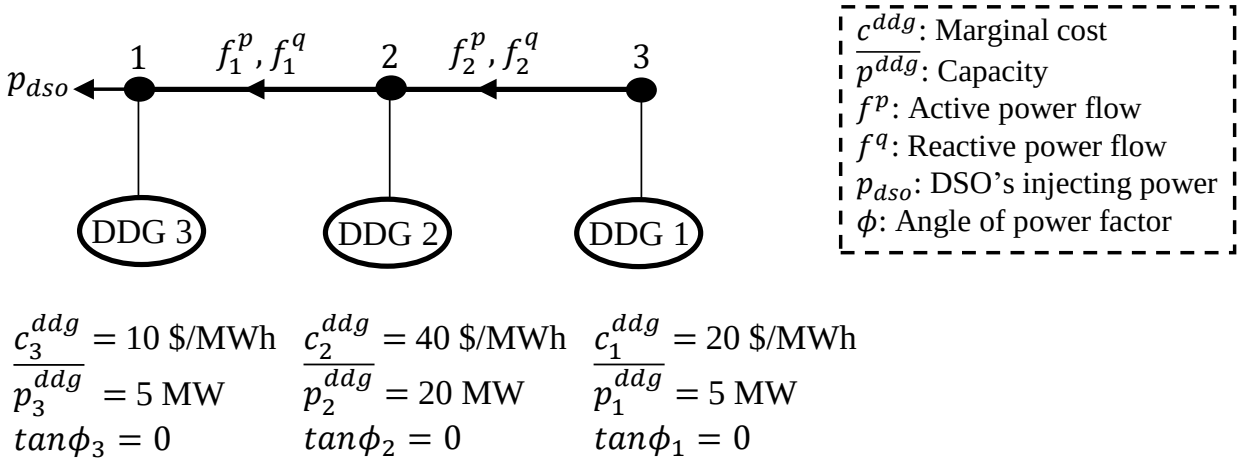

Figure 4.1: A balanced illustrative example system.

Equation (4.1e) imposes limits on the active power of each aggregator in relation to their respective capacities. Equation (4.1f) sets restrictions on the flow along each branch, considering the branch capacity limits. Equation (4.1g) defines the voltage level at each node. Finally, Equation (4.1h) places constraints on the voltage at each node based on predefined voltage limits.

By defining p_j^{dso} is defined as a parameter, Problem (4.1) is a parametric linear programming (LP) problem [35], since 1) piecewise-linear cost functions are adopted in our proposed ISO-DSO coordination framework, which fully comply with today's wholesale market clearing rules in US; and 2) linearized distribution power flow [30] is adopted to model the real/reactive power balance constraints, line flow constraints, and voltage constraints.

Although off-the-shelf parametric LP solvers [44–48] can have polynomial ($O(n^k)$) time complexity in some special cases [45, 46], the worst-case time complexity of general large-scale parametric LP is still exponential ($O(2^n)$) [49]. As the DSO problem size grows significantly (when numerous DERs enter DSO), these off-the-shelf algorithms will be inefficient for online computations.

4.3 Algorithm Structure

In this section, the proposed algorithm is explained in detail. Generally, the algorithm consists of two parts. The first algorithm solves the problem without considering any voltage constraints. Then, the second algorithm incorporates all the voltage constraints through cutting planes. Following this, we will elaborate on each algorithm in detail. To facilitate readers' understanding of the algorithm structures, we initially elucidate both algorithms through an illustrative example. Subsequently, we dive into the general formulations and details of the algorithms' mathematics.

4.3.1 Illustrative Example

Consider the system depicted in Fig. 4.1, which comprises three nodes and three DDGs. The system's data is also presented in Fig. 4.1. The DSO's bid-in cost function formulation is as follows.

$$c(p^{dso}) = \text{Min} \quad 20p_1^{ddg} + 40p_2^{ddg} + 10p_3^{ddg} \tag{4.2a}$$
$$\text{s.t.} \quad p_1^{ddg} - f_2^p = 0 \tag{4.2b}$$
$$p_2^{ddg} + f_2^p - f_1^p = 0 \tag{4.2c}$$
$$p_3^{ddg} + f_1^p - p^{dso} = 0 \tag{4.2d}$$
$$0 \le p_1^{ddg} \le 5 \tag{4.2e}$$
$$0 \le p_2^{ddg} \le 20 \tag{4.2f}$$
$$0 \le p_3^{ddg} \le 5 \tag{4.2g}$$
$$-50 \le f_1^p, f_2^p \le 50 \tag{4.2h}$$
$$0.95^2 \le U_2 = 1+2(0.1f_1^p + 0.1f_1^q) \le 1.05^2 \tag{4.2i}$$
$$0.95^2 \le U_3 = U_2+2(0.1f_2^p + 0.1f_2^q) \le 1.05^2 \tag{4.2j}$$

Algorithm 1

Let us remove all the voltage constraints (4.2i)-(4.2j) and consider we want to solve this problem.

First, we find the minimum value of p^{dso}, which in this case will be zero because we do not have any demand response aggregator.

Next, we sort all the DDGs based on their offering price from minimum to maximum. We start with the DDG offering the lowest price, which is DDG3. We assess how much power can be provided from this DDG before moving on to the next. Since DDG3 is connected directly to the substation, there is no branch limit, allowing us to utilize its full capacity of 5 MW. Therefore, the first breakpoint is determined to be (5 MW, \$10/MWh). This means that from zero to 5 MW, the cost of providing power from this DSO is \$10/MWh.

Beyond 5 MW, we proceed to the next cheapest DDG, which is DDG1. We continue to provide power from this DDG until its capacity is reached or the limit of the line connecting this DDG to the substation is met. Given the minimum of 5 MW and 50 MW is 5 MW, we can utilize the full capacity of this DDG, setting the next breakpoint at (10 MW, \$20/MWh). Subsequently, we update the line capacity connecting DDG1 to the substation, resulting in a new capacity of 45 MW for these lines.

Moving to the next cheapest DDG, which is DDG2, the minimum of the line capacity of line 2, which connects this DDG to the substation, and the capacity of this DDG is the lesser of 35 MW and

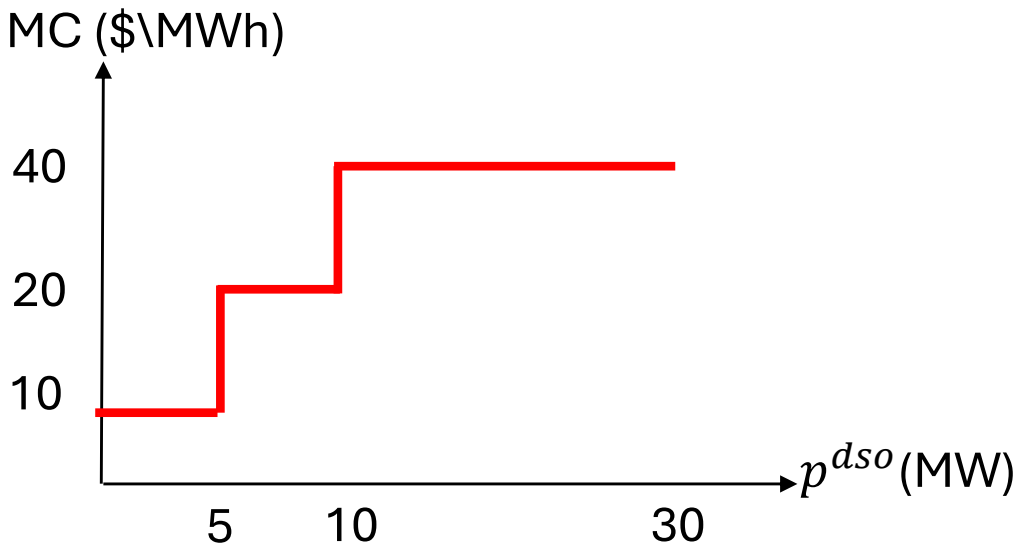

Figure 4.2: Marginal cost curve.

20 MW, which is 20 MW. Therefore, the next breakpoint is (30 MW, $40/MWh), marking the final breakpoint as no DDGs are left. Beginning with a baseline of zero, if we link these breakpoints, it results in the formation of the marginal cost curve, as outlined in Fig. 4.2 and breakpoints given in Table 4.1.

Algorithm 2

Before initiating Algorithm 2, it's necessary to refine the formulation by eliminating all flow variables and substituting them with voltage constraints. The formulation, after removing all the

flow variables and substituting the voltage constraints, is as follows:

$$\text{Min}_{\boldsymbol{p}^{ddg}} \quad 10p_1^{ddg} + 30p_2^{ddg} + 10p^{dso} \tag{4.3a}$$
$$\text{s.t.} \quad p_1^{ddg} - 5 \leq 0, -p_1^{ddg} \leq 0 \tag{4.3b}$$
$$p_2^{ddg} - 20 \leq 0, -p_2^{ddg} \leq 0 \tag{4.3c}$$
$$p_3^{ddg} - 5 \leq 0, -p_3^{ddg} \leq 0 \tag{4.3d}$$
$$p_1^{ddg} + p_2^{ddg} - 50 \leq 0 \tag{4.3e}$$
$$p_1^{ddg} - 50 \leq 0 \tag{4.3f}$$
$$-p_1^{ddg} - p_2^{ddg} - 50 \leq 0 \tag{4.3g}$$
$$-p_1^{ddg} - 50 \leq 0 \tag{4.3h}$$
$$0.1p_1^{ddg} + 0.1p_2^{ddg} - 0.025 \leq 0 \tag{4.3i}$$
$$-0.1p_1^{ddg} - 0.1p_2^{ddg} - 0.025 \leq 0 \tag{4.3j}$$
$$0.2p_1^{ddg} + 0.1p_2^{ddg} - 0.025 \leq 0 \tag{4.3k}$$
$$-0.2p_1^{ddg} - 0.1p_2^{ddg} - 0.025 \leq 0 \tag{4.3l}$$

We initiate the analysis at each breakpoint as determined by Algorithm 1, which is presented in Table 4.1. Our first step is to assess any potential violations of voltage constraints. This evaluation process is graphically illustrated in Fig. 4.3, where breakpoints are represented on the $(p_1^{ddg}, p_2^{ddg}, p^{dso})$ plane. In Fig. 4.3, the breakpoints are depicted as red dots, each encircled by a number. Breakpoints 1 through 3 comply with all voltage constraints; however, breakpoint 4 exhibits violations.

To address these violations, we incorporate the violated voltage constraints as cutting planes and calculate their intersection with the line connecting the third and fourth breakpoints, referred to as the marginal line. Subsequently, we calculate the marginal cost from breakpoint 3 to each point of intersection, selecting the one with the lowest marginal cost. For instance, if plane a imposes the voltage constraint resulting in the minimum marginal cost, this intersection point is designated as the new breakpoint, denoted as $4'$.

Next, we need to identify the marginal line. Given the three-dimensional nature of the plane, each point represents the intersection of three planes. We have already selected one of these planes—the one generating the new fourth breakpoint. Considering that the marginal line is defined by two planes in this three-dimensional space, we consider two potential paths for the marginal line: plane a and one of the planes from the previous marginal line that connected the third to the fourth breakpoint. We then examine the intersections of these potential marginal lines with all voltage and non-voltage constraints, calculating the marginal costs to identify the minimum, which in our case is the intersection of plane b and marginal line α. Following this, no feasible increase in p^{dso} can be observed, indicating the identification of the fifth breakpoint which is the final breakpoint. The resulted breakpoints are presented in Table 4.2.

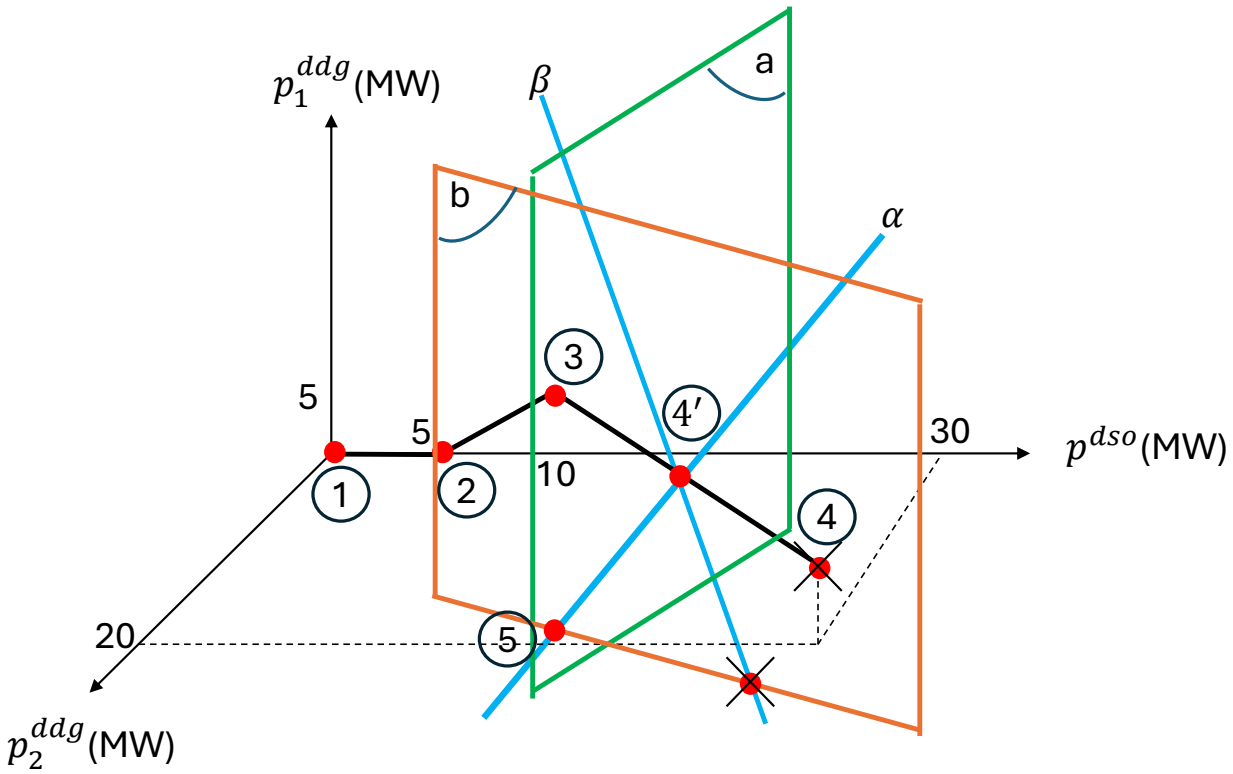

Figure 4.3: Break points using Algorithm 2.

Table 4.1: Breakpoints using Algorithm 1 for the balanced illustrative example

p_1^{ddg} (MW)	p_2^{ddg} (MW)	p_3^{ddg} (MW)	p^{dso} (MW)
0	0	0	0
0	0	5	5
5	0	5	10
5	20	5	30

Table 4.2: Breakpoints using Algorithm 2 for the balanced illustrative example

p_1^{ddg} (MW)	p_2^{ddg} (MW)	p_3^{ddg} (MW)	p^{dso} (MW)
0	0	0	0
0	0	5	5
5	0	5	10
5	12.5	5	22.5
2	20	5	27

4.3.2 Generalized Formulation of Algorithms

To start, we eliminate all the dependent decision variables in the DSO parametric LP problem. For each equality constraint in (4.1), we can eliminate one dependent decision variable. Let n denote the number of nodes in the distribution system. Considering the radial feature of the distribution network, we'll have a total of $n-1$ lines, subsequently leading to $n-1$ active power flow variables. In parallel, we'll also have n active power balance constraints. This presents an opportunity to employ these equality constraints for substituting all the active power flow variables, along with utilizing one remaining equality constraint to eliminate one of the decision variables associated with the power provided/consumed by aggregators. Note that we have the same procedure for eliminating the reactive power flow variables. Consider the following representation of Problem (4.1):

$$\begin{aligned} \text{Min} \quad & CX && \text{(4.4a)} \\ \text{s.t.} \quad & AX = B && \text{(4.4b)} \\ & DX \leq E && \text{(4.4c)} \end{aligned}$$

To eliminate power flow variables, let us open up equation (4.4b):

$$\begin{bmatrix} A_1 & A_2 \\ A_3 & A_4 \end{bmatrix} \begin{bmatrix} X_1 \\ X_2 \end{bmatrix} = \begin{bmatrix} B_1 \\ B_2 \end{bmatrix} \tag{4.5}$$

If we multiply the first row of Equation (4.5), we obtain the following:

$$X_2 = A_4^{-1}(B_2 - A_3 X_1) \tag{4.6}$$

Then we can substitute X_2 into the first row equation:

$$A_1 X_1 + A_2 A_4^{-1}(B_2 - A_3 X_1) = B_1 \tag{4.7}$$

By utilizing Equation (4.7), we can proceed to eliminate an additional dependent decision variable. Ultimately, we can substitute all the flow variables and one of the decision variables ($p_{i,j}^{agg}$), and incorporate these replacements into Problem (4.4) which will lead to the following optimization problem:

$$\begin{aligned} \text{Min} \quad & C_1 X_1 + C_2 A_4^{-1}(B_2 - A_3 X_1) && \text{(4.8a)} \\ \text{s.t.} \quad & D_1 X_1 + D_2 A_4^{-1}(B_2 - A_3 X_1) \leq E_1 && \text{(4.8b)} \\ & D_3 X_1 + D_4 A_4^{-1}(B_2 - A_3 X_1) \leq E_2 && \text{(4.8c)} \end{aligned}$$

Problem (4.8) does not include any flow variables and has one of the decision variables ($p_{i,j}^{agg}$) reduced compared to Problem (4.4).

4.3.3 Algorithm 1: ISO-DSO coordination problem without voltage constraints

In the proposed algorithm, initially, we eliminate all the voltage constraints and employ the following algorithm to determine the breakpoints.

Algorithm 1 Solving problem (4.1) without voltage constraints

Sort DRs decreasing based on offering price.
Sort DDGs increasing based on offering price.

$i \in \mathcal{N}^{dr}$Min $[\overline{f}_{k=n_i:n_s}, \overline{p}_i^{dr}]$
Update p^{dso}, p_i^{dr} and $\overline{f}_{k=n_i:n_s}$
Calculate $left_i = \overline{p}_i^{dr} - p_i^{dr}$
$left_i = 0$ Continue; Define $\mathcal{N}_i^c = \{j | j \in \mathcal{N}^{ddg}, c_j^{dr} \geq c_j^{ddg}\}$
$left_i, \mathcal{N}_i^c \neq 0$Min $[left_i, \overline{p}_z^{ddg}, \overline{f}_{k=n_i:n_z}]$
Update $left_i$, p^{dso}, p_i^{dr}, p_z^{ddg} and $\overline{f}_{k=n_i:n_z}$
$z \leftarrow z + 1 \quad \mathcal{N}^{agg} \leftarrow \mathcal{N}^{ddg} \cup \mathcal{N}^{dr}$
$c^{agg} \leftarrow \text{sort}(c^{ddg} \cup c^{dr})$
$i \in \mathcal{N}^{agg}$Calculate $left_i = \overline{p}_i^{agg} - p_i^{agg}$
$left_i \leftarrow$ Min $[\overline{f}_{k=n_i:n_s}, left_i]$
$left_i$ =0Continue Update p^{dso}, p_i^{agg}, and $\overline{f}_{k=n_i:n_s}$
$c^{dso} \leftarrow c^{dso} \cup c_i^{agg}$

Algorithm 1 consists of two main steps: Step 1 which includes lines 1-14; Step 2 which includes lines 15-23:

- **Step 1 (lines 1-14):** We begin by sorting DRs in decreasing order and DDGs in increasing order. The primary objective of this step is to identify the initial conditions for each aggregator's power injection or consumption value and for p^{dso}. In line 2, we determine the minimum value between the DR's capacity and the capacities of all lines connecting the DR to the substation. Subsequently, we update the values in line 5 and compute the remaining capacity for the DR in line 6. If there is no capacity left, we move on to the next DR. Then, in line 10, we establish a set to collect all the DDGs with offering prices lower than that of the DR. In line 12, we choose the minimum capacity between the line connecting the DR to the DDG and the capacity of that DDG until there is no capacity left for the DR or the DDGs. This process is repeated for all DRs.

- **Step 2 (lines 15-23):** We unify all DRs and DDGs, sorting them in ascending order in lines 15-16. We then iterate through each of them to compute the available capacity in line 18. This is determined by selecting the minimum value between the remaining capacity of the aggregator and the capacity of all lines connecting that aggregator to the substation. If no capacity remains, we proceed to the next aggregator and update the values in line 22. At this stage, we also consider the aggregator's cost as the cost of the DSO. This process is repeated for all the aggregators.

Theorem 6. *Algorithm 1 yields optimal solutions (i.e., breakpoints in the piecewise-linear DSO bid-in cost function) and the optimal bid cost function for the parametric LP DSO in Problem (4.1) without voltage constraints.*

Proof. See Appendix.

4.3.4 ISO-DSO coordination problem considering voltage constraints

In the previous section, we determined all the breakpoints for the piecewise-linear DSO bid-in cost function by excluding voltage constraints and utilizing Algorithm 1. In this section, our focus shifts to reintroducing all voltage constraints and deriving breakpoints while taking these constraints into account.

Algorithm 2 Solving problem (4.1) considering voltage constraints

$i \in Br B_i^f \leftarrow$ set of binding non voltage constants
$B_i^v \leftarrow$ set of binding voltage constants
$C \leftarrow$ total cost of Br_i
$B_i^v \neq 0 \;\; \& \;\; B_{i-1}^v = 0 \; CB_i \leftarrow B_{i-1}^f \cap B_i^f$
$j \in B_i^v A_j, B_j \leftarrow Eq(CB_j \cup B_j^v)$
$X_j \leftarrow A_j^{-1} B_j, C_j(X_j)$ **if** up:
$Br_i \leftarrow \{X_j \mid C_j(X_j)$ is minimum$\}$
if dn:
$Br_i \leftarrow \{X_j \mid C_j(X_j)$ is maximum$\}$
$BC \leftarrow B_j^v$
$\Delta p^{dso} \leftarrow p_j^{dso}$-$p_i^{dso}$
$\Delta p^{dso} \neq 0 \; k \in CB_j Ml_k \leftarrow B_{i \neq k}^f \cup BC \; j \in B_i^v \; kA_k, B_k \leftarrow Eq(Ml_j \cup B_j^v)$
$X_k \leftarrow A_k^{-1} B_k, C_k(X_k)$ **if** $B_{X_k}^f || B_{X_k}^v > 0$: delete X_k
if up: $\tilde{Br}_j \leftarrow \{X_k \mid C_k(X_k)$ is minimized$\}$
if dn: $\tilde{Br}_j \leftarrow \{X_k \mid C_k(X_k)$ is maximized$\}$
$j \in B^f \; kA_k, B_k \leftarrow Eq(Ml_j \cup B_j^v)$
$X_k \leftarrow A_k^{-1} B_k, C_k(X_k)$ **if** $B_{X_k}^f || B_{X_k}^v > 0$: delete X_k
if up: $\tilde{Br}_j \leftarrow \{X_k \mid C_k(X_k)$ is minimized$\}$
if dn: $\tilde{Br}_j \leftarrow \{X_k \mid C_k(X_k)$ is maximized$\}$
if up:$Br_i \leftarrow \{\tilde{Br}_j \mid C_j(\tilde{Br}_j)$ is minimized$\}$
if dn:$Br_i \leftarrow \{\tilde{Br}_j \mid C_j(\tilde{Br}_j)$ is maximized$\}$
Update Ml, BC , Δp^{dso}

Algorithm 2 comprises the following steps:

- **Step 1 (lines 1-15):** For each breakpoint determined using Algorithm 1, we establish a set of binding voltage constraints and a set of binding non-voltage constraints in lines 2-3. Next, we compute the total cost for the current breakpoint in line 4. If it is the first breakpoint, we proceed to the next breakpoint and repeat the process. Following that, we check whether any voltage constraint is violated when transitioning from the previous breakpoint to the current breakpoint in line 5. If that's the case, we proceed to identify the line that connects the previous breakpoint to the current breakpoint in line 6. It's important to note that if we have

n as the dimension, line 6 yields $n-1$ equations, which essentially determine a line in an n-dimensional space. Consequently, we can intersect this line with all the violated voltage constraints. For each violated voltage constraint, we combine the equations corresponding to the lines determined in line 6 with the violated voltage constraint, thereby deriving the coefficient matrices for these n sets of equations in line 8. In line 9, we determine the intersection point and calculate the total cost associated with this point. Once we have calculated all these intersection points for the violated voltages, we select the one with the minimum marginal cost if we are moving forward and the one with the maximum marginal cost if we are moving downward in lines 10-13. We store this point as the new breakpoint in line 14 and calculate the difference between the p^{dso} of the current breakpoint and the previous breakpoint in line 15.

- **Step 2 (lines 16-35):** We define Δp^{dso} and initiate a loop while Δp^{dso} has a positive value. When determining the new breakpoint, we also need to find the new marginal line to intersect with the subsequent voltage and non-voltage constraints. To achieve this, we generate all potential marginal lines in lines 17-18. These lines are derived by considering the previous marginal line and replacing one of them with the newly violated constraints from the previous breakpoint determination. Notably, this generates $n-1$ potential marginal lines. We aim to intersect each set of these potential marginal lines with all the voltage constraints (lines 19-25) and non-voltage constraints (lines 26-32) and select the optimal one. In lines 21-22, we intersect these lines with the current voltage constraint within the loop, determine the intersection point, and calculate the total cost associated with this intersection point. In line 23, we conduct a feasibility test to ensure that none of the constraints are violated by this intersection point, removing it if necessary. For each voltage constraint in the loop, we select the intersection point that has the minimum marginal cost when moving forward and the maximum marginal cost when moving downward in lines 24-25. We repeat the same procedure for non-voltage constraints in lines 26-32. This results in having all the intersections for both voltage and non-voltage constraints. We then choose the one with the minimum marginal cost when moving forward and the maximum marginal cost when moving downward in lines 33-34. In line 35, we update the candidate marginal lines, breakpoint and the Δp^{dso}. To update the marginal lines, we substitute the new binding constraints with all the elements of the selected marginal line and generate the new set of marginal lines.

Theorem 7. *Algorithm 2 yields optimal breakpoints and the optimal bid cost function for Problem (4.1) after considering all the voltage constraints.*

Proof. See Appendix.

4.4 Algorithm Extensions for Unbalanced Systems

The algorithm explained in the previous section is extended to accommodate unbalanced distribution systems. The formulation for unbalanced distribution systems was introduced in our prior work [3].

4.4.1 Extension of Algorithm 1

Consider the unbalanced DSO formulation proposed in our previous work [3]. When we eliminate all the voltage constraints, each of the three phases becomes independent of the others, as no constraints or equations connect them. We can then employ Algorithm 1 to determine the breakpoints and bid in cost function independently for each phase.

The objective function for the parametric programming dispatch problem in a three-phase unbalanced system is as follows:

$$\text{Min} \quad p_A^{dso}\pi_A + p^{dso}\pi_B + p_C^{dso}\pi_C \tag{4.9}$$

On the transmission side, everything must be balanced ($p_A^{dso} = p_B^{dso} = p_C^{dso} = \frac{p^{dso}}{3}$). Therefore, we can reformulate the objective function as follows:

$$\text{Min} \quad p^{dso}\frac{\pi_A + \pi_B + \pi_C}{3} \tag{4.10}$$

This implies that to find the total bid in cost function of the distribution system, we must intersect all the bid cost functions from each phase along the p^{dso} axis. Regarding the price axis, it needs calculating the average of the bid cost functions from the three phases. This process is shown in Algorithm 3

Algorithm 3 Extension to Algorithm 1 for unbalanced systems.

$p_A^{dso}, c_A^{dso} \leftarrow$ Algorithm 1 on phase A
$p_B^{dso}, c_B^{dso} \leftarrow$ Algorithm 1 on phase B
$p_C^{dso}, c_C^{dso} \leftarrow$ Algorithm 1 on phase C
$p^{dso} \leftarrow p_A^{dso} \cup p_B^{dso} \cup p_C^{dso}$
$c^{dso} \leftarrow \frac{1}{3}(c_A^{dso} + c_B^{dso} + c_C^{dso})$

4.4.2 Extension of Algorithm 2

Once we've utilized Algorithm 1 to calculate the bid in cost function for the unbalanced distribution system, the next step involves incorporating all the voltage constraints to determine the actual breakpoints. Algorithm 2 can be effectively employed for this purpose while considering all the voltage constraints. However, a problem can occur in some rare conditions in the case of the three-phase unbalanced system.

In the generation of marginal lines, we previously assumed that one voltage constraint could be added at a time. This assumption holds true for balanced test systems because in such systems, the voltage at each node is a function of the voltage at previous nodes, and there exists a recursive relationship between them. However, in three-phase transmission systems, there may be rare instances where three voltage constraints jointly contribute to generating new marginal lines. This scenario might lead us to identify a breakpoint that is not valid. Nevertheless, we have demonstrated

that this does not pose a significant issue because we can readily identify the invalid breakpoint through a post-processing procedure.

In this post-processing step, we use monotonically increasing feature of the bid in cost function to pinpoint breakpoints where the marginal cost is not monotonically increasing. This indicates that the breakpoint is not on the optimal path and should be discarded. This allows us to efficiently remove redundant breakpoints and retain only the optimal ones. This extension is given in Algorithm 4

Algorithm 4 Extension to Algorithm 2 for unbalanced systems.

$Br \leftarrow$ Algorithm 2
$i \in BrMC \leftarrow$ marginal cost of Br_{i-1} to Br_i
$MC_i \leq MC_{i-1}$ delete Br_i

4.5 Case Studies

In this section, case studies have been conducted. Two case studies were performed on larger test cases, comprising a balanced test system consisting of 33 nodes and an unbalanced test system with 240 nodes.

In our prior work [35], we conducted simulations using a 33-node test system and a 240-node test system, employing the YALMIP parametric programming solver [48]. Here, we applied our proposed algorithm to determine the DSO's bid-in cost function for both of these systems and compared the solution times of our algorithm and YALMIP. It's important to note that both our algorithm and YALMIP yield the same results as previously proposed in [35], and these results are not reiterated here.

The simulation results were generated using a computer equipped with a 2.3 GHz, 8-core CPU and 16 GB of RAM. The solution times are presented in Table 4.3. The table provides a breakdown of each algorithm's performance, as well as the total time consumed by both algorithms combined. In the case of the 33-node test system, voltage violations occurred, necessitating the use of Algorithm 2. However, for the 240-node test system, no voltage violations were encountered, explaining the 0 time in the table.To evaluate our algorithm under conditions where violations occur, we modified the 240-node test system. We increased the capacities of all DDGAGs by a factor of 15, all DRAGs by a factor of 16, and REAGs by a factor of 16. A comparison of solution times between YALMIP and our algorithm reveals an exponential increase in solution time for YALMIP. However, our algorithm demonstrates significantly shorter solution times compared to YALMIP.

A comparison of the computational performance of both algorithms and YALMIP reveals that these algorithms are significantly faster, particularly as the system scale increases.

4.6 Conclusion

We previously introduced an ISO-DSO coordination framework based on parametric programming. Solving parametric programming problems is generally time-consuming and challenging. In this chapter, we present an efficient algorithm designed to address the ISO-DSO coordination framework

Table 4.3: Computational performance of the algorithms and YALMIP.

Method	33 node	240 node	Modified 240 node
Algorithm 1	0.02 s	0.02 s	0.02
Algorithm 2	0.37 s	0 s	12.5
Both Algorithms	0.39 s	0.02 s	12.52
YALMIP	0.77 s	30.91 s	270 s

by leveraging the characteristics of the distribution system. We propose two algorithms, one of which can be employed after removing all voltage constraints and is exceptionally swift in determining breakpoints. The other algorithm is intended for use when voltage constraints are added. Importantly, we provide mathematical proof that both algorithms yield optimal solutions for the DSO's bid cost function.

To validate our approach, we conducted case studies on two illustrative examples, comprising both balanced and unbalanced test systems, as well as two large test systems: a balanced 33-node test system and an unbalanced 240-node test system. Our results demonstrated the remarkable efficiency of both proposed algorithms, particularly when compared to the computation time of off-the-shelf parametric programming solver in YALMIP. It was evident that the algorithm's performance surpassed that of YALMIP, especially as the system's scale increased.

Appendix

Proof of Theorem 6

Here, we show that Algorithm 1 is based on KKT conditions. Hence, it gives the optimal solution. Let's consider the parametric programming DSO dispatch problem in which the flow variables have been removed. The problem is as follows:

$$\text{Min} \sum_{i \in \mathcal{N}_{agg}} c_i^{agg} p_i^{agg} \tag{4.11a}$$

$$\text{s.t.} \sum p_i^{agg} - \sum l_n = p^{dso};\ [\lambda] \tag{4.11b}$$

$$0 \le p_i^{agg} \le \overline{p_i^{agg}};\ \forall i \in \mathcal{N}_{agg};\ [\alpha_i^-, \alpha_i^+] \tag{4.11c}$$

$$-\overline{f_k} \le f_k(p_{1\dots n}^{agg}) \le \overline{f_k};\ \forall k \in \mathcal{N}_J;\ [\mu_k^-, \mu_k^+] \tag{4.11d}$$

We can write the Lagrangian function as follows:

$$\begin{aligned}
\mathcal{L} = & \sum_{i \in \mathcal{N}_{agg}} c_i^{agg} p_i^{agg} + \sum_{i \in \mathcal{N}_{agg}} \alpha_i^-(-p_i^{agg}) \\
& + \sum_{i \in \mathcal{N}_{agg}} \alpha_i^+(p_i^{agg} - \overline{p_i^{agg}}) \\
& + \sum_{\forall k \in \mathcal{N}_J} \mu_k^-(-\overline{f_k} - f_k(p_{1\dots n}^{agg})) \\
& + \sum_{\forall k \in \mathcal{N}_J} \mu_k^+(f_k(p_{1\dots n}^{agg}) - \overline{f_k}) \\
& + \lambda(p^{dso} - \sum p_i^{agg} + \sum l_n)
\end{aligned} \tag{4.12}$$

We can formulate the KKT conditions as follows:

$$c_i^{agg} - \lambda - \alpha_i^- + \alpha_i^+ + \sum_{k \in \mathcal{K}_i} (\mu_k^+ - \mu_k^-) = 0; \quad \forall i \in \mathcal{N}_{agg} \tag{4.13a}$$

$$p^{dso} - \sum p_i^{agg} + \sum l_n = 0 \tag{4.13b}$$

$$\mu_k^-(-\overline{f_k} - f_k(p_{1\dots n}^{agg})) = 0;\ \forall k \in \mathcal{N}_J \tag{4.13c}$$

$$\mu_k^+(f_k(p_{1\dots n}^{agg}) - \overline{f_k}) = 0;\ \forall k \in \mathcal{N}_J \tag{4.13d}$$

$$\alpha_i^-(-p_i^{agg}) = 0;\ \forall i \in \mathcal{N}_{agg} \tag{4.13e}$$

$$\alpha_i^+(p_i^{agg} - \overline{p_i^{agg}}) = 0;\ \forall i \in \mathcal{N}_{agg} \tag{4.13f}$$

The only unknown variable in the set of equations (4.13) is p^{dso}. A closed-loop solution to the KKT conditions is not possible.

To solve the system of equations in (4.13), we must partition the variable p^{dso} in a way that maintains the same marginal unit within each partition. This approach comes from the key features related to the structure of optimization problem (4.11) and insights from economic dispatch problems.

In the optimization problem (4.11), the marginal unit is always a single generator, and there is no possibility of a combination of multiple generators acting as the marginal unit. This feature comes from the fact that the coefficients of all the constraints are either +1 or -1. When we successfully partition p^{dso} and identify a specific unit as the marginal unit, it leads to conditions such as $\alpha_1^- = \alpha_1^+ = \sum_{k \in \mathcal{K}i}(\mu k^+ - \mu_k^-) = 0$. Using equation (4.13a), it implies that $c_i^{agg} = \lambda$ in this case, indicating that the price of the DSO within that partition is equal to the offering price of the corresponding aggregator.

The process begins with the search for the minimum value of p^{dso} and progressively increasing it while monitoring changes in the group of generators. Each transition in this group marks the occurrence of a breakpoint, signifying a shift in the cost associated with providing the next megawatt (MW).

To determine the lowest value of p^{dso}, we maximize the dispatch of DRs up to the constraints imposed by line capacity. This process allows us to identify the minimum value of p^{dso}. The limiting factors in this process include the capacity of the DR or the capacity of the lines connecting the DR to the substation. This approach is implemented in step 1 of Algorithm 1, as outlined in lines 3-6.

Additionally, we need to determine the minimum value for DDGs. Here, we draw from the intuition derived from economic dispatch. When the offering price of DR is higher than the offering price of DDG, redirecting power from DDG to DR reduces the objective function. This insight guides the sorting of DRs and DDGs. The approach in Algorithm 1, detailed in lines 7-14, incorporates this logic.

With the minimum value of p^{dso} identified and the initial values of other aggregators established, we proceed to increase p^{dso} incrementally, adhering to the sorted list of aggregators. Beginning with the aggregator offering the lowest price, we determine the capacity of the lines connecting this aggregator to the substation, denoted as $\overline{f}k = n_i : n_s$. This information allows us to increase p^{dso} from its minimum to $min\{\overline{p_1^{agg}}, \overline{f}k = n_i : n_s\}$ while keeping the first aggregator as the marginal unit. This is the logic used in lines 18-19 of Algorithm 1. Utilizing complementary slackness, resulting in conditions such as $\alpha_1^- = \alpha_1^+ = \sum_{k \in \mathcal{K}i}(\mu k^+ - \mu_k^-) = 0$. Consequently, we determine that $\lambda = c_1^{agg}$, which is indicated in line 23 of Algorithm 1.

To further increase p^{dso}, we must move beyond this value and employ the next cheapest aggregator, which is the second aggregator. We apply the same principles to this partition of p^{dso}, resulting in $\lambda = c_2^{agg}$. This process continues until all aggregators are fully utilized or the line limit is reached, as described in the second step of Algorithm 1.

Proof of Theorem 7

In the preceding section, we established that all the breakpoints determined using Algorithm 1 are optimal and aligned with the KKT conditions. In Algorithm 2, we initiate our analysis with the breakpoints identified through Algorithm 1. Consequently, as long as there are no voltage constraints being violated, we remain on the optimal route. However, if a voltage violation occurs, we pinpoint all potential candidates by intersecting it with all the breakpoints, and we select the breakpoint for which $\frac{\Delta Cost}{\Delta p^{dso}}$ is minimized.

Drawing upon the Lagrangian function and employing the Envelope theorem, we recognize that $\frac{\partial Cost}{\partial p^{dso}}$ is equivalent to $\frac{\partial \mathcal{L}}{\partial p^{dso}}$, and we further know that $\frac{\partial \mathcal{L}}{\partial p^{dso}} = \lambda$. Hence, our selection process focuses on the partition of p^{dso} with the minimum marginal cost, which aligns with the ultimate goal of determining the bid-in cost function.

References

[1] Y. Chen, T. Zheng, X. Wang, and S. Oren, "Der market integration – opportunities and challenges," in *Panel session at 2020 IEEE Power and Energy Society General Meeting*, 2020.

[2] Federal Energy Regulatory Commission, "Order no. 2222: Participation of distributed energy resource aggregations in markets operated by regional transmission organizations and independent system operators," 2020.

[3] M. Mousavi and M. Wu, "A dso framework for market participation of der aggregators in unbalanced distribution networks," *IEEE Transactions on Power Systems*, 2021.

[4] H. Chen, L. Fu, L. Bai, T. Jiang, Y. Xue, R. Zhang, B. Chowdhury, J. Stekli, and X. Li, "Distribution market-clearing and pricing considering coordination of dsos and iso: An epec approach," *IEEE Trans. Smart Grid*, 2021.

[5] A. Hassan and Y. Dvorkin, "Energy storage siting and sizing in coordinated distribution and transmission systems," *IEEE Trans. Sustain. Energy*, vol. 9, no. 4, pp. 1692–1701, 2018.

[6] T. Jiang, C. Wu, R. Zhang, X. Li, H. Chen, and G. Li, "Flexibility clearing in joint energy and flexibility markets considering tso-dso coordination," *IEEE Transactions on Smart Grid*, 2022.

[7] K. Steriotis, P. Makris, G. Tsaousoglou, N. Efthymiopoulos, and E. Varvarigos, "Co-optimization of distributed renewable energy and storage investment decisions in a tso-dso coordination framework," *IEEE Transactions on Power Systems*, 2022.

[8] M. Zhang, Y. Xu, and H. Sun, "Optimal coordinated operation for a distribution network with virtual power plants considering load shaping," *IEEE Transactions on Sustainable Energy*, 2022.

[9] M. A. El-Meligy, M. Sharaf, and A. T. Soliman, "A coordinated scheme for transmission and distribution expansion planning: A tri-level approach," *Electric Power Systems Research*, vol. 196, p. 107274, 2021.

[10] F. Moret, A. Tosatto, T. Baroche, and P. Pinson, "Loss allocation in joint transmission and distribution peer-to-peer markets," *IEEE Transactions on Power Systems*, vol. 36, no. 3, pp. 1833–1842, 2020.

[11] Y. K. Renani, M. Ehsan, and M. Shahidehpour, "Optimal transactive market operations with distribution system operators," *IEEE Transactions on Smart Grid*, vol. 9, no. 6, pp. 6692–6701, 2017.

[12] S. Wang, B. Sun, X. Tan, T. Liu, and D. H. Tsang, "Real-time coordination of transmission and distribution networks via nash bargaining solution," *IEEE Trans. Sustain. Energy*, 2021.

[13] S. Yin, J. Wang, and H. Gangammanavar, "Stochastic market operation for coordinated transmission and distribution systems," *IEEE Trans. Sustain. Energy*, 2021.

[14] R. Haider, S. Baros, Y. Wasa, J. Romvary, K. Uchida, and A. M. Annaswamy, "Toward a retail market for distribution grids," *IEEE Transactions on Smart Grid*, vol. 11, no. 6, pp. 4891–4905, 2020.

[15] M. Bragin and Y. Dvorkin, "Tso-dso operational planning coordination through l 1-proximal surrogate lagrangian relaxation," *IEEE Transactions on Power Systems*, 2021.

[16] M. Khodadadi, M. H. Golshan, and M. P. Moghaddam, "Non-cooperative operation of transmission and distribution systems," *IEEE Trans. Ind. Informat.*, 2020.

[17] Z. Yuan and M. R. Hesamzadeh, "Hierarchical coordination of tso-dso economic dispatch considering large-scale integration of distributed energy resources," *Applied energy*, vol. 195, pp. 600–615, 2017.

[18] C. Lin, W. Wu, X. Chen, and W. Zheng, "Decentralized dynamic economic dispatch for integrated transmission and active distribution networks using multi-parametric programming," *IEEE Transactions on Smart Grid*, vol. 9, no. 5, pp. 4983–4993, 2017.

[19] X. Zhou, C.-Y. Chang, A. Bernstein, C. Zhao, and L. Chen, "Economic dispatch with distributed energy resources: Co-optimization of transmission and distribution systems," *IEEE Control Systems Letters*, vol. 5, no. 6, pp. 1994–1999, 2020.

[20] T. Jiang, C. Wu, R. Zhang, X. Li, and F. Li, "Risk-averse tso-dsos coordinated distributed dispatching considering renewable energy and demand response uncertainties," *Applied Energy*, vol. 327, p. 120024, 2022.

[21] Y. Liu, L. Wu, Y. Chen, and J. Li, "Integrating high der-penetrated distribution systems into iso energy market clearing: A feasible region projection approach," *IEEE Transactions on Power Systems*, vol. 36, no. 3, pp. 2262–2272, 2020.

[22] Y. Liu, L. Wu, Y. Chen, J. Li, and Y. Yang, "On accurate and compact model of high der-penetrated sub-transmission/primary distribution systems in iso energy market," *IEEE Transactions on Sustainable Energy*, vol. 12, no. 2, pp. 810–820, 2020.

[23] W. Lin, Z. Yang, J. Yu, G. Yang, and L. Wen, "Determination of transfer capacity region of tie lines in electricity markets: Theory and analysis," *Applied Energy*, vol. 239, pp. 1441–1458, 2019.

[24] Y. Guo, L. Tong, W. Wu, B. Zhang, and H. Sun, "Multi-area economic dispatch via state space decomposition," in *2016 American Control Conference (ACC)*. IEEE, 2016, pp. 1440–1445.

[25] M. Mousavi and M. Wu, "A dso framework for comprehensive market participation of der aggregators," in *2020 IEEE Power Energy Society General Meeting (PESGM)*, 2020, pp. 1–5.

[26] M. Mousavi and M. Wu, "A two-stage stochastic programming dso framework for comprehensive market participation of der aggregators under uncertainty," in *2020 52nd North American Power Symposium (NAPS)*. IEEE, 2021, pp. 1–6.

[27] ——, "Iso and dso coordination: A parametric programming approach," in *2022 IEEE Power & Energy Society General Meeting (PESGM)*. IEEE, 2022, pp. 1–5.

[28] C. Chen, S. Bose, T. D. Mount, and L. Tong, "Wholesale market participation of dera part i: Dso-dera-iso coordination," *arXiv preprint arXiv:2307.01999*, 2023.

[29] A. Bemporad and C. Filippi, "An algorithm for approximate multiparametric convex programming," *Computational optimization and applications*, vol. 35, no. 1, pp. 87–108, 2006.

[30] L. Gan and S. H. Low, "Convex relaxations and linear approximation for optimal power flow in multiphase radial networks," in *2014 Power Systems Computation Conference*, Aug 2014, pp. 1–9.

[31] J. Löfberg, "Yalmip : A toolbox for modeling and optimization in matlab," in *In Proceedings of the CACSD Conference*, Taipei, Taiwan, 2004.

[32] "Ieee 118 bus test system, 2015." [Online]. Available: http://motor.ece.iit.edu/data/118bus_ro.xls

[33] M. Mousavi, A. M. Ranjbar, and A. Safdarian, "Optimal dg placement and sizing based on micp in radial distribution networks," in *2017 Smart Grid Conference (SGC)*, 2017, pp. 1–6.

[34] F. Bu, Y. Yuan, Z. Wang, K. Dehghanpour, and A. Kimber, "A time-series distribution test system based on real utility data," *arXiv preprint arXiv:1906.04078*, 2019.

[35] M. Mousavi and M. Wu, "Transmission and distribution coordination for der-rich energy markets: A parametric programming approach," 2023.

[36] S. Shao, F. Gao, and J. Wu, "Distributed multi-area intraday economic dispatch using modified critical region projection algorithm," *IEEE Transactions on Automation Science and Engineering*, pp. 1–14, 2023.

[37] W. Wei, D. Wu, Z. Wang, S. Mei, and J. P. S. Catalão, "Impact of energy storage on economic dispatch of distribution systems: A multi-parametric linear programming approach and its implications," *IEEE Open Access Journal of Power and Energy*, vol. 7, pp. 243–253, 2020.

[38] Z. Guo, W. Wei, L. Chen, Z. Y. Dong, and S. Mei, "Impact of energy storage on renewable energy utilization: A geometric description," *IEEE Transactions on Sustainable Energy*, vol. 12, no. 2, pp. 874–885, 2021.

[39] E. C. Umeozor and M. Trifkovic, "Operational scheduling of microgrids via parametric programming," *Applied Energy*, vol. 180, pp. 672–681, 2016. [Online]. Available: https://www.sciencedirect.com/science/article/pii/S0306261916310960

[40] S. Liu, Z. Yang, Q. Xia, W. Lin, L. Shi, and D. Zeng, "Power trading region considering long-term contract for interconnected power networks," *Applied Energy*, vol. 261, p. 114411, 2020. [Online]. Available: https://www.sciencedirect.com/science/article/pii/S0306261919320987

[41] Z. Yang, H. Zhong, W. Lin, J. Lin, Y. Chen, Q. Xia, W. Liu, and X. Zhang, "Mapping between transmission constraint penalty factor and opf solution in electricity markets: analysis and fast calculation," *Energy*, vol. 168, pp. 1181–1191, 2019. [Online]. Available: https://www.sciencedirect.com/science/article/pii/S0360544218322527

[42] E. C. Umeozor and M. Trifkovic, "Energy management of a microgrid via parametric programming," *IFAC-PapersOnLine*, vol. 49, no. 7, pp. 272–277, 2016, 11th IFAC Symposium on Dynamics and Control of Process SystemsIncluding Biosystems DYCOPS-CAB 2016. [Online]. Available: https://www.sciencedirect.com/science/article/pii/S2405896316304852

[43] G. Yang, M. Xu, W. Wang, and S. Lei, "Coordinated dispatch optimization between the main grid and virtual power plants based on multi-parametric quadratic programming," *Energies*, vol. 16, no. 15, 2023. [Online]. Available: https://www.mdpi.com/1996-1073/16/15/5593

[44] F. Borrelli, A. Bemporad, and M. Morari, "Geometric algorithm for multiparametric linear programming," *Journal of optimization theory and applications*, vol. 118, no. 3, pp. 515–540, 2003.

[45] I. Adler and R. D. Monteiro, "A geometric view of parametric linear programming," *Algorithmica*, vol. 8, pp. 161–176, 1992.

[46] A. Bemporad, F. Borrelli, M. Morari *et al.*, "Model predictive control based on linear programming˜ the explicit solution," *IEEE transactions on automatic control*, vol. 47, no. 12, pp. 1974–1985, 2002.

[47] M. Herceg, M. Kvasnica, C. N. Jones, and M. Morari, "Multi-parametric toolbox 3.0," in *2013 European Control Conference (ECC)*, 2013, pp. 502–510.

[48] J. Lofberg, "Yalmip : a toolbox for modeling and optimization in matlab," in *2004 IEEE International Conference on Robotics and Automation (IEEE Cat. No.04CH37508)*, 2004, pp. 284–289.

[49] K. G. Murty, "Computational complexity of parametric linear programming," *Mathematical programming*, vol. 19, no. 1, pp. 213–219, 1980.